Clemson University
TigerPrints

All Dissertations | Dissertations

5-2017

Acetate Transport Is Essential for Survival and Virulence of *Cryptococcus neoformans*

Grace Naanyu Kisirkoi
Clemson University, gkisirk@g.clemson.edu

Follow this and additional works at: https://tigerprints.clemson.edu/all_dissertations

Recommended Citation
Kisirkoi, Grace Naanyu, "Acetate Transport Is Essential for Survival and Virulence of *Cryptococcus neoformans*" (2017). *All Dissertations*. 1915.
https://tigerprints.clemson.edu/all_dissertations/1915

This Dissertation is brought to you for free and open access by the Dissertations at TigerPrints. It has been accepted for inclusion in All Dissertations by an authorized administrator of TigerPrints. For more information, please contact kokeefe@clemson.edu.

ACETATE TRANSPORT IS ESSENTIAL FOR SURVIVAL AND VIRULENCE OF *CRYPTOCOCCUS NEOFORMANS*

A Dissertation
Presented to
the Graduate School of
Clemson University

In Partial Fulfillment
of the Requirements for the Degree
Doctor of Philosophy
Genetics

---

by
Grace Naanyu Kisirkoi
May 2017

Accepted by:
Kerry S. Smith, Committee Chair
Cheryl Ingram-Smith
Lukasz Kozubowski
Julia Frugoli
Meredith Morris

Abstract

Cryptococcus neoformans is a basidiomycetous fungal pathogen that claims 625,000 lives annually worldwide. Particularly among the immunocompromised, it is the leading cause of fungal meningitis following pulmonary colonization and dissemination to the central nervous system via the blood-brain barrier. The success of *C. neoformans* as a pathogen is largely attributable to metabolic scavenging during starvation conditions within the host's environment. Lung alveolar macrophages, which are among the first immune effectors to combat an initial pulmonary infection, present a glucose- and amino acid-poor environment that likely necessitates metabolism of nonpreferred carbon sources such as lactate and acetate for establishment of a pulmonary infection. While acetate transporters have been characterized in ascomycetous fungi such as *Saccharomyces cerevisiae*, *Candida albicans*, *Aspergillus nidulans* and *Yarrowia lipolytica* the role of acetate production and transport in *C. neoformans* is not well understood and its importance in infection has not been established. Putative acetate transporter genes, designated as *ADY2* and *ATO2*, from the GPR1/FUN34/YAAH family have been identified in *C. neoformans* and are highly expressed during infection in the lung and during growth on acetate as sole carbon source. Studies have identified acetate as one of the metabolites in brain tissue biopsies of infected rats and in culture supernatant. We propose that Ady2 and Ato2 have a role in acetate transport as a metabolic adaptation during starvation and stressful environmental conditions. Growth of the *ady2* single mutant, and the *ady2ato2* double mutant, but not *ato2* single mutant, was severely impaired in 1 mM versus 10 mM acetate plates, suggesting that Ady2 is the

essential acetate importer during growth on low acetate. Intensity of growth defects was emphasized by a 137-fold overexpression of *ADY2* during growth on acetate in relation to growth on glucose. The role of Ato2 during prolonged starvation was highlighted by diminished acetate uptake in the *ato2* single mutant after glucose-grown cells were passaged into minimal media with acetate as sole carbon source. This study also uncovered a role of Ady2 and Ato2 in ammonia export and that they preferentially import acetate versus other carboxylates. Major *C. neoformans* virulence factors: growth at 37°C and capsule synthesis were impaired by loss of Ady2 and Ato2. Moreover, Ady2 and Ato2 were essential for virulence in mice such that *ady2ato2* infected mice survived as long as uninfected controls. Additionally, Ady2 and Ato2 were additively required during coculture with human and mouse-derived phagocytes. Therefore, acetate transporters play a significant role in the survival and virulence of *C. neoformans*.

Dedication

To the great fountain of knowledge, the Creator; to the ever - nourishing bonds of family and irrevocable friendship, and to my unyielding ‘eternal optimist’ - thou knowest thyself!

Acknowledgements

I am very thankful for my parents: dad- Samson Ole Kisirkoi and mom- Florence Kanorio Kisirkoi who encouraged me into furthering education with a lot of confidence in my abilities. My siblings: sister- Sarah Naserian, brothers- Timothy Lemayian and Caleb Lekishon, niece- Joy Enkirotet, best friends Winnie Selle, and Steven Cogill have been very patient sounding boards. I am grateful to Clemson University for an opportunity to pursue a PhD degree and providing an environment for collaborative research. The guidance of my advisor, Dr. Kerry Smith has been helpful towards gaining valuable skills and his recommendation letters have helped me obtain career-advancement opportunities for which I am grateful. My thanks extend to Dr. Cheryl-Ingram Smith, who has been a source of ideas during lab-meetings and as part of my thesis committee. I am filled with warmth at my numerous interactions with Dr. Julia Frugoli both during our lab TA appointments and as part of my committee. Besides gaining from her wealth of knowledge in science, teaching, and grant writing, I have enjoyed scrumptious meaty meals at her house parties. I am thankful for Drs. Frugoli's and Amy Lawton-Rauh's TA award nominations as well as for writing me recommendation letters to career advancement opportunities. The generosity of another one of my committee members, Dr. Meredith Morris has been helpful towards gaining cell biology skills by allowing our lab to access her lab space for flow cytometry and microscopy, thank you! I am also thankful to Dr. Lukasz Kozubowski, for thoughtful questions which spur curiosity and for generosity to provide vectors containing fluorescent tags. Support from Dr. Kerry Smith's senior graduate students- Drs. Tonya

Taylor and Katie Glenn, and Dr. Ingram-Smith's senior graduate student, Thanh Dang were a great help both in shaping my research and in adjusting to a new culture. The EPIC family at large has been instrumental in providing a collaborative environment for equipment and expertise-sharing. Especially, I am grateful to Drs. Kimberley Paul and Jimmy Suryadi for their help with troubleshooting my radiolabeled experiments. Dr. Paul went out of her way to connect me with Dr. Sandra Gray of the endocrine physiology lab (thank you so much!) when our scintillation counter broke down. Peipei Wu and Evan (Yijian) Qiu been a great source of support. Thanks Bridget Luckie for stimulating scientific discussions that made for an amazing final year! I have no words to thank Dr. Gary Powell and his wife, Connie Powell for their friendship, encouragement, generosity, and mentorship to me and my family. Levi Blue, Anna Williams, Ekei Eyo, Nicole Barclay, Kemi Hambolu, Martin Kimani, Wangechi Taiti, Betiglu Eshete and his family and the rest of my Clemson family, thank you for a home away from home! The 2016 Molecular Mycology Course held at MBL was a great platform to learn practical host-microbe interactions skills in a collaborative environment, thanks for the opportunity and scholarship award! I am obliged to the the Wade-Stackhouse fellowship, Professional Enrichment Grants, and the NIH and NSF, whose funding support has supported the work in this dissertation. My appreciation extends to Dr. Stuart Levitz who graciously opened his home and lab for a collaboration that has greatly enriched my PhD research. Dr. Charlie Specht and Chrono Lee of the Levitz lab have also been quite resourceful to my research topic, thanks! There is not enough room to thank all that contributed to my PhD journey, but my heartfelt gratitude goes to everyone for every little and big thing!

Table of Contents

Page

Table of Contents (continued)

List of Tables

Table **Page**

List of tables (Chapter 4)

List of tables (Chapter 6)

List of Figures

Figure **Page**

List of figures (Chapter 1)

List of figures (Chapter 2)

List of figures (Chapter 3)

List of Figures (continued)

Figure **Page**

List of figures (Chapter 4)

List of figures (Chapter 5)

List of figures (Chapter 6)

A review of acetate transport for microbial utilization and its role in pathogenesis

Grace N. Kisirkoi and Kerry S. Smith

Department of Genetics and Biochemistry

Eukaryotic Pathogens Innovation Center (EPIC)

Clemson University

Clemson, SC 29634

To whom correspondence should be addressed:

Kerry S. Smith

Office 864-656-6935

Email kssmith@clemson.edu

CHAPTER ONE: LITERATURE REVIEW

Global disease burden and control of *Cryptococcus neoformans*

The annual incidence of cryptococcal meningitis between 1997 and 2007 was estimated at 720,000 in Sub-Saharan Africa, 100,000 in Southeast Asia, 50,000 in Latin America, 20,000 in Europe and Central Asia and 5,000-20,000 in North America, the Caribbean, East Asia, Oceania, North Africa and the Middle East (Sloan and Parris, 2014). Of these cases, over 600,000 annual deaths occurred due to cryptococcosis, the bulk of which were in Sub-Saharan Africa (Sloan and Parris, 2014). *Cryptococcus neoformans* var *grubii* (capsular serotype D) is the most common subtype, causing 82 % of the global manifestation of cryptococcosis. The capsular serotype A (var *neoformans*) on the other hand is prevalent among the northern European (France, Italy and Denmark) HIV-infected population at a rate of up to 30 % (Franzot et al., 1999; Dromer et al., 1996; Tortorano et al., 1997). According to reports from the US (Pappas et al., 2001) and South East Asia (Lui et al., 2006), serotype D has been seen at higher incidence among the immunocompetent than serotype A. Unlike *Cryptococcus neoformans*, *Cryptococcus gattii* (serotypes B and C) are usually diagnosed among the immunocompetent with 218 cases having been identified on Vancouver Island between 1999 and 2010 (Sloan and Parris, 2014).

Most patients who develop cryptococcosis have defects in cell-mediated immunity, specifically in $CD4^+$ lymphocytes. Immune compromisation from AIDS predisposes these patients to secondary infections, with cryptococcosis being a leading cause of mortality as it has death rates ranging from 15-20 % in the US and 55-70 % in

Latin America and sub-Saharan Africa (Park, 2009). Solid organ transplant patients receiving immunosuppressive therapy are also at risk of *C. neoformans* infection. Cryptococcosis is the third most common invasive fungal infection in recipients of sold organ transplant (Neofytos et al., 2010; Pappas et al., 2010). Recent studies suggest that smoking, oral corticosteroids, and older age increase the risk of infection (reviewed in MacDougall, 2011).

Serotyping and diagnosing *Cryptococcus* infection

The biochemical characteristics conferred by the sugar envelope of *Cryptococcus* cells enables its grouping into serotypes, A, B, C, D (Kwon-Chung et al., 1982) and AD (Cherniak and Sundstrom, 1994; Okabayashi et al., 2006). This is done according to their respective antibody agglutination to antigens against the polysaccharide capsule. Specifically, the antigenic potential of the capsule is attributable to GXM (consists of polymerized mannose, xylose, glucuronic acid and *O*-acetyl galactoxylomannan (GalXM), and mannoprotein (MP) (Cherniak and Sundstrom, 1994). Specific patterns of immunological reactions are detectable in response to GXM and its conjugates. Serotypes A (mating type a) and D (mating type α) are two of three variants of *Cryptococcus neoformans* and their GXM antigens are conjugates such that one of their six *O*-acetyl groups (the *O*-2 group) is substituted with beta-D-xylopyranosyl groups. The AD *Cryptococcus neoformans* serotype is aneuploid or diploid and is heterozygous at the mating type locus with both the a and α mating alleles (Lengeler et al., 2001). The *Cryptococcus gattii* serotypes B and C are substituted with beta-D-xylopyranosyl at their *O*-2 and *O*-4 *O*-acetyl groups (Cherniak and Sundstrom, 1994).

Symptomatic cryptococcal patients may present with cutaneous lesions, cough, dyspnea, pulmonary ausculatory sounds, fever, fatigue, headache, stiff neck, papilledema, blurred vision, confusion and seizures (Darras-Joly et al., 1996; Barron and Madinger, 2008). To determine suspected infection, such clinical specimens as spinal fluid from lumbar puncture, tissue biopsies with granulomata and aspirates from skin lesions (Mitchell and Perfect, 1995), are stained with India ink, mucicarmine, Alcan Blue, Fontana-Mason silver, Gomor's methenamine or Calcofluor White then observed by light or fluorescent microscopy to detect yeast cells (Mustafa et al., 2014). From patient urine, serum and cerebrospinal fluid, cryptococcal capsular antigens can be sensitively detected and serotyped (Mitchell and Perfect, 1995).

Serological tests can accurately detect and quantify solubilized capsule antigens by agglutination with rabbit anti-*C. neoformans*-antiserum (Neill et al., 1951; Nogueira et al., 2017). Moreover, urine and blood specimens can be cultured for isolation of *C. neoformans* especially when fungal load is high as is typical of infection in the immunosuppressed host (Speed and Dunt, 1995). A suspected *C. neoformans* culture is usually substantiated by melanized yeast colony morphology on Staib's birdseed agar or caffeic acid medium (Staib, 1962). A rapid urease test can also presumptively indicate *C. neoformans* infection (Canteros et al., 1996). While standard mycological techniques can diagnose cryptococcosis to the species level, several molecular-based techniques have been used to distinguish strains and serotypes by conventional and real time PCR (Sidrim et al., 2010), random fragment length polymorphism, random amplified polymorphic DNA, and using specific probes and primers (Mitchell and Perfect, 1995). Chest

radiographs can be utilized to visualize lung colonization.

Anticryptococcal therapy

Despite mortality rates as high as malaria and a high global impact of the annual disease burden, investment in research and development towards anticryptococcal agents is less than 0.5 % of the global 2014 research and development funding (Moran et al., 2015; Rodrigues, 2016). The fungicidal polyene amphotericin B is a potent broad-spectrum antifungal agent (Odds et al., 2003). It binds to ergosterol, an abundant sterol in fungal membranes, causing leakage of cytoplasmic contents. However, despite structural distinction between fungal ergosterol and mammalian cholesterol, amphotericin B is prone to low selectivity of ergosterol over cholesterol causing toxicity to mammalian cells, especially nephrotoxicity (Odds, et al., 2003). Liposomal formulations of amphotericin B reduce nephrotoxicity by slowing its delivery rate to the kidneys (Odds et al., 2003).

Another effective anticryptococcal agent is the fluorinated pyrimidine analogue, 5-flucytosine. Its antifungal action is such that flucytosine is converted to 5-fluoroacil (5-FC) that is incorporated into fungal RNA, thus prematurely terminating transcription. Fungal cytosine permease catalyzes uptake of flucytosine, cytosine deaminase converts it to 5-FC and uracil phosphoribosyl transferase converts it to a substrate fit for synthesis of nucleic acids. 5-flucytosine also inhibits DNA synthesis by perturbing the function of thymidylate synthase. 5-flucytosine has excellent delivery due to good penetration even into cerebrospinal fluid (Odds et al., 2003). However, resistance to flucytosine has been reported due to mutations in fungal cytosine permease, deaminase, and phosphoribosyl

transferase (Odds et al., 2003).

The gold standard therapy for treatment of cryptococcosis is a combination of amphotericin B and 5-flucytosine (Krysan, 2015). Both amphotericin B and 5-flucytosine were discovered over half a century ago, yet it is only recently that a clinical trial demonstrated that the combination therapy is better than amphotericin B alone (Day et al., 2013). Not only is this gold-standard anticryptococcal therapy too costly to be made available in resource poor countries, which have the highest mortality from the infection, it also has an associated toxicity such that only 37 % of patients at a major medical center in the United States receive this combination therapy (Perfect, 2013).

The azoles (fluconazole, miconazole, ketoconazole, itraconazole) are a class of antifungal agents that function by perturbing membrane permeability and fluidity by depleting ergosterol. However, resistance has been reported due to mutations that alter cytochrome P450-Erg11 or Cyp51p, which are the targets for mode of action of these azoles (Odds et al., 2003). Due to economical constraints that preclude access to the gold standard anticryptococcal therapy, fluconazole is still the readily available anticryptococcal drug used in resource poor countries. Echinocandins are the newest class of antifungal drugs which were identified forty years ago then made available on the market twenty years afterwards (Espinel-Ingroff, 1998; Tawara et al., 2000). The echinocandins include caspofungin, micafungin, and anidulafungin, impede synthesis of fungal β1,3-glucan, a major component of the fungal cell wall, by inhibiting function of β1,3-glucan synthase, which catalyzes glucose polymerization through β1,3 linkages. However, *C. neoformans* is resistant to caspofungin both *in vitro* and *in vivo* (Maligie and

Selitrennikoff, 2005).

High drug toxicity and mounting cryptococcal resistance to antifungals are the main challenges that undermine treatment of both pulmonary and disseminated cryptococcosis. This challenge is further complicated by the characteristic immunocompromised state of most patients; hence relapse of infection despite stringent therapy (Odds, et al., 2003; Mitchell and Perfect, 1995). These challenges create urgency for a deeper understanding of indispensable virulence-associated genes, which could provide an effective target for anticryptococcal therapy.

Cryptococcus neoformans host-pathogen interactions

The host inhales the environmentally ubiquitous *C. neoformans*' desiccated cryptococcal cells or basidiospores. For progression to the lungs, *C. neoformans* cells must overcome the host's relatively elevated temperature of 37°C. Moreover, the pathogen must traverse the initial physical host barriers: skin and nasal mucosa (Rohatgi and Pirofski, 2015). With the aid of mucociliary movement and gravity, *C. neoformans* reaches the lungs causing pulmonary cryptococcosis (**Figure 1-1**) (Sabiiti and May, 2012). The cryptococcal cells then adhere to the host's pulmonary epithelial cells. This is promoted by the host's lung surfactant, which facilitates cryptococcal cells' opsonization, therefore enhancing phagocytosis by macrophages (Ganendren et al., 2006). An intact immune system responds with activated macrophages (AMΦ) killing or containing the infection in a granuloma (**Figure 1-1**). CD4 T cells can also recruit macrophages and granulocytes to sites of pulmonary infection (Huffnagle et al., 1994). In the absence of antigen stimulation, memory B cells also produce IgM which enhances innate immunity

by containing *C. neoformans* in alveolar macrophages and reducing its dissemination with a predilection to the host's brain (Rohatgi and Pirofski, 2012).

In opposition to host phagocyte activation, cryptococcal cells synthesize capsule and melanin which are protective against reactive oxygen species secreted by immune cells and phosphoglycerate E (PGE) downregulates host antimicrobial activity (Valdez et al., 2012). *C. neoformans* also upregulates its nutrient and ion acquisition (Ctr4-copper acquisition, Cft1/Cfo1-iron acquisition) to facilitate their survival in the nutrient poor lung environment (Hu et al., 2008). Resistance to harsh environments complicates cryptococcal clearance as the cells can survive and proliferate within the macrophages (Tucker and Casadevall, 2002). Should the patient's immunity become compromised, latent cryptococci in granulomas or engulfed in parasitized macrophages (PMΦ) can get reactivated and enter systemic circulation by riding in the PMΦ or non-lytically exiting into blood circulation, hence fungemia (**Figure 1-1**).

Alternatively, *C. neoformans* could grow into large cells that are refractory to phagocytosis and enter systemic circulation (**Figure 1-1**). The complement system is an essential anticryptococcal armour, substantiated by complement-deplete patients having characteristic higher fungaemea (Macher et al., 1978) and complement-sufficient animals being more resistant to cryptococcosis (Rhodes and Wicker, 1980). Cell-mediated immunity in concert with either the complement system or Fc-γ receptors of macrophages, dendritic cells and neutrophils also facilitate cryptococcal containment and clearance by phagocytosis of complement-opsonized yeast (Levitz and Tabuni, 1991); and binding to antibody-opsonized *C. neoformans* respectively (Griffin, 1981). Natural

killer (NK) cells have perforin-mediated anti-cryptococcal activity (Ma et al., 2004). Host resistance to *C. neoformans* is also mediated by secretion of IL-4 and IFN γ production, and Th1 pro-inflammatory cytokine responses following activation of NK T cells (Taniguchi et al., 2003). In the event of exaggerated anti-inflammatory response, the γδ T cells secrete anti-inflammatory Th2 cytokines to regain balance (Uezu et al., 2004). Activated CD8 T cells also secrete IFN γ production that inhibits growth of *C. neoformans* inside macrophages (Lindell et al., 2005).

The host's adaptive immunity elicits protective activation against such cryptococcal antigens as the GXM capsule, cell wall polysaccharides, and specific cryptococcal proteins. When patients were vaccinated with a GXM vaccine conjugate formulated to a T-dependent antigen, the GXM-tetanus toxoid (GXM-TT), IgG2 was found to be protective by enhancing phagocytosis by human mononuclear cells (Zhong and Pirofski, 1996). Moreover, a mouse monoclonal GXM IgG1 (mAB18B7) was promising as an approach to cryptoccocal meningitis treatment among HIV-infected patients at a phase 1 trial, which unfortunately lacked resources hence failed to proceed (Casadevall et al., 1998; Larsen et al., 2005). For a cryptococcal meningitis outcome, *C. neoformans* traverses the blood-brain barrier by (**Figure 1-1**): A) entry between endothelial cells, enhanced by damage to tight junctions facilitated by phospholipase B (PLB) which is degradative to membranes (Stie et al., 2009); B) adhering to brain microvascular endothelial cells (BMECs) and being internalized (Shi et al., 2010); or C) riding in parasitized immune cells such as PMΦ, hence the "Trojan horse" model of dissemination (Charlier et al., 2009; Sabiiti and May, 2012; Santiago-Tirado et al., 2017).

Dissemination to the brain results in cryptococcal meningoencephalitis, whose mortality in some populations can reach 100 % regardless of immune status and despite administration of antifungals (Mwaba et al., 2001; Lee et al, 2011). During disease progression of *C. neoformans* in the host, the pathogen encounters a variety of environments ranging from a glucose-limited, slightly acidic alveolar macrophage environment (Vylkova and Lorenz., 2014; Cox et al., 2003; Nyberg et al., 1992; Barelle et al., 2006), which mimics growing on acetate as a sole carbon source (Lorenz et al., 2004), to the more glucose-rich (0.1 %) and slightly alkaline conditions of the blood (O'Meara et al., 2010; Güemes et al., 2016). Glucose level in the brain is maintained at approximately 0.1 % - 0.2 % (Gruetter et al., 1992) at a slightly alkaline pH (O'Meara et al., 2010). (**Figure 1-1**).

Virulence determinants of *Cryptococcus neoformans*

Several traits that influence the degree of pathogenicity of *C. neoformans* have been extensively reviewed (Coelho et al., 2014; Kronstad et al., 2012). The three major virulence determinants are: ability to grow at 37°C, a polysaccharide capsule, and melanin formation (Coelho et al., 2014; Kronstad et al., 2012). To successfully cause disease, *C. neoformans* has to be able to grow at 37°C, which is uncharacteristic of such non-pathogenic strains as soil fungi (Coelho et al., 2014). The ability of *C. neoformans* to sense the environment and adjust to environmental stresses such as temperature is facilitated through signal transduction cascades such as the calcineurin pathway (Odom et al., 1997; Lengeler et al., 2000). The capsule is another major virulence determinant of *C. neoformans* (Kwon-Chung and Rhodes, 1986). Cell wall associated and secreted capsule

polysaccharides are immunomodulatory as exported capsule-associated mannoproteins stimulate T-cell mediated immune response. Acapsular mutants are typically avirulent except in the event of extreme immunosuppression (Kronstad et al., 2012). Moreover, the smaller the capsule size the more efficient the phagocytosis and clearance of cryptococcal cells by macrophages (Bojarczuk et al., 2016). Deposition of melanin in the cell wall poses an additional influence to the degree of pathogenicity of *C. neoformans* (Kwon-Chung and Rhodes, 1986). Cryptococcal cells synthesize melanin from catecholamine substrates with the aid of copper-dependent laccases (Eisenman and Casadevall, 2012; Almeida et al., 2015). The central nervous system is catecholamine rich and experimental evidence suggests that cryptococcal cells synthesize melanin within brain cells (Norsanchuk et al., 2000). Melanin confers protection to *C. neoformans* cells against antifungal agents, environmental radiation, and oxidative killing by phagocytes thus facilitating dissemination (Coelho et al., 2014; Kronstad et al., 2012) beyond the initial site of infection (lung colonization).

C. neoformans cells also secrete neutralizing enzymes and metabolites, among them enzymes conferring resistance to oxidative and nitrosative stress. Upon the loss of these enzymes, virulence is attenuated and susceptibility to killing by phagocytes is facilitated (Missal et al., 2006; Coelho et al., 2014; Broxton and Culotta, 2016). Cell wall localized laccases and phospholipase B are important enzymes classified as virulence factors that facilitate melanin formation, cell wall integrity, and dissemination of cryptococcal cells to extrapulmonary sites (Noverr et al., 2004; Coelho et al., 2014). Urease enzyme secretion is another important virulence-associated trait of *C.*

neoformans, which facilitates its crossing the blood-brain barrier following urea breakdown into ammonia and carbamate, thus raising the local pH (Cox et al., 2000; Olszewski et al., 2004). This increased pH has been suggested to cause toxicity to endothelial cells hence facilitating permeability of cryptococcal cells and their crossing the blood brain barrier (Shi et al., 2010).

Role of fungal acetate metabolism in *Cryptococcus neoformans* pathogenesis

Gene expression profiling during murine pulmonary infection revealed induction of the glyoxylate pathway, fatty acid beta-oxidation, gluconeogenesis and amino acid synthesis. The resident lung alveolar macrophages, which present an initial immune response against *C. neoformans* infection (Feldmesser et al., 2000; Feldmesser et al., 2001), have a characteristically glucose- and amino acid-poor environment (Barelle et al., 2006; Lorenz et al., 2004). Consequently, such nonpreferred carbon sources as lactate and acetate may be important for nutrient scavenging early in establishment of pulmonary infection (Price et al., 2011). It was therefore hypothesized that carbon-source limitation was experienced by *C. neoformans* thus requiring alternative carbon source scavenging (Hu et al., 2008). In agreement with this hypothesis, elevated transcript levels of the putative acetate transporters, *ADY2* (CNAG_05678) and *ATO2* (CNAG_05266), as well as the gene encoding acetyl-CoA synthetase (*ACS*) in infected mice led to a speculation that acetyl-CoA production provided a precursor for central carbon metabolism in *C. neoformans* during starvation.

Acs is generally considered to operate solely in the direction of acetate activation to acetyl-CoA during which it utilizes up ATP and CoA to form AMP and PP_i in *C.*

neoformans (Ingram-Smith, et al., 2006). An *acs* mutant was attenuated in virulence and could not utilize acetate as the sole carbon source (Hu et al., 2008). Furthermore, the virulence-associated role of *O*-acetylation of cryptoccocal capsule and cell wall chitin synthesis was suggested (Hu et al., 2008). The yeasts *Candida albicans* and *Saccharomyces cerevisiae* have two isoforms of Acs, termed Acs1 and Acs2. Cytosolic acetyl-CoA is likely generated by Acs2 during glucose utilization (Berg and Steensma, 1995; Carman et al., 2008). When growing on highly assimilable carbon sources such as glucose, fungi glycolytically execute either oxidative respiration or nonoxidative fermentation, with production of NAD^+ being far more efficient using the former route. As eukaryotes are typically facultative or obligate aerobes, aerophilic respiration occurs unless oxygen is depleted (Strijbis and Distel., 2010). For example, *C. albicans* glycolytically oxidizes glucose to pyruvate in the cytosol followed by further oxidization to CO_2 through the TCA cycle in the mitochondria. Like in prokaryotes, the *C. albicans* pyruvate dehydrogenase complex (Pda) evolves pyruvate to acetyl-CoA. The Pda associates to the mitochondrial membrane and acetyl-CoA once produced, gets released within the mitochondria where it remains until glucose becomes limiting (Strijbis and Distel., 2010).

Besides Acs, two other pathways involved in production of cytosolic acetyl-CoA were induced during pulmonary infection of mice with *C. neoformans* (**Figure 1-2**). Beta-oxidation multifunctional enzyme type 2 (Mfe2), which is an integral part of utilization of storage lipids and exogenous fatty acids to generate acetyl-CoA, was induced during pulmonary infection of mice (Hu et al., 2008). Mutants lacking Mfe2,

which catalyzes the second and third steps in peroxisomal fatty acid beta-oxidation, were defective in growth on fatty acids and acetate, melanin biogenesis and capsule formation, and had attenuated virulence (Kretschmer et al., 2012). Furthermore, a double deletion mutant of the genes encoding Mfe2 and hydroxyacyl-CoA dehydrogenase (Had1), which catalyzes the third step in mitochondrial beta-oxidation, resulted in full attenuation of virulence (Kretschmer et al., 2012). ATP-citrate lyase (Acl1), which converts citrate to acetyl-CoA, is the third source of cytosolic acetyl-CoA. Expression of *ACL1* is upregulated during macrophage coculture (Griffiths et al., 2012) and its loss resulted in capsule defect during growth on low iron medium (LIM) which contained 0.5 % glucose. However, upon replacing glucose with 0.5 % acetate, the capsule defect was rescued. This suggested a requirement of Acl1 for attainment of the threshold of capsule acetylation in the absence of acetate that would allow for its correct attachment. Loss of Acl1 also affected melanization in the absence of acetate. The mutants lacking Acl1 were altogether avirulent, had significantly low pulmonary fungal load, and had diminished dissemination into the BALB/c mouse brain (Griffiths et al., 2012).

The eukaryotic nature of fungi presents an additional layer of complexity: unlike prokaryotic cells, acetate metabolic pathways in such fungi as *C. albicans* and *S. cerevisiae* are compartmentalized in the nucleus, peroxisome, mitochondria and cytosol. Nuclear acetyl-CoA is the donor of acetyl units for histone acetylation (Takahashi et al., 2006) that directly impacts replication, DNA repair, transcription, cell cycle progression, and aging (Galdieri et al., 2014). Intracellular acetate transport within respective organellar sources is governed by inter-conversion of metabolite intermediates into

variants that are least toxic and easily transported across membranes. Acidity of acetate and other carboxylates could lower intracellular pH to toxic levels, thus necessitating detoxifying transport and conjugation mechanisms. The amphiphilic nature of cytosolic acetyl-CoA precludes its ability to diffuse across a membrane, particularly from the cytosolic pool into the mitochondria. To circumvent this, the activated acetyl group is transferred from CoA to carnitine by the carnitine acetyltransferase (Cat). The activated carnitine is then transported by an acetyl-carnitine/carnitine translocase (Cact) then reverted back to acetyl-CoA inside the mitochondria where it feeds into the TCA cycle for subsequent ATP generation. The two-carbon acetyl-CoA can also be a precursor for synthesis of sugars following production of four carbon intermediates through the glyoxylate pathway that allows fungal growth on non-fermentable carbon sources. This gives fungi the unique advantage of being able to subsist on fatty acids as the sole carbon source.

Mitochondrial acetyl-CoA hydrolases (Ach) in *S. cerevisiae* and *Neurospora crassa* are involved in detoxification of mitochondrial acetate by transferring CoASH from succinyl-CoA to acetate such that the energy intensive hydrolysis of acetyl-CoA is bypassed and instead mitochondrial acetate is detoxified (Buu et al., 2003; Fleck et al., 2009). Peroxisomal acetyl-CoA in *C. albicans* and *S. cerevisiae* is generated following oxidation of acyl-CoA during beta-oxidation of fatty acids by acyl-CoA oxidases and ketoacyl-CoA thiolases (Strijbis and Distel., 2010).

Not only is acetate among the most abundant metabolites recovered in culture supernatants during growth in glucose (Bubb et al., 1999), it has also been identified as

one of the most abundant metabolites in brain tissues of infected rats following cryptococcal dissemination through the blood-brain barrier (Himmelreich et al., 2003). Export of acetate among other carboxylic acids has been proposed to acidify the extracellular environment leading to altered chemotaxis of phagocytes towards cryptococcal cells, and induction of neutrophil necrosis (Wright et al., 2002). Genes encoding proteins involved in acetate production: pyruvate decarboxylase (Pdc), aldehyde dehydrogenase (Ald), xylulose 5-phosphate/fructose 6-phosphate phosphoketolase (Xfp) were induced during pulmonary infection by *C. neoformans* (Hu et al., 2008; Kronstad et al., 2012). Smith and coworkers (Ingram-Smith, et al., 2006) have identified two putative acetate-producing pathways (**Figure 1-3**), whose genes have been found to be upregulated during mice pulmonary infection (Hu et al., 2008). One pathway, previously thought to be present only in bacteria, consists of acetate kinase (Ack) partnering with xylulose 5-phosphate/fructose 6-phosphate phosphoketolase (Xfp) in a modification of the pentose-phosphate pathway to produce acetate from ketose sugars with the formation of ATP. The Ack-Xfp pathway is found in euascomycetes and some basiodiomycetes but is absent in yeasts such as *S. cerevisiae* and *C. albicans* (Ingram-Smith, et al., 2006).

The second possible acetate production pathway, pyruvate decarboxylase (Pdc) and acetaldehyde dehydrogenase (Ald), decarboxylates pyruvate to acetaldehyde, which is then oxidized to acetate in the presence of $NADP^+$ (Hu et al., 2008; Tielens et al., 2010). A third possible source of acetate in *C. neoformans* could be Acs. Upon acetylation of an unidentified lysine residue(s), *Aspergillus nidulans* Acs has been shown

to have increased affinity to acetyl-CoA, consequently catalyzing the reverse reaction to produce acetate and ATP in an acetyl-CoA dependent fashion under conditions of ammonia fermentation (Takasaki et al., 2004).

Acetate metabolism is also conserved among the prokaryotes. During exponential growth on preferred carbon sources such as glucose, bacteria excrete acetate and other carboxylic acids as part of their byproducts, which lowers extracellular pH (Wolfe, 2005). However, as these bacterial cells deplete the preferred carbon sources, growth slows down resulting in a switch to utilization of alternative carbon sources like acetate and catabolism of amino acids to produce ammonia. Consequently, the media becomes alkalinized (Prüß et al., 1994; Chang et al., 1999). Research substantiates that phosphorylation of acetyl units emanating from catabolism of glucose acts to signal a switch to metabolism of acetate and has regulatory consequences as far reaching as nitrogen assimilation, capsule synthesis, biofilm generation, and overall pathogenicity (Wolfe, 2005). In *Escherichia coli,* acetate production from breakdown of highly assimilable carbon sources serves to produce high energy ATP for the cell, restore NAD^+ spent during glucose catabolism by glycolysis and to recycle coenzyme A which is utilized upon (non)oxidative decarboxylation of pyruvate to acetyl-CoA, which could be fed into the TCA cycle and fully oxidized into CO_2 (Wolfe, 2005).

Despite conserved acetate producing pathways among both eukaryotic and prokaryotic microorganisms, a few pathways remain exclusively prokaryotic. Glycine metabolism is one such pathway among Gram positive bacteria like *Clostridium* and *Eubacterium*, resulting in acetyl phosphate formation, catalyzed by glycine reductase

(Stadtman and Davis 1991; Schräder and Andreesen, 1992; Wolfe, 2005). Overall, acetyl phosphate has been documented in *E. coli* to regulate acetylation of lysine peptide residues to regulate cell growth signaling (Weinert et al., 2013). A conserved lysine (609) residue of *Salmonella enterica* Acs inhibits its activity when acetylated (Starai et al., 2002) and this residue is conserved in *S. cerevisiae*, a lower eukaryote (Starai et al., 2003). Moreover, the deacetylated form of *E. coli* Acs is more active than its acetylated counterpart (Castaño-Cerezo et al., 2014). Across bacteria (excluding *E. coli*) catabolism of sulfonated compounds yields a key intermediate, sulfoacetaldehyde, which can be further evolved by the enzyme sulfoacetaldehyde acetyltransferase into acetyl phosphate and sulfite (Jürgen and Denger., 2003). Under glucose-derepressed conditions, acetate utilization helps cells scavenge for energy. Primarily, Acs is induced during low acetate (Brown et al., 1977; Kumari et al., 1995). This pathway catalyzes production of acetyl-CoA, PP_i and AMP from acetate, ATP and CoA under limiting acetate concentrations as excess acetate could drive the Ack-Pta pathway in the acetyl-CoA forming direction (Wolfe, 2005).

Export and uptake of weak carboxylic acids

Weak carboxylic acids such as pyruvate, acetate, and lactate accumulate during growth on highly assimilable carbon sources. These carboxylic acids dissociate partially in aqueous systems and exist in a pH-dependent equilibrium between the uncharged protonated and charged deprotonated forms of the acids (Casal et al., 2008). Since intracellular cytosolic pH is buffered at neutral-slightly alkaline while the pKa of acetate is 4.76, acetate dissociates to its deprotonated form, which confers an osmotic challenge

to the cell. Furthermore, the dissociated proton could be toxic as it rapidly acidifies the cytosol with the risk of inducing programmed cell-death (Giannattasio et al., 2013). Therefore, ability to activate acetate to acetyl-CoA relieves the cell of this toxicity challenge while providing an alternative carbon source. During growth on excess glucose and when acetate levels exceed the cells potential and need of activation, an export strategy becomes necessary. An ATP-binding cassette (ABC) efflux pump, Pdr12 from the Pleiotropic Drug Resistance (PDR) Subfamily is involved in efflux following induction by sorbic, benzoic, propionic acids and slightly by acetate in *S. cerevisiae* under the control of the War1p transcription factor (Holyoak et al., 1999; Piper et al., 1998; Piper, 2011). To counter the continued diffusion of acetate into the cell along a concentration gradient, which would cost cellular ATP to export, yeast cells remodel their membrane to diminish its porosity (Simoes et al., 2006). Little else is known of acetate efflux proteins.

As cells gradually deplete the preferred carbon sources, a switch to catabolism of the partially oxidized carboxylic acids generated through breakdown of the highly assimilable carbon sources is executed (Wolfe, 2005; Casal et al., 2008). Extracellularly secreted carboxylic acids exist in protonated and deprotonated forms relative to environmental pH. At a pH above their pKa, carboxylic acids are mostly deprotonated but stay associated and uncharged when the pH is below their pKa. These forms of carboxylic acids call for either of two transport mechanisms, the first being passive transport, which occurs by either i) simple diffusion or ii) facilitated diffusion using a permease or through a channel. Below their pKa, weak carboxylic acids exist in an

uncharged protonated form, which is lipid-soluble and can traverse membranes by simple diffusion. The neutral intracellular pH favors the charged, deprotonated form of the acid that is lipophobic and cannot readily diffuse outside the cell (Casal et al., 2008).

Experimental evidence in *S. cerevisiae* has identified Fps1p, a membrane aquaglyceroporin channel through which undissociated acetate traverses the membrane. Mutants lacking Fps1p accumulate acetate slower than wild type cells and are more resistant to acetate toxicity (Mollapour and Piper, 2007). The second mechanism of carboxylic acid transport is active transport, which is typically characterized by the charged acid entering the cell against a concentration gradient through a permease that acts as a secondary active transporter such as a proton symporter. This is usually enhanced by an energy-dependent electrochemical gradient, derived from secondary ions like Na^+, K^+, or H^+, which provides energy to shuttle the anion against a concentration gradient. As intracellular pH favours accumulation of the anionic acid, a primary active transport mechanism that spends ATP usually exports the charged acid by a pump (Casal et al., 2008).

Transport of acetate in bacteria and archaea

Two acetate transporters have been identified in *E. coli*. During nutrient deprivation, an acetate permease designated Actp is co-induced at the RNA level with Acs for scavenging micromolar concentrations of extracellular acetate (Gimenez et al., 2003). YaaH (SatP) is another acetate-proton symporter that has been characterized in *E. coli* and is competitively inhibited by succinate, hence classified as an acetate-succinate transporter with a higher affinity for acetate (Sá-Pessoa et al., 2013). *E. coli* Actp is a

member of the Sodium:Solute Symporter family while *E. coli* YaaH belongs to the YaaH family. This latter transporter functions mainly during exponential growth phase on glucose before the cells switch to start assimilating acetate while ActP functions during stationary phase once the acetate switch has been executed and the glyoxylate bypass activated (Sá-Pessoa et al., 2013). Genome analysis of *Geobacter sulfurreducens* identified four homologs of *E. coli* ActP (Risso et al., 2008). A monocarboxylic acid transporter (MctC) of the same Sodium:Solute Symporter family has been identified in *Corynebacterium glutamicum* as having a high affinity for acetate and propionate and a low affinity for pyruvate (Jolkver et al., 2009).

The first known evidence of acetate permease activity in *Archaea* was reported in *Natronococcus occultus* following [^{14}C]-acetate uptake assays (Kevbrina et al., 1989). Acetate permeases have been identified in methanoarchaea such as *Methanosaeta* (Smith and Ingram-Smith, 2007), and in *Methanosarcina spp*. such as *Methanosarcina mazei* MM_0903 (Welte et al., 2014). *Methanosarcina acetivorans* MA4008 homologs are highly induced during growth on acetate as sole carbon and energy source and upon their loss acetate uptake was impaired (Rohlin and Gunsaulus, 2010).

Transport of acetate in yeast and fungi

Two putative acetate transporters, designated as Ady2 and Ato2, from the Gpr1/Fun34/YaaH family of acetate transporters, have been identified in *C. neoformans* and are highly expressed during infection in the lung (Hu et al., 2008). Although not much else is known about acetate transport in *C. neoformans*, it has been investigated in other fungi. *S. cerevisiae ADY2* was shown to be essential for the activity of the

membrane transport protein, acetate permease in uptake of acetate and was upregulated following a switch of *S. cerevisiae* from glucose-rich medium to a nutrient-poor medium supplemented with acetate (Paiva, et al., 2004). While *S. cerevisiae* Jen1 is a dedicated lactate transporter whose loss abolishes lactate uptake (Pacheco et al., 2012), lactate transport can be restored by complementation with Ady2p^{Leu219Val} and Ady2p^{Ala252Gly} suggesting that these altered Ady2p alleles can function to transport lactate (de Kok et al., 2012). *S. cerevisiae* is able to actively transport acetate when only acetate or ethanol is present in media (Casal, et al., 1996).

Unlike *S. cerevisiae* Ady2 (Ato1p), two other homologs Fun34 (Ato2p) and Ato3 (Ato3p) did not exhibit as drastic an effect in acetate transport; hence their role in acetate transport could not be conclusively ascertained (Paiva et al., 2004). A role of all three genes in environment alkalinization was proposed following the observation that subcellular localization, and ammonia export was consistent with induction of these genes (Palková et al., 2002; Řičicová et al., 2007). Consistent with this observation, the *ady2*, *fun34*, and *ato3* deletion mutants had impaired ammonia export (Palková et al., 2002; Řičicová et al., 2007). Each of these three transporters is distributed differentially in ergosterol-rich fractions of the membrane. While Ato2p is diffuse uniformly in the membrane, Ato1p and Ato3p are enriched in lipid rafts. However, Ato1p's localization in this fraction is pH-regulated (Řičicová et al., 2007). With the aid of fluorescent life-time imaging (FLIM), fluorescent resonance energy transfer (FRET) and photobleaching, Strachotová et al., (2012) uncovered physical interactions between three *S. cerevisiae* transporters: Ato1p-Ato2p, Ato1p-Ato1p, Ato3p-Ato3p forming complexes within the

membrane. These interactions suggest that these proteins' functions are not redundant but may be synergistic.

In the euascomycete *A. nidulans*, the Ady2 homolog AcpA was essential for uptake of deprotonated acetate and exhibited acetate permease activity (Robellet, et al., 2008). When concentration of protonated, uncharged acetate was lower than that of deprotonated acid in nutrient-poor media, this *acpA* mutant had growth defects growth rates but it was able to grow to wild type levels when protonated acetate concentration was high. Complementation of the *acpA* knockout with *ACPA* rescued the mutant phenotype (Robellet, et al., 2008). Unlike *S. cerevisiae ADY2*, the *A. nidulans* ortholog *ACPA* is not under carbon catabolite repression and is not an ammonia exporter (Sá-Pessoa et al., 2015). However, short chain monocarboxylates such as benzoate, formate, butyrate and propionate competitively inhibit its function (Sá-Pessoa et al., 2015). Moreover, site-directed alterations and targeted truncation of parts of the open reading frames of the *S. cerevisiae* Ady2 (Ato1) and Ato2 (Fun34) led to hypersensitivity to acetate (Gentsch et al., 2007). Alterations of amino acids in the N-terminus of the yeast *Yarrowia lipolytica* Gpr1p causes hypersensitivity to protonated acetate. However, removal of the complete ORF has no such effect. This suggested that Gpr1p is involved in adaptation to acetate (Gentsch et al., 2007). The ability to raise pH through ammonia export may also play a significant role in adapting to the acidic pH of the phagolysosome. In the opportunistic fungal pathogen *C. albicans*, the ten genes of the *ATO* family raise both macrophage pH and *in vitro* through ammonia export (Danhof and Lorenz, 2015).

A pathogen's ability to sense and actively modulate their environment enhances

their remarkable ability to prevail despite host attempts to expel them by creating harsh microenvironments. Media alkalinization by *C. albicans* was observed to be virulence associated and inhibited by presence of glucose, hence hypothesized to be glucose repressible (Vylkova et al., 2011). While little is known about pH modulation in *C. neoformans*, the recovery of acetate during infection, and induction of acetate transporters whose homologs in *C. albicans* have a virulence-associated role in carbon source dependent pH modulation, suggest a similar role in *C. neoformans*. Iron acquisition in *C. albicans* is pH modulated and its limitation is consistent with upregulation of homologs of iron transporters. (Thewes et al., 2007). Iron transporters are also elevated during *C. neoformans* infection, suggestive of iron limitation during infection (Hu et al., 2008).

Role of acetate transport in nutrient sensing and cellular signaling cascades

SNF1, the yeast ortholog of mammalian Pka, which encodes a cellular energy sensor that acts as a master regulator of metabolism, facilitates catabolic pathways during energy limitation, and inhibits protein, carbohydrate, lipid biosynthesis, cell growth and proliferation (Hardie, 2007). Activation of Snf1 causes ATP production and may phosphorylate Gpr1/Fun34/YaaH proteins, thus regulating acetate uptake relative to cellular acetyl-CoA needs. Additionally, the SNF1/PKA pathway controls nucleosome structure and remodeling at the *ADY2* promoter as evidenced by abolished H3 acetylation at the -1 and +1 nucleosomes in a *SNF1* deletion mutant (Abate et al., 2012). Moreover, accumulation of *ADY2* mRNA was diminished in this mutant, suggesting an interaction between Ady2 and Snf1 (Abate et al., 2012). Similarly, acetate regulates *S. cerevisiae*

sporulation under the control of cAMP/PKA pathway in a pH-dependent manner (Jungbluth et al., 2012). Sporulation occurs following nutrient limitation that induces meiosis and ultimate nuclear packaging into compact spores (Neiman., 2011).

Evidence of *ADY2* involvement in cell cycle progression during meiosis was demonstrated in *S. cerevisiae* by Young et al., (2003) under the control of Adr1, a carbon source responsive transcriptional regulator that impacts induction of pathways which feed into the cellular acetyl-CoA pool, and requires upstream function of Snf1. Moreover, cAMP/PKA signaling is connected with the pH responsive transcription factor, Rim 101 which is required for correct capsule anchoring onto the *C. neoformans* cell surface and mutants lacking Rim 101 were defective in growth during alkaline conditions (Kronstad et al., 2011a). Pathogenic fungi characteristically induce virulence associated traits during growth in physiological pH, consequently mutants lacking Rim101 or other interacting factors such as Nrg1, a predicted transcription factor which is also regulated by cAMP/Pka pathway, are also defective in virulence (Alkan et al., 2013). Moreover, a high pH generally affects nutrient bioavailability relative to charge and transmembrane diffusibility, thus necessitating mechanisms of facilitated nutrient uptake (Kisirkoi et al., unpublished).

Due to a link between Snf1 protein complex's regulation of acetyl-CoA levels, nutrient sensing and epigenetic gene regulation (Zhang et al., 2013), one might expect that acetate uptake is coupled with a cellular signal transduction mechanism that allows the cell to master-regulate its physiological processes using acetyl-CoA levels from acetate metabolism. The induction of *S. cerevisiae* (Paiva et al., 2004) and *A. nidulans*

(Robellet et al., 2008) acetate transporters to utilize acetate may be contributing to fluctuations in the acetyl-CoA pool. As a result, there may be an interaction with adenylyl cyclase such that the consequent production of cyclic AMP (cAMP), a ubiquitous messenger of extracellular signals, leads to activation of an AMP activated protein kinase A (Pka) (**Figure 1-4**).

In the *Y. lipolytica* Gpr1p, Ser-37 is reversibly phosphorylated in the presence of acetate but not glucose (Gentsch et al., 2005). This fluctuating pool of cellular acetyl-CoA impacts cellular metabolic expenditures and the virulence-associated capsule acetylation thus undermining capsule attachment, histone acetylation and cell cycle arrest (Galdieri et al., 2014). From our review of literature on roles played by fungal Gpr1/Fun34/YaaH family members, we present a model (**Figure 1-4**) that is supported further by Alspaugh et al., (2002) who also demonstrated that *C. neoformans* adenylyl cyclase and its second messenger, cAMP are integral to capsule and melanin formation, two key virulence factors, and virulence in a mouse model.

Chapter summary

The first chapter serves to provide readers with a broad understanding of the disease burden associated with cryptococcal meningitis and to demonstrate a link between *C. neoformans* pathogenicity and acetate metabolism and transport. The discussions in this chapter further evaluate functional and translational analyses of acetate transport and their pertinent proteins. Chapter 2, goes deeper into expounding on a functional analysis of *C. neoformans* acetate transporters as studied and provides experimental evidence of *C. neoformans* Ady2 and Ato2 of involvement in and

requirement for acetate transport. Further, Chapter 3 delineates the role of acetate transport in pathogenesis of *C. neoformans*. In Chapter 4, we provide experimental details and evidence for the roles of Ady2 and Ato2 in virulence in an invertebrate model, *Galleria mellonella*. Experimental detail on Ady2 fluorescent tagging are provided in Chapter 5 followed by applications of yeast protein isolation and western blotting techniques to investigate the construct. Chapter 6 provides inferences of our overarching findings while highlighting opportunities for continued investigations.

Why study acetate transport in *Cryptococcus neoformans*?

Despite an importance of acetate transport and metabolism during *C. neoformans* infection, knowledge of acetate transport in this pathogen is still very limited. Acetate transport during infection by *C. neoformans* could provide an anticryptococcal target against this pathogen that causes a significant annual death toll of an increasingly global reach. Current treatment regimens against *C. neoformans* are challenged with developing drug resistance and toxicity to patients, hence the need for alternative drug targets. Identification of Ady2 as a putative acetate transporter upregulated during *C. neoformans* infection and recovery of acetate in *C. neoformans*-infected tissue call for a study on acetate transporter genes that when disrupted, could diminish or sever availability of acetate as an alternative carbon source and possibly hinder this pathogen's survival. Acetate transporters' possible role in facilitating switches to catabolism of secondary metabolites essential for fungal survival during starvation could provide a broad anti-fungal target. This possibility underscores the importance of examining the roles that acetate transporters play during *C. neoformans* infection.

References

Abate G, Bastonini E, Braun KA, Verdone L, Young ET and Caserta M, 2012. Snf1/AMPK regulates Gcn5 occupancy, H3 acetylation and chromatin remodelling at *S. cerevisiae ADY2* promoter. *Biochimica et biophysica acta (BBA)-Gene Regulatory Mechanisms*, **1819:**419-427.

Alkan N, Espeso EA and Prusky D, 2013. Virulence regulation of phytopathogenic fungi by pH. *Antioxidants & redox signaling*, **19:**1012-1025.

Almeida F, Wolf JM and Casadevall A, 2015. Virulence-associated enzymes of *Cryptococcus neoformans*. *Eukaryotic Cell*, **14:**1173-1185.

Alspaugh JA, Pukkila-Worley R, Harashima T, Cavallo LM, Funnell D, Cox GM, Perfect JR, Kronstad JW and Heitman J, 2002. Adenylyl cyclase functions downstream of the Gα protein Gpa1 and controls mating and pathogenicity of *Cryptococcus neoformans*. *Eukaryotic Cell*, **1:**75-84.

Barelle CJ, Priest CL, MacCallum DM, Gow NA, Odds FC and Brown AJ, 2006. Niche-specific regulation of central metabolic pathways in a fungal pathogen. *Cellular Microbiology*, **8:**961-971.

Barron MA and Madinger NE, 2008. Opportunistic fungal infections, part 2: *Candida* and *Aspergillus*. *Infections In Medicine*, **25:**498-505.

Berg MA and Steensma HY, 1995. *ACS2*, a *Saccharomyces cerevisiae* gene encoding acetyl-Coenzyme A synthetase, essential for growth on glucose. *European Journal of Biochemistry*, **231:**704-713.

Bojarczuk A, Miller KA, Hotham R, Lewis A, Ogryzko NV, Kamuyango AA, Frost H, Gibson RH, Stillman E, May RC, Renshaw SA, 2016. *Cryptococcus neoformans* intracellular proliferation and capsule size determines early macrophage control of infection. *Scientific Reports*, **6**.

Brown TDK, Jones-Mortimer MC and Kornberg HL, 1977. The enzymic interconversion of acetate and acetyl-coenzyme A in *Escherichia coli*. *Microbiology*, **102:**327-336.

Broxton CN and Culotta VC, 2016. SOD enzymes and microbial pathogens: Surviving the oxidative storm of infection. *PLoS Pathogens*, **12:**1005295.

Bubb WA, Wright LC, Cagney M, Santangelo RT, Sorrell TC and Kuchel PW, 1999. Heteronuclear NMR studies of metabolites produced by *Cryptococcus neoformans* in culture media: identification of possible virulence factors. *Magnetic Resonance in Medicine*, **42:**442-453.

Buu LM, Chen YC and Lee FJS, 2003. Functional characterization and localization of acetyl-CoA hydrolase, Ach1p, in *Saccharomyces cerevisiae*. *Journal of Biological Chemistry*, **278:**17203-17209.

Canteros CE, Rodero L, Rivas MC and Davel G, 1996. A rapid urease test for presumptive identification of *Cryptococcus neoformans*. *Mycopathologia*, **136:**21-23.

Carman AJ, Vylkova S. and Lorenz MC, 2008. Role of acetyl coenzyme A synthesis and breakdown in alternative carbon source utilization in *Candida albicans*. *Eukaryotic Cell*, **7:**1733-1741.

Casadevall A, Cleare W, Feldmesser M, Glatman-Freedman A, Goldman DL, Kozel TR, Lendvai N, Mukherjee J, Pirofski LA, Rivera J and Rosas AL, 1998. Characterization of a murine monoclonal antibody to *Cryptococcus neoformans* polysaccharide that is a candidate for human therapeutic studies. *Antimicrobial Agents and Chemotherapy*, **42:**1437-1446.

Casal M, Cardoso H and Leao C, 1996. Mechanisms regulating the transport of acetate in *Saccharomyces cerevisiae*. *Microbiology*, **142:**1385-1390.

Casal M, Paiva S, Queirós O and Soares-Silva I, 2008. Transport of carboxylic acids in yeasts. *FEMS Microbiology Reviews*, **32:**974-994.

Castaño-Cerezo S, Bernal V, Post H, Fuhrer T, Cappadona S, Sánchez-Díaz NC, Sauer U, Heck AJ, Altelaar AM and Cánovas M, 2014. Protein acetylation affects acetate metabolism, motility and acid stress response in *Escherichia coli*. *Molecular Systems Biology*, **10:**762.

Chang DE, Shin S, Rhee JS. and Pan JG, 1999. Acetate metabolism in a *pta* mutant of *Escherichia coli* w3110: Importance of maintaining acetyl coenzyme a flux for growth and survival. *Journal of Bacteriology*, **181:**6656-6663.

Charlier C, Nielsen K, Daou S, Brigitte M, Chretien F, Dromer F, 2009. Evidence of a role for monocytes in dissemination and brain invasion by *Cryptococcus neoformans*. *Infection and Immunity*, **77:**120-7.

Cherniak R and Sundstrom JB, 1994. Polysaccharide antigens of the capsule of *Cryptococcus neoformans*. *Infection and Immunity*, **62:**1507-1512.

Coelho C, Bocca AL and Casadevall A, 2014. The tools for virulence of *Cryptococcus neoformans*. *Advances in Applied Microbiol*ogy, **75:**1-41.

Cox GM, Mukherjee J, Cole GT, Casadevall A and Perfect JR, 2000. Urease as a virulence factor in experimental cryptococcosis. *Infection and Immunity*, **68:**443-448.

Cox GM, Harrison TS, McDade HC, Taborda CP, Heinrich G, Casadevall A and Perfect JR, 2003. Superoxide dismutase influences the virulence of *Cryptococcus neoformans* by affecting growth within macrophages. *Infection and Immunity*, **71:**173-180.

Danhof HA, and Lorenz MC, 2015. The *Candida albicans ATO* gene family promotes neutralization of the macrophage phagolysosome. *Infection and Immunity*, **83:**4416-4426.

Darras-Joly C, Chevret S, Wolff M, Matheron S, Longuet P, Casalino E, Joly V, Chochillon C, Bédos JP, 1996. *Cryptococcus neoformans* infection in France: epidemiologic features of and early prognostic parameters for 76 patients who were infected with human immunodeficiency virus. *Clinical Infectious Diseases*, **23:**369-76.

Day JN, Chau TT, Wolbers M, Mai PP, Dung NT, Mai NH, Phu NH, Nghia HD, Phong ND, and Thai LH, 2013. Combination antifungal therapy for cryptococcal meningitis. *New England Journal of Medicine*, **368:**1291-1302.

de Kok S, Nijkamp JF, Oud B, Roque FC, de Ridder D, Daran JM, Pronk JT and van Maris AJ, 2012. Laboratory evolution of new lactate transporter genes in a jen1Δ mutant of *Saccharomyces cerevisiae* and their identification as *ADY2* alleles by whole-genome resequencing and transcriptome analysis. *FEMS Yeast Research*, **12:**359-374.

Dromer F, Mathoulin S, Dupont B, Letenneur L, Ronin O and French. Cryptococcosis Study Group, 1996. Individual and environmental factors associated with infection due to *Cryptococcus neoformans* serotype D. *Clinical Infectious Diseases*, **23:**91-96.

Eisenman HC and Casadevall A, 2012. Synthesis and assembly of fungal melanin. *Applied Microbiology and Biotechnology*, **93:**931-940.

Espinel-Ingroff A, 1998. Comparison of in vitro activities of the new triazole SCH56592 and the echinocandins MK-0991 (L-743,872) and LY303366 against opportunistic filamentous and dimorphic fungi and yeasts. *Journal of Clinical Microbiology*, **36:**2950-2956.

Feldmesser M, Kress Y, Novikoff P and Casadevall A, 2000. *Cryptococcus neoformans* is a facultative intracellular pathogen in murine pulmonary infection. *Infection and Immunity*, **68:**4225-4237.

Feldmesser M, Tucker S and Casadevall A, 2001. Intracellular parasitism of macrophages by *Cryptococcus neoformans*. *Trends in Microbiology*, **9:**273-278.

Fleck CB and Brock M, 2009. Re-characterisation of *Saccharomyces cerevisiae* Ach1p: fungal CoA-transferases are involved in acetate detoxification. *Fungal Genetics and Biology*, **46:**473-485.

Franzot SP, Salkin IF and Casadevall A, 1999. *Cryptococcus neoformans* var. *grubii*: separate varietal status for *Cryptococcus neoformans* serotype A isolates. *Journal of Clinical Microbiology*, **37:**838-840.

Galdieri L, Zhang T, Rogerson D, Lleshi R and Vancura A, 2014. Protein acetylation and acetyl coenzyme a metabolism in budding yeast. *Eukaryotic Cell*, **13:**1472-1483.

Ganendren R, Carter E, Sorrell T, Widmer F and Wright L, 2006. Phospholipase B activity enhances adhesion of *Cryptococcus neoformans* to a human lung epithelial cell line. *Microbes and Infection*, **8:**1006-1015.

Gentsch M and Barth G, 2005. Carbon source dependent phosphorylation of the Gpr1 protein in the yeast *Yarrowia lipolytica*. *FEMS Yeast Research*, **5:**909-917.

Gentsch M, Kuschel M, Schlegel S and Barth G, 2007. Mutations at different sites in members of the Gpr1/Fun34/YaaH protein family cause hypersensitivity to acetate in *Saccharomyces cerevisiae* as well as in *Yarrowia lipolytica*. *FEMS Yeast Research*, **7:**380-390.

Giannattasio S, Guaragnella N, Ždralević M and Marra E, 2013. Molecular mechanisms of *Saccharomyces cerevisiae* stress adaptation and programmed cell death in response to acetate. *Frontiers in Microbiology*, **4:**33.

Gimenez R, Nuñez MF, Badia J, Aguilar J and Baldoma L, 2003. The gene yjcG, cotranscribed with the gene acs, encodes an acetate permease in *Escherichia coli*. *Journal of Bacteriology*, **185:**6448-6455.

Griffin FM, 1981. Roles of macrophage Fc and C3b receptors in phagocytosis of immunologically coated *Cryptococcus neoformans*. *Proceedings of the National Academy of Sciences*, **78:**3853-3857.

Griffiths EJ, Hu G, Fries B, Caza M, Wang J, Gsponer J, Gates-Hollingsworth MA, Kozel TR, De Repentigny L and Kronstad JW, 2012. A defect in ATP-citrate lyase links acetyl-CoA production, virulence factor elaboration and virulence in *Cryptococcus neoformans*. *Molecular Microbiology*, **86:**1404-1423.

Güemes M, Rahman SA and Hussain K, 2016. What is a normal blood glucose? *Archives of Disease in Childhood*, **101:**569-574.

Gruetter R, Novotny EJ, Boulware SD, Rothman DL, Mason GF, Shulman GI, Shulman RG and Tamborlane WV, 1992. Direct measurement of brain glucose concentrations in humans by 13C NMR spectroscopy. *Proceedings of the National Academy of Sciences*, **89:**1109-1112.

Hardie DG, 2007. AMP-activated/SNF1 protein kinases: conserved guardians of cellular energy. *Nature Reviews Molecular Cell Biology*, **8:**774-785.

Himmelreich U, Allen C, Dowd S, Malik R, Shehan BP, Mountford C and Sorrell TC, 2003. Identification of metabolites of importance in the pathogenesis of pulmonary cryptococcoma using nuclear magnetic resonance spectroscopy. *Microbes and Infection*, **5:**285-290.

Holyoak CD, Bracey D, Piper PW, Kuchler K and Coote PJ, 1999. The *Saccharomyces cerevisiae* weak-acid-inducible ABC transporter Pdr12 transports fluorescein and preservative anions from the cytosol by an energy-dependent mechanism. *Journal of Bacteriology*, **181:**4644-4652.

Hu G, Cheng PY, Sham A, Perfect JR and Kronstad JW, 2008. Metabolic adaptation in *Cryptococcus neoformans* during early murine pulmonary infection. *Molecular Microbiology*, **69:**1456-1475.

Huffnagle GB, Lipscomb MF, Lovchik JA, Hoag KA and Street NE, 1994. The role of CD4+ and CD8+ T cells in the protective inflammatory response to a pulmonary cryptococcal infection. *Journal of Leukocyte Biology*, **55:**35-42.

Idnurm A, Giles SS, Perfect JR and Heitman J, 2007. Peroxisome function regulates growth on glucose in the basidiomycete fungus *Cryptococcus neoformans*. *Eukaryotic Cell*, **6:**60-72.

Ingram-Smith C, Martin SR and Smith KS, 2006. Acetate kinase: not just a bacterial enzyme. *Trends in Microbiology*, **14:**249-253.

Jolkver E, Emer D, Ballan S, Krämer R, Eikmanns BJ, Marin K, 2009. Identification and characterization of a bacterial transport system for the uptake of pyruvate, propionate, and acetate in *Corynebacterium glutamicum*. *Journal of Bacteriology*, **191**:940-948.

Jungbluth M, Mösch HU and Taxis C, 2012. Acetate regulation of spore formation is under the control of the Ras/cyclic AMP/protein kinase A pathway and carbon dioxide in *Saccharomyces cerevisiae*. *Eukaryotic Cell*, **11:**1021-1032.

Jürgen RUFF and Denger K, 2003. Sulphoacetaldehyde acetyltransferase yields acetyl phosphate: purification from *Alcaligenes defragrans* and gene clusters in taurine degradation. *Biochemical Journal*, **369:**275-285.

Kevbrina MV, Zvyagintseva IS and Plakunov VK, 1989. Uptake of C-14 acetate in *Natronococcus-occultus*. *Microbiology*, **58:**719-723.

Kretschmer M, Wang J and Kronstad JW, 2012. Peroxisomal and mitochondrial β-oxidation pathways influence the virulence of the pathogenic fungus *Cryptococcus neoformans*. *Eukaryotic Cell*, **11:**1042-1054.

Kronstad JW, Hu G and Choi J, 2011a. The cAMP/protein kinase. A pathway and virulence in *Cryptococcus neoformans*. *Mycobiology*, **39:**143-150.

Kronstad JW, Attarian R, Cadieux B, Choi J, D'Souza CA, Griffiths EJ, Geddes JM, Hu G, Jung WH, Kretschmer M and Saikia S, 2011b. Expanding fungal pathogenesis: *Cryptococcus* breaks out of the opportunistic box. *Nature Reviews Microbiology*, **9:**193-203.

Kronstad J, Saikia S, Nielson ED, Kretschmer M, Jung W, Hu G, Geddes JM, Griffiths EJ, Choi J, Cadieux B and Caza M, 2012. Adaptation of *Cryptococcus neoformans* to mammalian hosts: integrated regulation of metabolism and virulence. *Eukaryotic Cell*, **11:**109-118.

Krysan DJ, 2015. Toward improved anti-cryptococcal drugs: Novel molecules and repurposed drugs. *Fungal Genetics and Biology*, **78:**93-98.

Kumari S, Tishel R, Eisenbach M and Wolfe AJ, 1995. Cloning, characterization, and functional expression of acs, the gene which encodes acetyl coenzyme A synthetase in *Escherichia coli*. *Journal of Bacteriology*, **177:**2878-2886.

Kwon-Chung KJ and Rhodes JC, 1986. Encapsulation and melanin formation as indicators of virulence in *Cryptococcus neoformans*. *Infection and Immunity*, **51:**218-223.

Kwon-Chung KJ, Polacheck ITZHACK and Bennett JE, 1982. Improved diagnostic medium for separation of *Cryptococcus neoformans* var. *neoformans* (serotypes A and D) and *Cryptococcus neoformans* var. *gattii* (serotypes B and C). *Journal of Clinical Microbiology*, **15:**535-537.

Larsen RA, Pappas PG, Perfect J, Aberg JA, Casadevall A, Cloud GA, James R, Filler S and Dismukes WE, 2005. Phase I evaluation of the safety and pharmacokinetics of murine-derived anticryptococcal antibody 18B7 in subjects with treated cryptococcal meningitis. *Antimicrobial Agents and Chemotherapy*, **49:**952-958.

Lee YC, Wang JT, Sun HY and Chen YC, 2011. Comparisons of clinical features and mortality of cryptococcal meningitis between patients with and without human immunodeficiency virus infection. *Journal of Microbiology, Immunology and Infection*, **44:**338-345.

Lengeler KB, Cox GM and Heitman J, 2001. Serotype AD strains of *Cryptococcus neoformans* are diploid or aneuploid and are heterozygous at the mating-type locus. *Infection and Immunity*, **69:**115-122.

Lengeler KB, Davidson RC, D'souza C, Harashima T, Shen WC, Wang P, Pan X, Waugh M and Heitman J, 2000. Signal transduction cascades regulating fungal development and virulence. *Microbiology and Molecular Biology Reviews*, **64:**746-785.

Levitz SM and Tabuni A, 1991. Binding of *Cryptococcus neoformans* by human cultured macrophages. Requirements for multiple complement receptors and actin. *Journal of Clinical Investigation*, **87:**528.

Lindell DM, Moore TA, McDonald RA, Toews GB and Huffnagle GB, 2005. Generation of antifungal effector CD8+ T cells in the absence of CD4+ T cells during *Cryptococcus neoformans* infection. *The Journal of Immunology*, **174:**7920-7928.

Lorenz MC, Bender JA and Fink GR, 2004. Transcriptional response of *Candida albicans* upon internalization by macrophages. *Eukaryotic Cell*, **3:**1076-1087.

Lui G, Lee N, Ip M, Choi KW, Tso YK, Lam E, Chau S, Lai R and Cockram CS, 2006. Cryptococcosis in apparently immunocompetent patients. *Quarterly Journal of Medicine*, **99:**143-151.

Ma LL, Wang CL, Neely GG, Epelman S, Krensky AM and Mody CH, 2004. NK cells use perforin rather than granulysin for anticryptococcal activity. *The Journal of Immunology*, **173:**3357-3365.

MacDougall L, 2011. Risk factors for *Cryptococcus gattii* infection, British Columbia, Canada-*Emerging Infectious Disease Journal-CDC,* **17**.

Macher AM, Bennett JE, Gadek JE and Frank MM, 1978. Complement depletion in cryptococcal sepsis. *The Journal of Immunology*, **120:**1686-1690.

Maligie MA and Selitrennikoff CP, 2005. *Cryptococcus neoformans* resistance to echinocandins: (1,3) β-glucan synthase activity is sensitive to echinocandins. *Antimicrobial Agents and Chemotherapy*, **49:**2851-2856.

Missall TA, Pusateri ME, Donlin MJ, Chambers KT, Corbett JA and Lodge JK, 2006. Posttranslational, translational, and transcriptional responses to nitric oxide stress in *Cryptococcus neoformans*: implications for virulence. *Eukaryotic Cell*, **5:**518-529.

Mitchell TG and Perfect JR, 1995. Cryptococcosis in the era of AIDS--100 years after the discovery of *Cryptococcus neoformans*. *Clinical Microbiology Reviews*, **27:**515-548.

Mollapour M and Piper PW, 2007. Hog1 mitogen-activated protein kinase phosphorylation targets the yeast Fps1 aquaglyceroporin for endocytosis, thereby rendering cells resistant to acetate. *Molecular and Cellular Biology*, **27:**6446-6456.

Moran M, Chapman N, Abela-Oversteegen L, Doubell A, Whittall C, Howard R, Farrell P, Halliday D, and Hirst C, 2015. Funding by disease. *Neglected Disease Research and Development: the Ebola effect*. Policy Cures, **8:**13-85.

Mota S, Alves R, Carneiro C, Silva S, Brown AJ, Istel F, Kuchler K, Sampaio P, Casal M, Henriques M and Paiva S, 2015. *Candida glabrata* susceptibility to antifungals and phagocytosis is modulated by acetate. *Frontiers in Microbiology*, **6:**919.

Mustafa M, Salih FM, Parash MTH, Shimmi CS and Rahman MS, 2014. *Cryptococcus* Meningitis, in the patients with Human Immunodeficiency Virus Infection. *International Journal of Pharmaceutical Science Invention*, **3:**60-65.

Mwaba P, Mwansa J, Chintu C, Pobee J, Scarborough M, Portsmouth S and Zumla A, 2001. Clinical presentation, natural history, and cumulative death rates of 230 adults with primary cryptococcal meningitis in Zambian AIDS patients treated under local conditions. *Postgraduate Medical Journal*, **77:**769-773.

Neill JM, Sugg JY and McCauley DW, 1951. Serologically reactive material in spinal fluid, blood, and urine from a human case of cryptococcosis (torulosis). *Experimental Biology and Medicine*, **77:**775-778.

Neiman AM, 2011. Sporulation in the budding yeast *Saccharomyces cerevisiae*. *Genetics*, **189:**737-765.

Neofytos D, Fishman JA, Horn D, Anaissie E, Chang CH, Olyaei A, Pfaller M, Steinbach WJ, Webster KM, and Marr KA, 2010. Epidemiology and outcome of invasive fungal infections in solid organ transplant recipients. *Transplant Infectious Disease*, **12:**220-229.

Nogueira F, Istel F, Pereira L, Tscherner M and Kuchler K, 2017. Immunological identification of fungal species. *Human Fungal Pathogen Identification: Methods and Protocols*, **1508:**339-359.

Norsanchuk JD, Rosas AL, Lee SC and Casadevall A, 2000. Melanisation of *Cryptococcus neoformans* in human brain tissue. *The Lancet*, **355:**2049-2050.

Noverr MC, Williamson PR, Fajardo RS and Huffnagle GB, 2004. CNLAC1 is required for extrapulmonary dissemination of *Cryptococcus neoformans* but not pulmonary persistence. *Infection and Immunity*, **72:**1693-1699.

Nyberg K, Johansson U, Johansso A and Camner P, 1992. Phagolysosomal pH in alveolar macrophages. *Environmental Health Perspectives*, **97:**149.

Odds FC, Brown AJ and Gow NA, 2003. Antifungal agents: mechanisms of action. *Trends in Microbiology*, **11:**272-279.

Odom A, Muir S, Lim E, Toffaletti DL, Perfect J and Heitman J, 1997. Calcineurin is required for virulence of *Cryptococcus neoformans*. *The EMBO Journal*, **16:**2576-2589.

Okabayashi K, Kano R, Nakamura Y, Watanabe S and Hasegawa A, 2006. Capsule-associated genes of serotypes of *Cryptococcus neoformans*, especially serotype AD. *Medical Mycology*, **44:**127-132.

Olszewski M A, Noverr MC, Chen GH, Toews GB, Cox GM, Perfect JR, Huffnagle GB. 2004. Urease expression by *Cryptococcus neoformans* promotes microvascular sequestration, thereby enhancing central nervous system invasion. *The American Journal of Pathology*, **164:**1761-1771.

O'Meara TR, Norton D, Price MS, Hay C, Clements MF, Nichols CB and Alspaugh JA, 2010. Interaction of *Cryptococcus neoformans* Rim101 and protein kinase A regulates capsule. *PLoS Pathogens*, **6:**1000776.

Pacheco A, Talaia G, Sá-Pessoa J, Bessa D, Gonçalves MJ, Moreira R, Paiva S, Casal M and Queirós O, 2012. Lactic acid production in *Saccharomyces cerevisiae* is modulated by expression of the monocarboxylate transporters Jen1 and Ady2. *FEMS Yeast Research*, **12:**375-381.

Paiva S, Devaux F, Barbosa S, Jacq C and Casal M, 2004. Ady2p is essential for the acetate permease activity in the yeast *Saccharomyces cerevisiae*. *Yeast*, **21:**201-210.

Palková Z, Devaux F, Řicˇicová M, Mináriková L, Le Crom S and Jacq C, 2002. Ammonia pulses and metabolic oscillations guide yeast colony development. *Molecular Biology of the Cell*, **13:**3901-3914.

Pappas PG, Perfect JR, Cloud GA, Larsen RA, Pankey GA, Lancaster DJ, Henderson H, Kauffman CA, Haas DW, Saccente M and Hamill RJ, 2001. Cryptococcosis in human immunodeficiency virus-negative patients in the era of effective azole therapy. *Clinical Infectious Diseases*, **33:**690-699.

Pappas PG, Alexander BD, Andes DR, Hadley S, Kauffman CA, Freifeld A, Anaissie EJ, Brumble LM, Herwaldt L, Ito J and Kontoyiannis DP, 2010. Invasive fungal infections among organ transplant recipients: results of the Transplant-Associated Infection Surveillance Network (TRANSNET). *Clinical Infectious Diseases*, **50:**1101-1111.

Park BJ, Wannemuehler KA, Marston BJ, Govender N, Pappas PG, and Chiller TM, 2009. Estimation of the current global burden of cryptococcal meningitis among persons living with HIV/AIDS. *Aids*, **23:**525-530.

Perfect JR, 2013. Efficiently killing a sugar-coated yeast. *New England Journal of Medicine,* **368:**1354-1356

Piper P, Mahé Y, Thompson S, Pandjaitan R, Holyoak C, Egner R, Mühlbauer M, Coote P and Kuchler K, 1998. The Pdr12 ABC transporter is required for the development of weak organic acid resistance in yeast. *The EMBO Journal*, **17:**4257-4265.

Piper P, 2011. Resistance of yeasts to weak organic acid food preservatives. *Advances in Applied Microbiology*, **77:** 97-113.

Price MS, Betancourt-Quiroz M, Price JL, Toffaletti DL, Vora H, Hu G, Kronstad JW and Perfect JR, 2011. *Cryptococcus neoformans* requires a functional glycolytic pathway for disease but not persistence in the host. *MBio*, **2:**00103-11.

Prüß BM, Nelms JM, Park C and Wolfe AJ, 1994. Mutations in NADH: ubiquinone oxidoreductase of *Escherichia coli* affect growth on mixed amino acids. *Journal of Bacteriology*, **176:**2143-2150.

Rhodes JC, Wicker LS and Urba WJ, 1980. Genetic control of susceptibility to *Cryptococcus neoformans* in mice. *Infection and Immunity*, **29:**494-499.

Řičicová M, Kučerová H, Váchová L and Palková Z, 2007. Association of putative ammonium exporters Ato with detergent-resistant compartments of plasma membrane during yeast colony development: pH affects Ato1p localisation in patches. *Biochimica et Biophysica Acta (BBA)-Biomembranes*, **1768:**1170-1178.

Risso C, Methe BA, Elifantz H, Holmes DE, Lovley DR, 2008. Highly conserved genes in Geobacter species with expression patterns indicative of acetate limitation. *Microbiology*, **154**:2589-2599.

Robellet X, Flipphi M, Pégot S, MacCabe AP and Vélot C, 2008. AcpA, a member of the GPR1/FUN34/YaaH membrane protein family, is essential for acetate permease activity in the hyphal fungus *Aspergillus nidulans*. *Biochemical Journal*, **412:**485-493.

Rodrigues ML, 2016. Funding and Innovation in Diseases of Neglected Populations: The Paradox of Cryptococcal Meningitis. *PLoS Neglected Tropical Diseases*, **10:**e0004429.

Rohatgi S and Pirofski LA, 2012. Molecular characterization of the early B cell response to pulmonary *Cryptococcus neoformans* infection. *The Journal of Immunology*, **189:**5820-5830.

Rohatgi S and Pirofski LA, 2015. Host immunity to *Cryptococcus neoformans*. *Future Microbiology*, **10:**565-581.

Rohlin L and Gunsalus RP, 2010. Carbon-dependent control of electron transfer and central carbon pathway genes for methane biosynthesis in the Archaean, *Methanosarcina acetivorans* strain C2A. *BMC Microbiology* **10:** 62.

Santiago-Tirado FH, Onken MD, Cooper JA, Klein RS, and Doering TL, 2017. Trojan horse transit contributes to blood-brain barrier crossing of a eukaryotic pathogen. *mBio*, **8:**e02183-16.

Sá-Pessoa J, Paiva S, Ribas D, Silva IJ, Viegas SC, Arraiano CM and Casal M, 2013. SATP (YaaH), a succinate–acetate transporter protein in *Escherichia coli*. *Biochemical Journal*, **454:**585-595.

Sá-Pessoa J, Amillis S, Casal M and Diallinas G, 2015. Expression and specificity profile of the major acetate transporter AcpA in *Aspergillus nidulans*. *Fungal Genetics and Biology*, **76:**93-103.

Sabiiti W and May RC, 2012. Mechanisms of infection by the human fungal pathogen *Cryptococcus neoformans*. *Future Microbiology*, **7:**1297-1313.

Schräder T and Andreesen JR, 1992. Purification and characterization of protein PC, a component of glycine reductase from *Eubacterium acidaminophilum*. *European Journal of Biochemistry*, **206:**79-85.

Shi M, Li SS, Zheng C, Jones GJ, Kim KS, Zhou H, Kubes P and Mody CH, 2010. Real-time imaging of trapping and urease-dependent transmigration of *Cryptococcus neoformans* in mouse brain. *The Journal of Clinical Investigation*, **120:**1683-1693.

Sidrim JJC, Costa AKF, Cordeiro RA, Brilhante RSN, Moura FEA, Castelo-Branco DSCM, Neto MPDA and Rocha MFG, 2010. Molecular methods for the diagnosis and characterization of Cryptococcus: a review. *Canadian Journal of Microbiology*, **56:**445-458.

Simoes T, Mira NP, Fernandes AR and Sá-Correia I, 2006. The SPI1 gene, encoding a glycosylphosphatidylinositol-anchored cell wall protein, plays a prominent role in the development of yeast resistance to lipophilic weak-acid food preservatives. *Applied and Environmental Microbiology*, **72:**7168-7175.

Sloan DJ and Parris V, 2014. *Cryptococcal meningitis*: epidemiology and therapeutic options. *Clinical Epidemiology*, **6:**169-182.

Smit G, Straver MH, Lugtenberg BJ and Kijne JW, 1992. Flocculence of *Saccharomyces cerevisiae* cells is induced by nutrient limitation, with cell surface hydrophobicity as a major determinant. *Applied and Environmental Microbiology*, **58:**3709-3714.

Smith KS and Ingram-Smith C, 2007. *Methanosaeta*, the forgotten methanogen. *Trends in Microbiology* **15:**150-155.

Speed B, Dunt D, 1995. Clinical and host differences between infections with the two varieties of *Cryptococcus neoformans*. *Clinical Infectious Diseases*. **21:**28-34.

Stadtman TC and Davis JN, 1991. Glycine reductase protein C. Properties and characterization of its role in the reductive cleavage of Se-carboxymethyl-selenoprotein A. *Journal of Biological Chemistry*, **266:**22147-22153.

Staib F, 1962. *Cyptococcus neoformans* und *Guizotia abyssinica* (syn. G. oleifera DC). *Medical Microbiology and Immunology*, **148:**466-475.

Starai VJ, Celic I, Cole RN, Boeke JD and Escalante-Semerena JC, 2002. Sir2-dependent activation of acetyl-CoA synthetase by deacetylation of active lysine. *Science*, **298:**2390-2392.

Starai VJ, Takahashi H, Boeke JD, and Escalante-Semerena JC, 2003. Short-chain fatty acid activation by acyl-coenzyme A synthetases requires SIR2 protein function in *Salmonella enterica* and *Saccharomyces cerevisiae*. *Genetics*, **163:**545-555.

Stie J, Bruni G and Fox D, 2009. Surface-associated plasminogen binding of *Cryptococcus neoformans* promotes extracellular matrix invasion. *PloS One*, **4:**5780.

Strachotová D, Holoubek A, Kučerová H, Benda A, Humpolíčková J, Váchová L and Palková Z, 2012. Ato protein interactions in yeast plasma membrane revealed by fluorescence lifetime imaging (FLIM). *Biochimica et Biophysica Acta (BBA)-Biomembranes*, **1818:**2126-2134.

Strijbis K and Distel B, 2010. Intracellular acetyl unit transport in fungal carbon metabolism. *Eukaryotic Cell*, **9:**1809-1815.

Takahashi H, McCaffery JM, Irizarry RA and Boeke JD, 2006. Nucleocytosolic acetyl-coenzyme a synthetase is required for histone acetylation and global transcription. *Molecular Cell*, **23:**207-217.

Takasaki K, Shoun H, Yamaguchi M, Takeo K, Nakamura A, Hoshino T and Takaya N, 2004. Fungal ammonia fermentation, a novel metabolic mechanism that couples the dissimilatory and assimilatory pathways of both nitrate and ethanol role of acetyl-CoA synthetase in anaerobic ATP synthesis. *Journal of Biological Chemistry*, **279:**12414-12420.

Taniguchi M, Harada M, Kojo S, Nakayama T and Wakao H, 2003. The regulatory role of Vα14 NKT cells in innate and acquired immune response. *Annual Review of Immunology*, **21:**483-513.

Tawara S, Ikeda F, Maki K, Morishita Y, Otomo K, Teratani N, Goto T, Tomishima M, Ohki H, Yamada A and Kawabata K, 2000. *In vitro* activities of a new lipopeptide antifungal agent, FK463, against a variety of clinically important fungi. *Antimicrobial Agents and Chemotherapy*, **44:**57-62.

Thewes S, Kretschmar M, Park H, Schaller M, Filler SG and Hube B, 2007. *In vivo* and *ex vivo* comparative transcriptional profiling of invasive and non-invasive *Candida albicans* isolates identifies genes associated with tissue invasion. *Molecular Microbiology*, **63:**1606-1628.

Tielens AG, van Grinsven KW, Henze K, van Hellemond JJ and Martin W, 2010. Acetate formation in the energy metabolism of parasitic helminths and protists. *International Journal for Parasitology*, **40:**387-397.

Tortorano AM, Viviani MA, Rigoni AL, Cogliati M, Roverselli A and Pagano A, 1997. Prevalence of serotype D in *Cryptococcus neoformans* isolates from HIV positive and HIV negative patients in Italy. *Mycoses*, **40:**297-302.

Tucker SC and Casadevall A, 2002. Replication of *Cryptococcus neoformans* in macrophages is accompanied by phagosomal permeabilization and accumulation of vesicles containing polysaccharide in the cytoplasm. *Proceedings of the National Academy of Sciences*, **99:**3165-3170.

Uezu K, Kawakami K, Miyagi K, Kinjo Y, Kinjo T, Ishikawa H and Saito A, 2004. Accumulation of γδ T cells in the lungs and their regulatory roles in Th1 response and host defense against pulmonary infection with *Cryptococcus neoformans*. *The Journal of Immunology*, **172:**7629-7634.

Valdez PA, Vithayathil PJ, Janelsins BM, Shaffer AL, Williamson PR and Datta SK, 2012. Prostaglandin E2 suppresses antifungal immunity by inhibiting interferon regulatory factor 4 function and interleukin-17 expression in T cells. *Immunity*, **36:**668-679.

Vylkova S, Carman AJ, Danhof HA, Collette JR, Zhou H and Lorenz MC, 2011. The fungal pathogen *Candida albicans* autoinduces hyphal morphogenesis by raising extracellular pH. *MBio*, **2:**e00055-11.

Vylkova S and Lorenz MC, 2014. Modulation of phagosomal pH by *Candida albicans* promotes hyphal morphogenesis and requires Stp2p, a regulator of amino acid transport. *PLoS Pathogens*, **10:**1003995.

Weinert BT, Iesmantavicius V, Wagner SA, Schölz C, Gummesson B, Beli P, Nyström T and Choudhary C, 2013. Acetyl-phosphate is a critical determinant of lysine acetylation in *E. coli*. *Molecular Cell*, **51:**265-272.

Welte C, Kröninger L and Deppenmeier U, 2014. Experimental evidence of an acetate transporter protein and characterization of acetate activation in aceticlastic methanogenesis of *Methanosarcina mazei*. *FEMS Microbiology Letters*, **359:**147-153.

Wolfe AJ, 2005. The acetate switch. *Microbiology and Molecular Biology Reviews*. **69:**12-50.

Wright L, Bubb W, Davidson J, Santangelo R, Krockenberger M, Himmelreich U and Sorrell T, 2002. Metabolites released by *Cryptococcus neoformans* var. *neoformans* and var. *gattii* differentially affect human neutrophil function. *Microbes and Infection*, **4:**1427-1438.

Young ET, Dombek KM, Tachibana C and Ideker T, 2003. Multiple pathways are co-regulated by the protein kinase Snf1 and the transcription factors Adr1 and Cat8. *Journal of Biological Chemistry*, **278:**26146-26158.

Zhang M, Galdieri L, and Vancura A, 2013. The yeast AMPK homolog SNF1 regulates acetyl coenzyme A homeostasis and histone acetylation. *Molecular and Cellular Biology*, **33:**4701-4717.

Zhong Z and Pirofski LA, 1996. Opsonization of *Cryptococcus neoformans* by human anticryptococcal glucuronoxylomannan antibodies. *Infection and Immunity*, **64:**3446-3450.

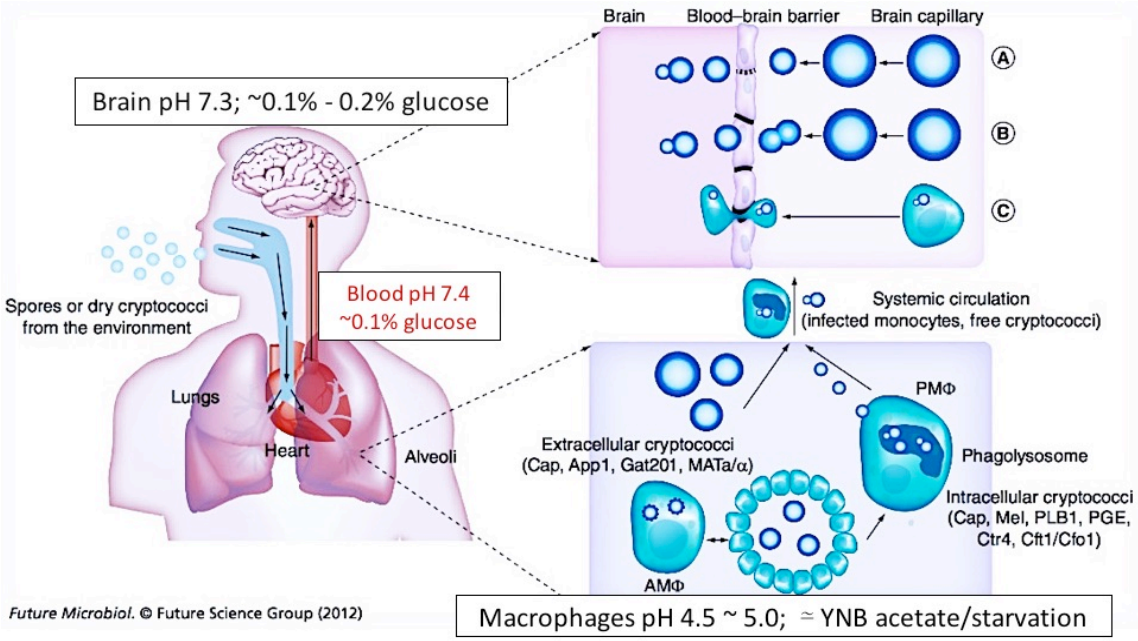

Figure 1-1: Pathogenesis of *Cryptococcus neoformans*. Dessicated cryptococcal cells or basidiospores are inhaled. They reach the lungs during which transporters of alternative carbon sources such as acetate are upregulated (Mota et al., 2015) and can be contained in granuloma or get phagocytosed by alveolar macrophages which is a nutrient poor environment (Barelle et al., 2006; Lorenz et al., 2004), at a slightly acidic pH (Vylkova and Lorenz., 2014; Cox et al., 2003; Nyberg et al., 1992). When immunity is compromised, cryptococci can enter blood circulation and traverse the blood brain barrier by A) entry between endothelial cells; B) adhering to being internalized by brain microvascular endothelial cells (BMECs); or C) riding in parasitized macrophages (PMΦ) (Sabiiti and May, 2012). Blood glucose level is maintained at approximately 0.1 % (Güemes et al., 2016) and 0.1 % - 0.2 % in the brain (Gruetter et al., 1992) in a slightly alkaline pH (O'Meara et al., 2010). This figure was reproduced with minor edits from (Sabiiti and May, 2012) with permission from the *Future Microbiology* journal editor.

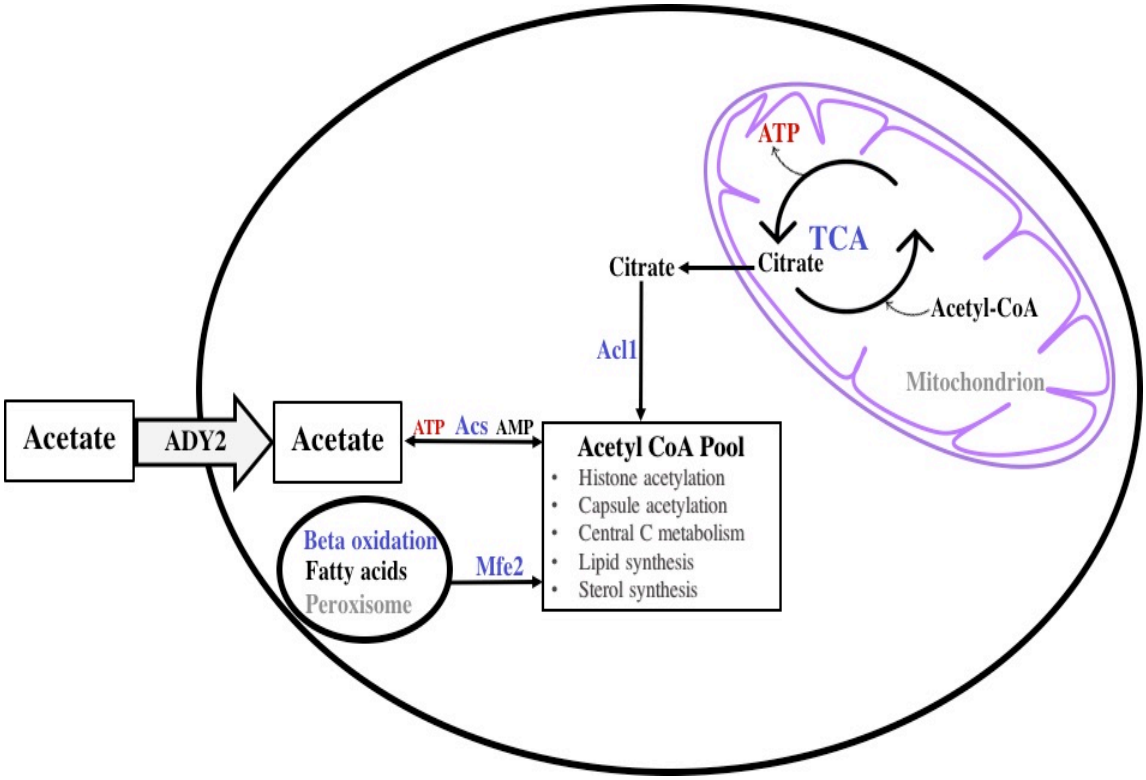

Figure 1-2: Acetate utilization in *Cryptococcus neoformans*. In eukaryotic cells, the pool of intracellular acetyl-CoA is essential for numerous cellular processes governed by histone acetylation and biosynthesis of various metabolic intermediates with energy potential. Cytosolic acetyl-CoA is mainly generated from beta-oxidation of fatty acids, oxidation of mitochondrial citrate by ATP-citrate lyase (Acl), and activation of acetate by AMP-forming acetyl-CoA synthetase (Acs). The *C. neoformans* acetate transporter, Ady2 is essential for facilitated uptake of deprotonated or low levels of acetate when present in nutrient-limiting condition (Dissertation Chapter 2).

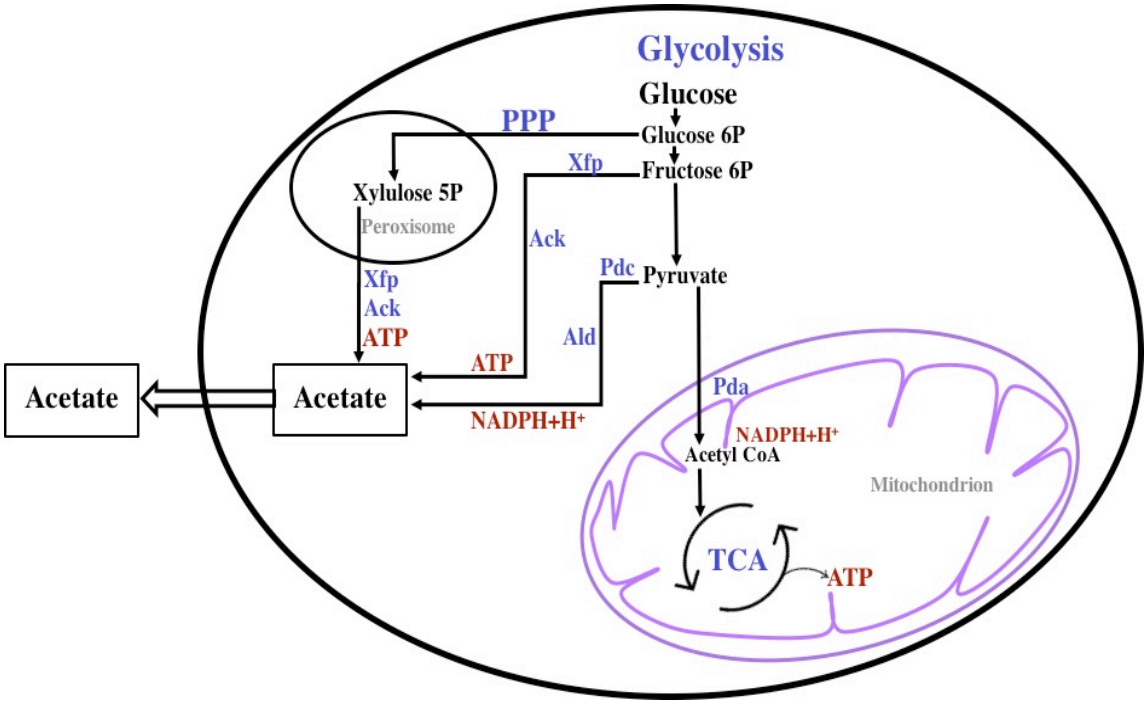

Figure 1-3: Acetate production in *Cryptococcus neoformans*. Metabolic fates of acetate in *C. neoformans*, *C. albicans* and *S. cerevisiae* are compartmentalized in the cytosol, peroxisome and the mitochondria (Idnurm et al., 2007; Kretschmer et al., 2012). Two of these consist of acetate kinase (Ack) partnering with xylulose 5-phosphate/fructose 6-phosphate phosphoketolase (Xfp) in a modification of the pentose-phosphate pathway (PPP) to produce acetate from ketose sugars with the formation of ATP (Ingram-Smith, et al., 2006). The third uses pyruvate decarboxylase and acetaldehyde dehydrogenase to decarboxylate pyruvate to acetaldehyde, which is then oxidized to acetate in the presence of $NADP^+$ (Hu et al., 2008).

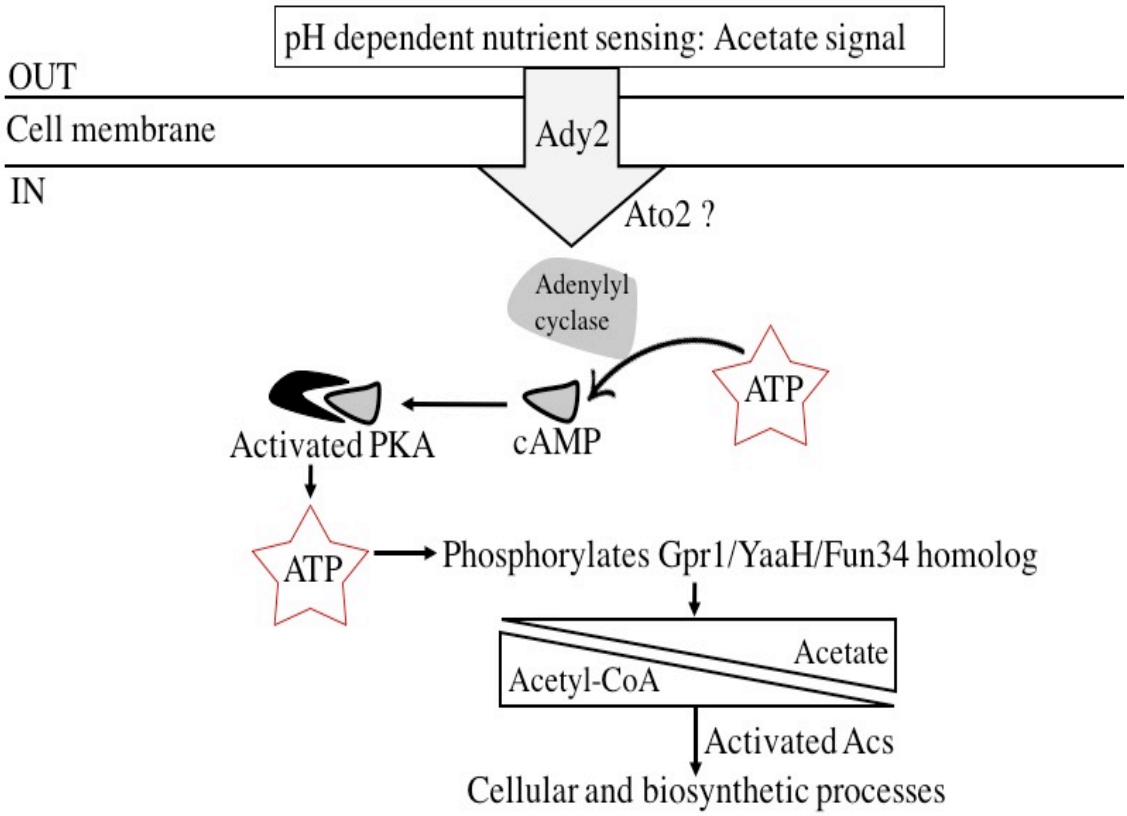

Figure 1-4: Role of acetate transporters in signaling cascade. This model suggests that Ady2 plays a role in pH dependent nutrient sensing in response to the acetate signal and interacts with the cAMP/PKA pathway responding to cellular levels of acetyl-CoA to regulate function of cellular and biosynthetic processes.

The role of *Cryptococcus neoformans* Ady2 and Ato2 in acetate transport

Grace N. Kisirkoi, Yijian Qiu, James Morris and Kerry S. Smith

Department of Genetics and Biochemistry

Eukaryotic Pathogens Innovation Center (EPIC)

Clemson University

Clemson, SC 29634

CHAPTER TWO

Abstract

The success of *Cryptococcus neoformans* as a pathogen is largely attributable to metabolic scavenging during starvation and mounting resistance to antifungals. Lung alveolar macrophages, which present a first line of host defense against *C. neoformans* infection provide a glucose- and amino acid-poor environment, and nonpreferred carbon sources such as lactate and acetate may be essential during initial pulmonary infection. Acetate transporters are required in fungi for the transport and subsequent utilization of acetate as a carbon source. While acetate transporters have been characterized in other fungi such as *Saccharomyces cerevisiae*, *Candida albicans*, *Aspergillus nidulans* and *Yarrowia lipolytica*, the role of acetate production and transport in *C. neoformans* is not well understood and its importance in infection has not been established. Putative acetate transporter genes, designated as *ADY2* and *ATO2*, from the Gpr1/Fun34/YaaH family have been identified in *C. neoformans* and are highly expressed during infection in the lung and during growth on acetate as sole carbon source. We propose that Ady2 and Ato2 have a role in acetate transport as a metabolic adaptation during starvation and stressful environmental conditions. Growth of the *ady2* mutant and the *ady2ato2* double mutant, but not the *ato2* mutant, was severely impaired when growing on 1 mM versus 10 mM acetate plates, suggesting that Ady2 is the essential acetate importer during growth on low acetate. Furthermore, *ADY2* was induced 137-fold during growth on acetate in relation to growth on glucose. The role of Ato2 during prolonged starvation was highlighted by diminished acetate uptake by the *ato2* mutant after glucose-grown cells

were passaged into minimal media with acetate as sole carbon source. This study also uncovered a role of Ady2 and Ato2 in ammonia export revealing they preferentially import acetate uninhibited by the presence of other carboxylates.

Introduction

Cryptococcus neoformans is an invasive basidiomycetous saprophytic yeast that annually infects one million people globally causing over 600,000 deaths (Park et al., 2009). While it largely co-occurs in sub-Saharan Africa among the immunocompromised, especially HIV/AIDs patients whose $CD4^+$ count has dropped below 100 cells/μL (Jarvis and Harrison, 2007; Kisenge et al., 2007), *C. neoformans* var *grubii* has been documented in the US (Pappas et al., 2001) and Asia (Lui et al., 2006) as having higher incidences among the immunocompetent than previously estimated. Var. *neoformans* (serotype A) on the other hand has higher incidences in France, Italy and Denmark (Franzot et al., 1999; Dromer et al., 1996; Tortorano et al., 1997), causing 20-30 % of cryptococcal meningitis cases among HIV/AIDs patients. Spores and desiccated yeast cells are *C. neoformans*' infectious agents. They occur ubiquitously in the environment following aerosolization from bird guano, decomposing organic substances, and soil (Sanfelice, 1894; Velagapudi et al., 2009). Relevant mammalian hosts can inhale aerosolized spores or dried yeast cells, developing initial pulmonary infection with a predilection to the brain (Sabiiti and May, 2012; Velagapudi et al., 2009). Metabolic adaptability and flexibility are important attributes for fungal pathogens to successfully infect and cause disease.

Although carbon metabolism is critical for virulence in *C. neoformans* (Price et al., 2011), very little is known about which carbon sources are utilized during infection. Serial analysis of gene expression study of cryptococcal cells during murine lung infection revealed elevated expression of genes involved in acetyl-CoA utilization (Hu et al., 2008), implying that acetate is utilized as a carbon source during infection. Among

the genes identified were *ADY2* (CNAG_05678) and *ATO2* (CNAG_05266), encoding homologs of Gpr1/Fun34/YaaH family of acetate transporters, and *ACS*, encoding acetyl-CoA synthetase that catalyzes the activation of acetate to acetyl-CoA (Hu et al., 2008). A *C. neoformans acs* knockout mutant was unable to utilize acetate, glycerol, and ethanol as carbon sources but did not have a phenotype with respect to capsule or melanin formation, known *C. neoformans* virulence factors (Hu et al., 2008). However, survival of mice infected with this strain was prolonged as compared to the wild type strain, but ultimately the mice did succumb to the infection. These findings point to an involvement of acetate metabolism during pathogenesis of *C. neoformans*. However, the role of Ady2 and Ato2 in *C. neoformans* metabolism and virulence has not been reported.

Here, we report the characterization of Ady2 and Ato2 in *C neoformans* and provide experimental evidence of the function of Ady2 as a high affinity, substrate specific acetate importer whose expression is induced by acetate. We profile substrate requirements of Ady2 and Ato2 to suggest that Ady2 is required for acetate uptake during growth on low acetate while Ato2 is required during prolonged starvation in low acetate. Ady2 transcript levels are increased ~2.5-fold during fluconazole treatment (Kim et al., 2015) leading us to hypothesize a possible role of Ady2 and Ato2 in membrane integrity and susceptibility to fluconazole. On the other hand, these proteins are not required for acetate export, suggesting that there may be another transporter or mechanism to export deprotonated acetate out of the cell when necessary. We also rule out roles of acetate transporters in membrane integrity or fluconazole susceptibility under the conditions tested.

Materials and methods

Cryptococcus neoformans strains

Individual and double knockouts of *ADY2* and *ATO2* were kindly provided by the Kronstad Lab. Independently created mutants of *ADY2* and *ATO2* from the Madhani collection (Jung et al., 2015) were checked for the same phenotypes as mutants obtained from the Kronstad Lab. A cross between the double mutant and the wild type of the opposite mating type-KN99a was set up and single mutant strains obtained from this cross were confirmed to have lost the distinguishing phenotypic traits of the double mutant. In order to achieve this, an equivalent of OD 600 = 2.0 of wild type KN99 (mating type a) was pelleted and mixed with the same inoculum size of *ady2ato2* (mating type α), resuspended in 500 μL of sterile nanopure water then spotted onto Murashige and Skoog (MS) medium (4.3 g/L Murashige and Skoog basal salt mixture from Sigma-Aldrich, 1 mL/L of 1000x Murashige and Skoog vitamin solution from Sigma-Aldrich, filter sterilized, mixed with 4 % sterile agar and adjusted to pH 5) and left to sporulate in the dark for two weeks at ambient temperature. Resulting spores from this cross were patched onto YPD containing 100 μg/mL neomycin or nourseothricin.

To select progeny that had undergone homologous recombination thus regaining *ADY2* or *ATO2* to become single mutant *ato2* or *ady2* strains respectively, we genotyped spores and the parental strains. To do this, we confirmed that the wild type KN99a had wild type *ADY2* and *ATO2* and was susceptible to both neomycin (Neo^S) and nourseothricin (Nat^S) and could grow on yeast nitrogen broth (YNB; Difco™) supplemented with 0.2 % acetate. We also confirmed that mutants lacking *ADY2* or

ATO2 had instead neomycin resistance (Neo^R) or nourseothricin resistance (Nat^R) and thus could grow in the presence of 100 μg/mL of respective antibiotics when included in yeast extract peptone dextrose (YPD) media. We also distinguished the Nat^R *ato2* from the Neo^R *ady2* and the *ady2ato2* strains due to a requirement of *ADY2* during growth on YNB supplemented with 0.2% acetate. Similarly, the *ato2* mutant strain regenerated from this cross replaced the parental strain's (*ady2ato2*) Neo^R property with a functional *ADY2* as evidenced by a regained ability to grow to wild type levels on YNB supplemented with 0.2 % acetate while still maintaining its Nat^R in place of the *ATO2* open reading frame (ORF). Further to these phenotypes, primers that amplified *ADY2* and *ATO2* confirmed the presence of the *ADY2* and the absence of *ATO2* ORFs in the newly generated Nat^R *ato2*; as well as the presence of *ATO2* and the absence of *ADY2* ORFs in the Neo^R *ady2* cross progeny.

Growth in various carbon sources

Overnight cultures of individual and double mutants lacking *ADY2* and *ATO2* along with their wild type background (H99) were washed twice by pelleting 1 mL of culture in the same volume of sterile nanopure water, centrifuged at 3000 x g then resuspended in sterile nanopure water at an OD 600 of 0.2. Their cell densities were then confirmed by a hemocytometer. These strains were grown in liquid YNB supplemented with 10 mM glucose, 60 mM acetate and 6 mM acetate. In addition, four 10-fold serial dilutions were spotted in minimal media, YNB agar supplemented with glucose, galactose, xylose, lactate, pyruvate, glycerol, ethanol, propionate, butyrate and acetate then incubated at 30ºC. The plates were incubated observed once every 24 hours. These

studies were performed in independent triplicates and data presented as mean ± the standard deviation were plotted using JMP® Pro 12.1.0 software and significant P values determined by comparing individual mutants to the wildtype H99 using the unpaired t test (GraphPad 7, Inc.).

Measuring [^{14}C] acetate uptake

The strains H99, *ady2*, *ato2* and *ady2ato2* were grown in liquid YPD cultures to an OD 600 of 1.0 at 30ºC then washed thrice in sterile nanopure water and resuspended to a final concentration of $1x10^5$ cells/µL in 100 µL of sterile nanopure water. Following a ten-minute incubation at 37ºC, 5 µL of 750 mM, 500 mM, 250 mM and 50 mM of unlabeled sodium acetate spiked with labeled sodium acetate (pH 5) in the ratio: 40 mM unlabeled sodium acetate to 1mM labeled sodium acetate ([^{14}C] acetate sodium salt solution of specific activity 59 mCi/mmol; American Radiolabelled Chemicals) was added to the cells homogenously. This reaction was incubated at 37ºC for 5 minutes. At 5 minutes, 1 mL of sterile ice cold nanopure water was immediately added to the cells to stop the uptake reaction followed by three washes using cold sterile nanopure water through a Vacuum filtration manifold, Millipore® model 1225 through Whatman filter papers. These washes alleviated trapping of extracellular [^{14}C] acetate between cells in suspension and resolved signal to noise ratio. The filter papers were left to air dry and inserted into scintillation vials after which 5 mL of scintillation fluid was added. Radioactivity was quantified using a Beckman LS 6000 liquid scintillation counter.

Measuring acetate export and media alkalinization

The strains H99, *ady2*, *ato2* and *ady2ato2* were grown overnight in YPD and subcultured into YNB supplemented with 2 % glucose, 0.2 % glucose for 20 hours; and 0.5 % acetate for 20 hours to a cell density of 100,000 cells/μL. At the respective time points, 500 μL of the cell suspension was pelleted and 225 μL of the cell lysate was collected and used to perform the hydroxamate assay as described by (Aceti and Ferry., 1988). To generate a standard curve from which to derive concentrations of acetate, the assay was first performed on standard concentrations of acetate ranging from 0.1 mM-50 mM. The hydroxamate reaction mixture used consisting of 0.4 M Tris at pH 7.5, 80 mM $MgCl_2$, 2.4 M hydroxylamine, and 90 uM ATP disodum salt hydrate was constituted. Of this reaction mixture 75 μL was mixed with 225 μL of the standard solution to the desired concentration of acetate, or 225 μL of respective culture supernatant's filtrate. The mixture was agitated thoroughly to ensure mixing after which it was incubated for 5 minutes at 37ºC. *Methanosarcina thermophila* acetate kinase (Ack) was added to the reaction to a concentration of 0.023 ng/μL, homogenously mixed and incubated at 37ºC for 15 minutes. At the 15-minute time point, the reaction was stopped with a 1:1 ratio of 20 % trichloroacetate and $FeCl_3$. The absorbance was read at 540 nm by a spectrophotometer with a monochromator set at 1 nm bandwidth.

To detect media alkalinization due to ammonia (NH_3) export, growth on GM-BCP agar containing glycerol, yeast extract, and the pH indicator bromocresol purple and adjusted to pH 3.3 was used to detect media alkalinization. 1 mL cultures of H99, *ady2*, *ato2*, and *ady2ato2* grown overnight at 30ºC were collected and washed twice with sterile

nanopure water before resuspending in 1 mL of sterile nanopure water to an OD 600 of 0.2. Homogenous cell density across the strains was then confirmed by hemocytometer. Four 10-fold serial dilutions of these cells were spotted onto this GM-BCP agar to determine media alkalinization and on YNB supplemented with 100 mM ammonium sulfate to investigate a converse role of Ady2 and Ato2 in ammonia export.

Gene expression of *ADY2*, *ATO2* and *ATO3* during growth on acetate versus growth on glucose

We measured the expression of three putative acetate transporters- *ATO3* (CNAG_04787), *ADY2* (CNAG_05678) and *ATO2* (CNAG_05266) in order to determine their induction in response to acetate, relative to the preferred carbon source, glucose. The wild type H99 was grown in an overnight YPD starter culture at 30ºC after which they were washed thrice in sterile nanopure water. Cells were resuspended to an OD 600 of 0.05 and allowed to grow for 20 hours on YNB supplemented with 0.5 % acetate, and YPD. Total RNA was isolated according to the specifications of Aurum™ Total RNA Mini Kit (Bio-Rad™). Quantitative RT-PCR (RT-qPCR) was performed according to the specifications of the Verso 1-step RT-qPCR SYBR Green ROX kit (ThermoFisher). This kit allowed for one step conversion of RNA to cDNA and further cycles to amplify the target relative to its abundance using the program: 1 cycle of cDNA synthesis at 50ºC for 15 minutes, 1 cycle of Thermo-Start polymerase activation at 95ºC for 15 minutes, then 40 cycles of denaturation at 95ºC for 15 seconds, annealing at 60ºC for 30 seconds and extension at 72ºC for 30 seconds. The reference gene to which relative abundance of target gene transcripts was normalized was *UBC6* (CNAG_05765) because its expression

remained highly stable during more than thirty different metabolic growth conditions conditions (Llanos et al., 2015).

The internal control gene used was actin (*ACT1*; CNAG_00483) as 18srRNA (CNAG_10502) was not utilized after we observed its differential regulation under variable conditions (data not shown). Data were analyzed using $2^{\Delta\Delta CT}$ n to determine expression fold change relative to the reference gene as described by Schmittgen TD and Livak KJ., 2008. This double delta Ct method compares the number of RT-qPCR cycles completed before a fluorescent signal crosses the background noise's threshold, that is the Cycle threshold (Ct) values. Hence the smaller the Ct value, the more abundant the target nucleic acid. We used the comparative delta Ct method to contrast up/downregulation of *ADY2*, *ATO2* and *ATO3*, our target genes, relative to *UBC6*, the reference control gene whose expression must not change regardless of experimental manipulations. The *ACT1* gene, our internal control of relative gene expression, was compared against the reference gene, *UBC6* as a quality check. Ct values of *ADY2, ATO2,* and *ATO3* against *UBC6* were presented in the form of fold change of gene expression in YNB supplemented with 0.5 % acetate, relative to fold change of gene expression in nutrient rich YPD, which contains 2 % glucose.

Predicting Ady2 and Ato2 membrane topology and examining cell wall and membrane stress

Predictions of the membrane topologies of *C. neoformans* Ady2 and Ato2 were performed by inserting amino acid sequences of Ady2 and Ato2 into the user interface of Protter. Using protein topology information, annotation, proteolytic peptides and

experimental proteomics data from Uniprot, Phobius, PeptideCutter and such databases as PeptideAtlas, consensus structural and feature predictions were performed (Omasits, et al., 2013)

To examine whether loss of Ady2 and Ato2 resulted in increased susceptibility to cell wall and membrane stressors, 1 mL cultures of H99, *ady2*, *ato2*, and *ady2ato2* grown overnight at 30 ºC were collected and twice washed with sterile nanopure water before resuspending the cells in 1 mL of sterile nanopure water to an OD 600 of 0.2. The cell density was then confirmed by hemocytometer. Four 10-fold serial dilutions were spotted onto YPD plates containing the membrane destabilizing agents, SDS and the cell wall stressor, Congo red at a concentration of 1 mg/mL. These plates were incubated at 30ºC and observed once every 24 hours.

Investigating susceptibility to fluconazole

The role of Ady2 and Ato2 during fluconazole treatment was investigated by subjecting null mutants and wild type *C. neoformans* to fluconazole. This was accomplished by first growing the H99, *ady2, ato2,* and the *ady2ato2* strains overnight in YPD at 30ºC. Cell pellets equivalent from these overnight cultures were collected and washed twice by centrifugation in sterile water before resuspension to the same volume at an OD 600 of 1.0. Using a hemocytometer, 100-fold dilutions of the strains were counted to confirm equal cell counts. These strains were inoculated to an OD 600 = 0.2 into liquid YNB media supplemented with 0.2 % glucose containing either no fluconazole (control environment) or varying concentrations of fluconazole (8 μg/mL, 15 μg/mL, 25 μg/mL and 35 μg/mL). Equal cell densities of the strains were ascertained by counting using a

hemocytometer. Relative growth inhibition was observed after 16 hours of incubation at 30ºC by comparing the OD 600 values of the different strains in varying concentrations of fluconazole against their respective control strain growing in YNB 0.2 % glucose lacking any fluconazole. Growth curves of were also performed in YNB supplemented with 0.2 % glucose containing 8 μg/mL fluconazole and compared to growth in the absence of fluconazole to determine statistical significance by ANOVA (GraphPad 7, Inc.).

Results

Role of Ady2 and Ato2 during carbon source utilization following acetate uptake

To examine whether Ady2 or Ato2 influences carbon source utilization, the wildtype, *ady2*, *ato2*, and *ady2ato2* strains were grown on media containing a variety of carbon sources. There was no requirement of *ADY2* or *ATO2* when *C. neoformans* cells were grown on YPD, YNB supplemented with 2 % glucose, 2 % galactose, 2 % acetate, 2 % glycerol, 2 % ethanol, or 2 % xylose (**Figure 2-1a**). While both wild type and mutant *C. neoformans* strains displayed robust growth on 10 mM glucose (~0.2 %) (**Figure 2-1b**), the cells lacking Ady2 had a slight growth defect on 10 mM acetate but not during growth (**Figure 2-1b**). This phenotype was exaggerated when the acetate concentration was dropped 10-fold, such that *ady2* mutant did not grow (**Figure 2-1b**). The *ato2* mutant did not display any observable growth defect under these conditions. Neither 10 mM propionate nor 10 mM butyrate supported growth of *C. neoformans* wildtype and mutant strains while 10 mM pyruvate and 10 mM lactate supported slight growth of *C. neoformans* but there was no requirement for *ADY2* or *ATO2* (**Figure 2-1b**).

Liquid media was able to highlight a contribution of Ato2 in carbon source utilization because *ato2* cells while they grew to wildtype levels in plate media, their growth diminished relative to wildtype in liquid cultures. Although both the wild type and mutant strains thrived in 10 mM glucose, loss of Ady2 and Ato2 additively diminished growth as demonstrated by the slightly slower growth of the individual mutants and even slower growth of the double mutant (**Figure 2-2**). Similarly, during

growth on the relative high acetate concentration of 60 mM (0.5 %) contained in liquid YNB cultures, all wild type and mutant *C. neoformans* thrived but *ady2* and *ato2* single mutants lagged slightly relative to wild type H99. Absence of Ady2 and Ato2 in the double mutant led to additively slower growth (**Figure 2-3**). Upon reducing the acetate concentration 10-fold in the liquid YNB cultures, the requirement for Ady2 was further pronounced such that both the single mutant lacking Ady2 and the double mutant lacking Ady2 and Ato2 had an exaggerated growth defect. Moreover, cells lacking Ato2 had a slight defect under these conditions. There was no additive effect from loss of both Ady2 and Ato2 in the *ady2ato2* strain (**Figure 2-4**).

For our gene expression studies, we were able to extend our scope of investigations to include *ATO3* in addition to *ADY2* and *ATO2* since it is also classified under the Gpr1/Fun34/YaaH superfamily of acetate transporters and its role in acetate transport has not been characterized. Unlike *ADY2* and *ATO2*, transcripts of *ATO3* were not elevated during mouse infection (Hu et al., 2008), hence we had not included *ato3* strains in growth studies to characterize *ady2* and *ato2*. To do this, we investigated the expression fold change of *ADY2, ATO2,* and *ATO3* in response to the alternative carbon source acetate relative to the preferred carbon source glucose. After 20 hours of culture, we found expression of *ADY2* was highly pronounced in 60 mM acetate relative to 100 mM glucose (137:1). The expression fold change of *ATO2* in 60 mM acetate relative to 100 mM glucose was slightly increased to the ratio of 1.91:1, while that of *ATO3* did not change (**Figure 2-5**).

Role of Ady2 and Ato2 in acetate uptake

To investigate the roles of Ady2 and Ato2 in acetate uptake, we incubated the wildtype, *ady2*, *ato2*, and *ady2ato2* strains with a 40:1 concentration of unlabeled to labeled acetate. We found that absence of Ady2 eliminated transport of acetate (**Figure 2-6**). The growth defect we observed when *ady2* and *ady2ato2* strains were growing on 6 mM acetate also coincided with the requirement of Ady2 for facilitated acetate uptake when glucose grown *C. neoformans* cells were incubated with a 40:1 homogenous mixture of unlabeled acetate to labeled acetate at varying concentrations (**Figure 2-4, Figure 2-6**). However, upon growing *C. neoformans* in acetate for 20 hours and then performing the acetate uptake assay, there was a requirement for both Ady2 and Ato2 for facilitated uptake of acetate demonstrated by the wild type H99 consistently having higher acetate uptake rates (**Figure 2-7**).

To examine the substrate specificity of Ady2 and Ato2, we performed competition experiments with the carboxylic acids propionate, butyrate, pyruvate, and lactate. During these conditions, Ady2 and Ato2 were also specific to acetate import as acetate uptake rates were not diminished by substituting unlabeled acetate with alternative carbon sources (**Figure 2-7**). We investigated whether acetate uptake would change in the presence of NH_3, due to a possible role of acetate transporters in acetate::NH_3 symport. We found that the presence of NH_3 during acetate uptake did not alter this pattern either (**Figure 2-7**).

Role of Ady2 and Ato2 in acetate export

We sought to investigate the roles of Ady2 and Ato2 in acetate export because acetate is the most abundant metabolite recovered in culture supernatants during growth in glucose (Bubb et al., 1999), and has been identified as the most abundant metabolites in brain tissues of infected rats (Himmelreich et al., 2003). When provided with 2 % and 0.05 % glucose, *C. neoformans* cells were able to utilize it and produce acetate that was detected in the extracellular environment of the culture supernatant after 20 hours of culture. However, we observed that loss of Ady2 and Ato2 did not impact acetate export when *C. neoformans* cells were growing in 2 % and 0.05 % glucose as there was no significant difference between acetate in the supernatant of the wild type and mutant *C. neoformans* strains ($P > 0.05$). (**Figure 2-8**). The hydroxamate assay correlation between the concentration of known standards and the assay 540nm absorbance signal between the ranges of 0.1 mM-2.0 mM (**Figure 2-9a**) beyond which the linear relationship was lost as the reaction rate slowed with increasing substrate (**Figure 2-9b**).

We investigated a possible role of acetate transporters in media alkalinization due to a likely excretion of NH_3 during culture and saw that Ady2 and Ato2 additively contributed to extracellular environment alkalinization by NH_3 export but were not required for NH_3 uptake (**Figure 2-9**). While the wild type and single mutants of Ady2 and Ato2 were able to alkalinize GM-BCP (adjusted to pH 3.3) containing glycerol, yeast extract, and the pH indicator bromocresol purple, the double mutant lacking both proteins was defective in extracellular environment alkalinization. Both Ady2 and Ato2 interacted to alkalinize the yellow acidic GM-BCP resulting in a purple hue around the colony

where the media had been alkalinized. This defect was not translated to the uptake of NH_3 as loss of Ady2 and Ato2 did not diminish ability to utilize minimal media supplemented with 100 mM ammonium sulfate, they all grew albeit slightly (**Figure 2-10**).

Role of Ady2 and Ato2 in adapting to cell wall and fluconazole antifungal stress

Using the program, Protter (Omasits et al., 2013) *C. neoformans* Ady2 and Ato2 were predicted to have six hydrophobic transmembrane proteins, as well as hydrophilic N and C termini that are intracellular in Ady2 but extracellular in Ato2. Since *C. neoformans* Ady2 and Ato2 are predicted to span the cryptococcal membrane multiple times, (**Figure 2-11a and Figure 2-11b**), we investigated whether the acetate uptake defect in mutants lacking Ady2 was a factor of compromised membrane integrity using the membrane perturbing agent SDS and the cell wall stressor, Congo red. We found that the loss of Ady2 or Ato2 did not differentially enhance susceptibility to SDS. Liquid media supplemented with 10 mM glucose and 1 mg/mL SDS enabled relative comparison of susceptibility of the wild type against mutants lacking Ady2 and Ato2. Comparing growth of a strain in SDS free media against 1 mg/mL SDS containing media allowed for distinguishing the effect of SDS from the growth phenotype due to carbon source requirement of the mutant strains. While SDS inhibited growth, the trend was consistent with growth rate during growth on 10 mM glucose lacking SDS but not differential susceptibility of mutants to SDS (**Figure 2-12a**). There was no growth defect during plate

spot assays of 1 mg/mL Congo red stress despite the cells having assimilated the toxic stain to appear as pink colonies (**Figure 2-12b, Figure 2-12c**).

To explore a possible link between acetate transport and fluconazole resistance, we determined the relative susceptibilities of H99, *ady2, ato2* and *ady2ato2* in the presence of fluconazole. We compared effects of growth over time in YNB containing 0.2 % glucose and 8 μg/mL fluconazole contrasted to corresponding growth rate in the absence of fluconazole (**Figure 2-13a**). While 8 μg/mL of fluconazole diminished *C. neoformans* growth, there was no differential susceptibility between the strains ($P>0.05$). We also determined growth differences of H99, *ady2, ato2* and *ady2ato2* in varying fluconazole concentrations compared to corresponding strains lacking fluconazole. Thus we revealed an overall susceptibility of *C. neoformans* to fluconazole but not enhanced or diminished by the loss either one or both of Ady2 and Ato2 (**Figure 2-13b**).

Discussion and conclusions

We hypothesized that Ady2 and Ato2 are essential for facilitated acetate uptake during carbon source poor conditions, especially to import charged deprotonated acetate. This is because conserved homologs of acetate transporters in other fungi have been implicated in acetate transport. An *ADY2* homolog in *S. cerevisiae* was essential for permease activity in uptake of acetate and lactate (Pacheco et al., 2012) and was upregulated following a switch from glucose-rich medium to a nutrient-poor medium supplemented with acetate (Paiva et al., 2004) or during stationary phase after growing in nutrient-rich media (Gasch et al., 2000). Our findings indicated that *ADY2* was selectively essential for growth of *C. neoformans* on acetate but was not required for growth on other carbon sources (**Figure 2-1, Figure 2-2**).

When acetate was increased to 60 mM in liquid media, the ability of the *ady2* and *ato2* mutants to grow to wild type levels (**Figure 2-3**) suggests that passive diffusion is sufficient in the absence of these transporters. However, the slight growth defect experienced by the *ato2* mutant strain during growth on minimal liquid media supplemented with 6 mM acetate (**Figure 2-4**) suggests a role for this transporter in very low acetate concentration. The severity of the phenotype of relative ability to grow on acetate was also reflected in the intensity of upregulation during growth on 60 mM acetate for 20 hours such that *ADY2* was upregulated dramatically while *ATO2* was slightly upregulated (**Figure 2-5a**). The requirement for Ady2 but not Ato2 during initial acetate uptake rates following *C. neoformans* growth on glucose was also confirmed with the dramatic upregulation of *ADY2* during growth on acetate but not glucose (**Figure 2-5,**

Figure 2-6).

However, upon passaging *C. neoformans* from glucose rich YPD (~100 mM glucose) into 20 hours of incubation in minimal YNB supplemented with 60 mM acetate before radiolabeled acetate uptake assays, a contribution of Ato2 was also demonstrated (**Figure 2-7**). These suggested that Ato2 plays a role in adaptation to prolonged exposure to starvation conditions. Effects of these mutations was reminiscent of observations in *A. nidulans* such that upon loss of the acetate permease AcpA, an Ady2 ortholog, there was a growth defect on acetate as a sole carbon source especially at higher pH of 6.8 and 8 when acetate was deprotonated, hence charged and unable to diffuse through the membrane (Robellet et al., 2008), suggesting that a transporter would be required for utilization of acetate as a sole carbon source at physiological pH of ~7. Moreover, this gene was induced by low acetate in *S. cerevisiae* and cells lacking Ady2 abolished saturable, mediated radiolabeled acetate uptake and could only take up acetate by diffusion (Paiva et al., 2004). Furthermore, amino acid substitutions in the N-terminus of *Y. lipolytica* Gpr1p induced sensitivity to protonated acetate but deletion of its complete ORF had no effect, leading to the hypothesis that this protein is involved in adaptation to acetate (Gentsch et al., 2007).

The function of acetate transporters has also been observed in bacteria and archaea. *Escherichia coli* has two acetate transporters that contribute to utilization of acetate as a sole carbon source: YaaH, which is specific to acetate and succinate, and ActP, a member of the Sodium:Solute Symporter Family (Saier et al., 2006, http://www.tcdb.org) that is highly specific for short chain aliphatic monocarboxylates

such as acetate, glycolate and propionate (Sá-Pessoa et al., 2013). Deletion of the genes encoding both ActP and YaaH was necessary to abolish acetate uptake (Sá-Pessoa et al., 2013). In *Methanosarcina acetivorans*, the gene MA4008 was highly expressed during growth on acetate versus methanol as a carbon and energy sources along with the genes encoding acetate utilizing enzymes, acetate kinase and phosphotransferase (Rohlin and Gunsalus, 2010).

An exploration into the substrate preferences of Ady2 and Ato2 indicated that Ady2 was specific for acetate. This is unlike the *A. nidulans* homolog, AcpA which was found to also transport short chain carboxylates albeit with lower efficiency, in addition to acetate such that these carboxylates competed with a diminished acetate uptake (Sá-Pessoa et al., 2015). While Ady2 mutants are severely defective in acetate uptake at low concentrations, they were still able to export acetate in conditions in which acetate was produced, indicating no apparent role of Ady2 in acetate export (**Figure 2-8**). Similarly, Ato2 was also not required for acetate export. However, the neutral intracellular pH, which is above the pKa of acetate, implies that intracellular acetate will exist in its deprotonated form and will require a dedicated transporter to export through the phospholipid bilayer of the cell wall since passive diffusion of a charged molecule would not be possible. Seeing that neither Ady2 nor Ato2 are required for acetate export, we hypothesize that yet another protein may be performing this task and efforts are underway to characterize Ato3, a third member of the Gpr1/Fun34/YaaH family in *C. neoformans*.

Acetate concentrations recovered in the culture supernatants fell between the linear range (0.1 mM-2.0mM) of the calibration curve which we used to correlate to hydroxamate assay absorbance signal (**Figure 2-9a**). Beyond 2 mM - 50 mM acetate, the linear relationship was lost as the *Methanosarcina thermophila* Ack became saturated resulting in slowed reaction rates (**Figure 2-9b**). Consistent with the findings of Vylkova et al., (2011) in *C. albicans*, the *C. neoformans* Ady2 and Ato2 were able to alkalinize the extracellular microenvironment from pH 3.3 to a more habitable neutral pH but deletion of both proteins caused a defect in pH alkalinization (**Figure 2-10**). This suggested that Ady2 and Ato2 compensate for each other and work in synchronously to alkalinize their environment such that a double mutation but not loss of one homolog impacts their pH homeostatic function. Efforts are underway to further characterize the mechanisms of this function by gene localization and expression. Since mutants lacking Ady2 and Ato2 were still able to grow on YNB plates containing 100 mM ammonium sulfate (**Figure 2-10**), it is hypothesized that the threshold at which Ady2 and Ato2 could be required for ammonium uptake had not been reached at this concentration. These observations also implied that the cell's ammonium needs may be adequately fulfilled through uptake of complexed ammonia, such as amino acids-which are present in YNB.

Since these proteins are predicted to span the cryptococcal membrane six times (**Figure 2-11a and Figure 2-11b**), we investigated whether the inability to take up acetate by null mutants of Ady2 was a factor of compromised membrane integrity and fluconazole resistance. Moreover, acetyl-CoA, a product of acetate metabolizing enzymes is a precursor for ergosterol synthesis and Ato homologs in *S. cerevisiae* were found to

localize to detergent resistant membranes enriched in ergosterol (Řičicová et al., 2007), the target of fluconazole. However, we found no differential susceptibility of the mutants to cell wall stressors (**Figure 2-12**) suggesting that there is no appreciable membrane damage associated to loss of these proteins under the conditions tested. Consequently, observed defects in growth may be isolated to the function of these proteins rather than a non-specific compromisation of the cell wall through which acetate transport would occur.

We also tested the susceptibility of the mutants when exposed to the cell wall and membrane damaging agents Congo red and SDS. The detergent properties of SDS cause it to solubilize membrane bilayers while Congo red interacts with cell wall beta-linked glucans *in vitro* and could bind nascent chitin chains causing inhibition of assembly of enzymes which polymerize chitin and beta-glucan resulting in a weakened cell wall (Ram and Klis et al., 2006). The ubiquitous occurance of fungal beta glucan, chitin and membrane lipid bilayers may have resulted in an overall similar effect to the cell walls of the H99, *ady2, ato2,* and *ady2ato2* strains. However, it is possible that the cell wall ultrastructure may have been differentially affected by loss of Ady2 or Ato2, and detailed analysis of cell wall ultrastructure through electron microscopy techniques may reveal inapparent cell membrane and cell wall damage.

Since acetate is a precursor for ergosterol synthesis, an essential target of such antifungal azoles as fluconazole, we hypothesized that loss of acetate transporters could enhance susceptibility to fluconazole. As conditional and differential gene overexpression are believed to highlight an organism's vulnerabilities when in such dynamic

environments as carbon source switches and antimicrobial agents, a potential role of Ady2 in fluconazole resistance was highlighted by its approximate 2.5-fold upregulation during fluconazole treatment (Kim et al, 2015). Furthermore, Vanden Bossche et al., (1992) found that the fluconazole resistant *C. glabrata* isolate (B57149) had a higher [^{14}C] acetate uptake rate and 50 % growth inhibition was not reached after 24 hours of incubation with high concentrations of fluconazole (100 μM).

We therefore hypothesize that during the conditions under which acetate uptake is essential, loss of function of Ady2 and Ato2 would enhance susceptibility to fluconazole due to diminished ergosterol formation. Nevertheless, under the conditions tested in this study of growth curve in 0.2 % glucose supplemented with 8μg/mL fluconazole (**Figure 2-13a**), and comparison of differential growth inhibition by 8μg/mL, 15 μg/mL fluconazole and 35 μg/mL fluconazole (**Figure 2-13b**), there was no differential susceptibility to fluconazole in the wild type versus the mutant strains (**Figure 2-13a** and **Figure 2-13b**). However, all strains wee uniformly susceptible to all fluconazole concentrations, suggesting that Ady2 and Ato2 do not result in enhanced susceptibility to fluconazole under the conditions tested. These findings do not however rule out a potential role of acetate transport and overall metabolism in fluconazole resistance. During growth on glucose, the acetate transporters are not essential, and intracellular acetyl-CoA levels may still be enough to support sufficient ergosterol synthesis such that differential susceptibility to fluconazole is not apparent. We are further characterizing the roles of Ady2 and Ato2 in fluconazole resistance during conditions highlighted in this study.

References

Aceti DJ and Ferry JG, 1988. Purification and characterization of acetate kinase from acetate-grown *Methanosarcina thermophila*. Evidence for regulation of synthesis. *Journal of Biological Chemistry*, **263:**15444-15448.

Bubb WA, Wright LC, Cagney M, Santangelo RT, Sorrell TC and Kuchel PW, 1999. Heteronuclear NMR studies of metabolites produced by *Cryptococcus neoformans* in culture media: identification of possible virulence factors. *Magnetic Resonance in Medicine*, **42:**442-453.

Dromer F, Mathoulin S, Dupont B, Letenneur L, Ronin O and French Cryptococcosis Study Group, 1996. Individual and environmental factors associated with infection due to *Cryptococcus neoformans* serotype D. *Clinical Infectious Diseases*, **23:**91-96.

Franzot SP, Salkin IF and Casadevall A, 1999. *Cryptococcus neoformans* var. grubii: separate varietal status for *Cryptococcus neoformans* serotype A isolates. *Journal of Clinical Microbiology*, **37:**838-840.

Gasch AP, Spellman PT, Kao CM, Carmel-Harel O, Eisen MB, Storz G, Botstein D and Brown PO, 2000. Genomic expression programs in the response of yeast cells to environmental changes. *Molecular Biology of the Cell*, **11:**4241-4257.

Gentsch M, Kuschel M, Schlegel S and Barth G, 2007. Mutations at different sites in members of the Gpr1/Fun34/YaaH protein family cause hypersensitivity to acetate in Saccharomyces cerevisiae as well as in *Yarrowia lipolytica*. *FEMS Yeast Research*, **7:**380-390.

Himmelreich U, Allen C, Dowd S, Malik R, Shehan BP, Mountford C and Sorrell TC, 2003. Identification of metabolites of importance in the pathogenesis of pulmonary cryptococcoma using nuclear magnetic resonance spectroscopy. *Microbes and Infection*, **5:**285-290.

Hu G, Cheng PY, Sham A, Perfect JR and Kronstad JW, 2008. Metabolic adaptation in *Cryptococcus neoformans* during early murine pulmonary infection. *Molecular Microbiology*, **69:**1456-1475.

Jarvis JN and Harrison TS, 2007. HIV-associated cryptococcal meningitis. *Aids*, **21:**2119-2129.

Jung KW, Yang DH, Maeng S, Lee KT, So YS, Hong J, Choi J, Byun HJ, Kim H, Bang S and Song MH, 2015. Systematic functional profiling of transcription factor networks in *Cryptococcus neoformans*. *Nature Communications*, **6:**1-14.

Kim H, Jung KW, Maeng S, Chen YL, Shin J, Shim JE, Hwang S, Janbon G, Kim T, Heitman J and Bahn YS, 2015. Network-assisted genetic dissection of pathogenicity and drug resistance in the opportunistic human pathogenic fungus *Cryptococcus neoformans*. *Scientific Reports*, **5:**8767.

Kisenge PR, Hawkins AT, Maro VP, Mchele JP, Swai NS, Mueller A and Houpt ER, 2007. Low CD4 count plus coma predicts cryptococcal meningitis in Tanzania. *BMC Infectious Diseases*, **7:**39.

Llanos A, François JM and Parrou JL, 2015. Tracking the best reference genes for RT-qPCR data normalization in filamentous fungi. *BMC Genomics*, **16:**1.

Lui G, Lee N, Ip M, Choi KW, Tso YK, Lam E, Chau S, Lai R and Cockram CS, 2006. Cryptococcosis in apparently immunocompetent patients. *Quarterly Journal of Medicine*, **99:**143-151.

Omasits U, Ahrens CH, Müller S, Wollscheid B, 2013. Protter: interactive protein feature visualization and integration with experimental proteomic data. *Bioinformatics,* **30:**884-886.

Pacheco A, Talaia G, Sá-Pessoa J, Bessa D, Gonçalves MJ, Moreira R, Paiva S, Casal M. and Queirós O, 2012. Lactic acid production in *Saccharomyces cerevisiae* is modulated by expression of the monocarboxylate transporters Jen1 and Ady2. *FEMS Yeast Research*, **12:**375-381.

Paiva S, Devaux F, Barbosa S, Jacq C and Casal M, 2004. Ady2p is essential for the acetate permease activity in the yeast *Saccharomyces cerevisiae*. *Yeast*, **21:**201-210.

Pappas PG, Perfect JR, Cloud GA, Larsen RA, Pankey GA, Lancaster DJ, Henderson H, Kauffman CA, Haas DW, Saccente M and Hamill RJ, 2001. Cryptococcosis in human immunodeficiency virus-negative patients in the era of effective azole therapy. *Clinical Infectious Diseases*, **33:**690-699.

Park BJ, Wannemuehler KA, Marston BJ, Govender N, Pappas PG and Chiller TM, 2009. Estimation of the current global burden of cryptococcal meningitis among persons living with HIV/AIDS. *Aids*, **23:**525-530.

Price MS, Betancourt-Quiroz M, Price JL, Toffaletti DL, Vora H, Hu G, Kronstad JW and Perfect JR, 2011. *Cryptococcus neoformans* requires a functional glycolytic pathway for disease but not persistence in the host. *MBio*, **2:**e00103-11.

Ram AF, Klis FM, 2006. Identification of fungal cell wall mutants using susceptibility assays based on Calcofluor white and Congo red. *Nature Protocols*. **1:**2253-6.

Řičicová M, Kučerová H, Váchová L and Palková Z, 2007. Association of putative ammonium exporters Ato with detergent-resistant compartments of plasma membrane during yeast colony development: pH affects Ato1p localisation in patches. *Biochimica et Biophysica Acta (BBA)-Biomembranes*, **1768:**1170-1178.

Robellet X, Flipphi M, Pégot S, MacCabe AP and Vélot C, 2008. AcpA, a member of the GPR1/FUN34/YaaH membrane protein family, is essential for acetate permease activity in the hyphal fungus *Aspergillus nidulans*. *Biochemical Journal*, **412:**485-493.

Rohlin L and Gunsalus RP, 2010. Carbon-dependent control of electron transfer and central carbon pathway genes for methane biosynthesis in the Archaean, *Methanosarcina acetivorans* strain C2A. *Bmc Microbiology*, **10:**62

Saier MH, Tran CV and Barabote RD, 2006. TCDB: The Transporter Classification Database for membrane transport protein analyses and information. *Nucleic Acids Research*, **34:**D181-D186 http://www.tcdb.org.

Sá-Pessoa J, Paiva S, Ribas D, Silva IJ, Viegas SC, Arraiano CM and Casal M, 2013. SATP (YaaH), a succinate–acetate transporter protein in *Escherichia coli*. *Biochemical Journal*, **454:**585-595.

Sá-Pessoa J, Amillis S, Casal M and Diallinas G, 2015. Expression and specificity profile of the major acetate transporter AcpA in *Aspergillus nidulans*. *Fungal Genetics and Biology*, **76:**93-103.

Sabiiti W and May RC, 2012. Mechanisms of infection by the human fungal pathogen *Cryptococcus neoformans*. *Future Microbiology*, **7:**1297-1313.

Sanfelice F, 1894. Contributo alle morfologia e biologia dei blastomiceti che si sviluppano nei succhi di alcuni frutti [Contribution to the morphology and biology of blastomiceti developing in some fruit juices] *Ann Isto Igiene* **4:**463–495.

Schmittgen TD and Livak KJ, 2008. Analyzing real-time PCR data by the comparative CT method. *Nature Protocols*, **3:**1101-1108.

Tortorano AM, Viviani MA, Rigoni AL, Cogliati M, Roverselli A and Pagano A, 1997. Prevalence of serotype D in *Cryptococcus neoformans* isolates from HIV positive and HIV negative patients in Italy. *Mycoses*, **40:**297-302.

Vanden Bossche H, Marichal PATRICK, Odds FC, Le Jeune L and Coene MC, 1992. Characterization of an azole-resistant *Candida glabrata* isolate. *Antimicrobial Agents and Chemotherapy*, **36:**2602-2610.

Velagapudi R, Hsueh YP, Geunes-Boyer S, Wright JR and Heitman J, 2009. Spores as infectious propagules of *Cryptococcus neoformans*. *Infection and Immunity*, **77:**4345-4355.

Vylkova S, Carman AJ, Danhof HA, Collette JR, Zhou H and Lorenz MC, 2011. The fungal pathogen *Candida albicans* autoinduces hyphal morphogenesis by raising extracellular pH. *MBio*, **2:**e00055-11.

a)

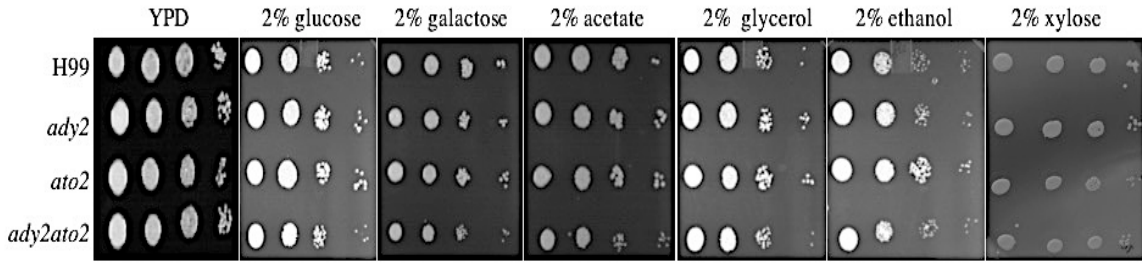

b)

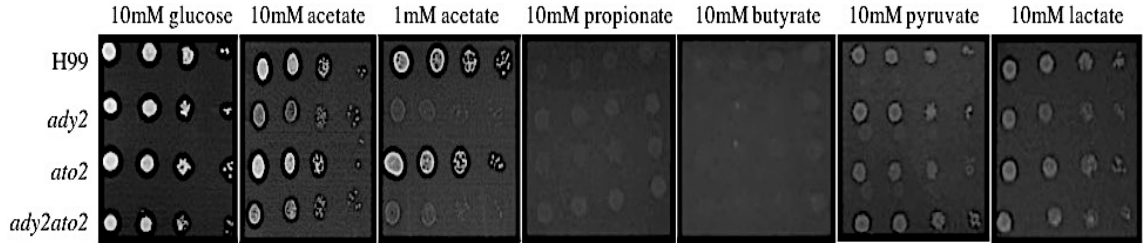

Figure 2-1.: Ady2 is required during growth on low acetate.

a) Plates of YPD, and of YNB supplemented with 2 % glucose, 2 % galactose, 2 % acetate, 2 % glycerol, 2 % ethanol and 2 % xylose were spotted with serial dilutions of H99, *ady2, ato2 and ady2ato2* cells. **b)** Plates of YNB supplemented with 10 mM glucose, 10 mM acetate, 1 mM acetate, 10 mM propionate, 10 mM pyruvate and 10 mM lactate were spotted with serial dilutions of H99, *ady2, ato2 and ady2ato2* cells.

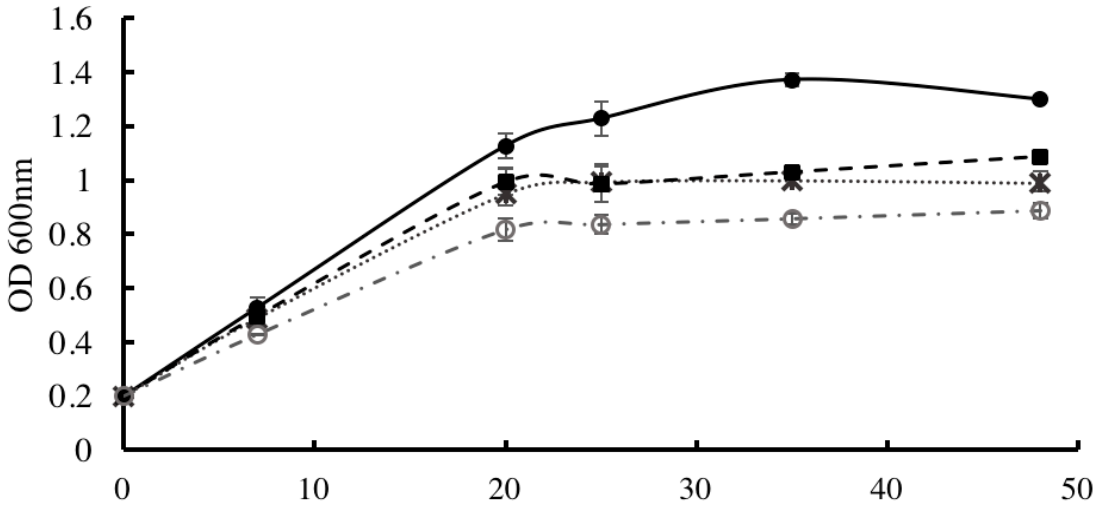

Figure 2-2. Ady2 and Ato2 additively contribute to growth in 10mM (~0.2 %) glucose. Overnight cultures of H99 —●—, *ady2* ···✱···, *ato2* - ■ -, and *ady2ato2* —○— that had been grown in YPD at 30ºC were subcultured into liquid YNB supplemented with 10 mM glucose (~0.2 %) at an OD 600 of 0.2 then growth was followed for up to 48 hours. Error bars indicate standard deviation from the mean of triplicate values.

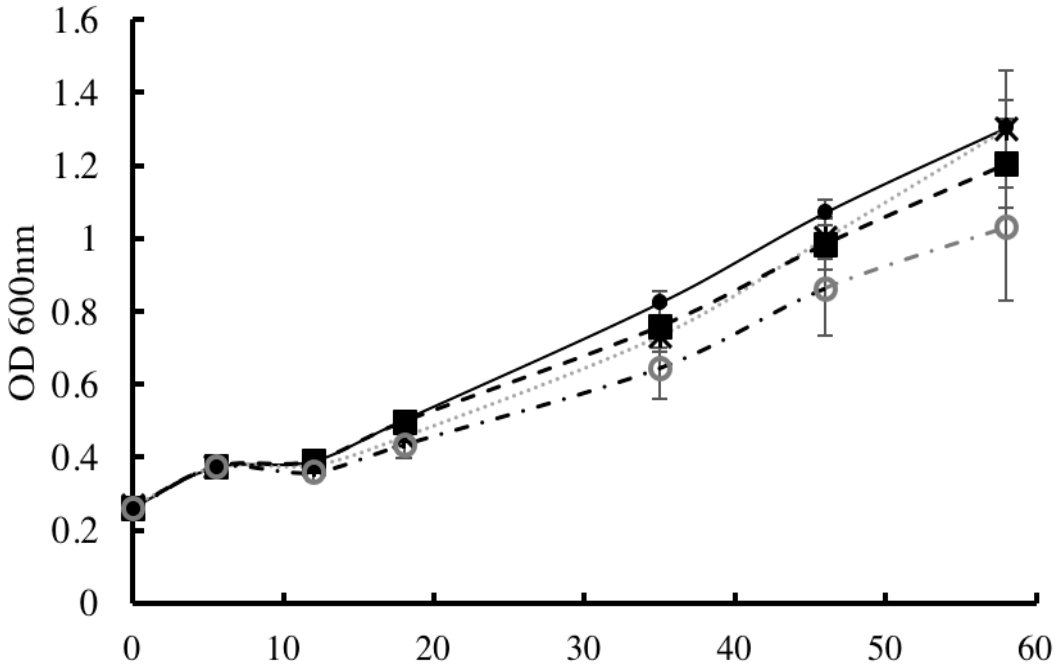

Figure 2-3. Ady2 and Ato2 additively contribute to growth in 60 mM acetate. Overnight cultures of H99 —●—, *ady2* ···■···, *ato2* - ■ -, and *ady2ato2* -○- that had been grown in YPD at 30ºC were subcultured into liquid YNB supplemented with 60 mM acetate (0.5 %) at an OD 600 of 0.2 then growth was followed for up to 48 hours. Error bars indicate standard deviation from the mean of triplicate values.

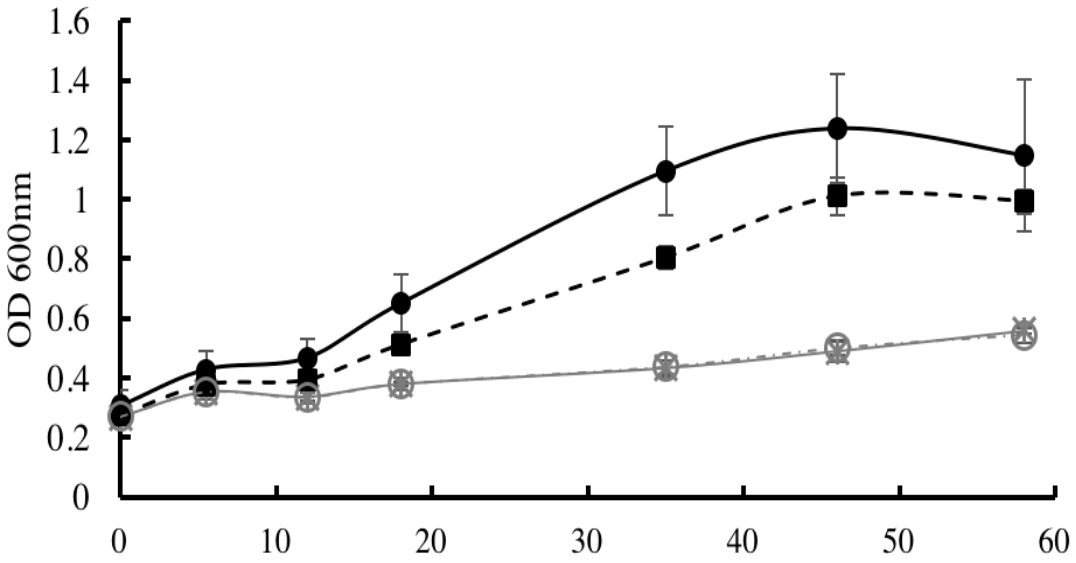

Figure 2-4. Ady2 is required while Ato2 contributes to growth in 6 mM acetate. Overnight cultures of H99 —●—, *ady2* ···■···, *ato2* - ■ -, and *ady2ato2* —○ – that had been grown in YPD at 30ºC were subcultured into liquid YNB supplemented with 6 mM acetate (0.05 %) at an OD 600 of 0.2 then growth was followed for up to 48 hours. Error bars indicate standard deviation from the mean of triplicate values.

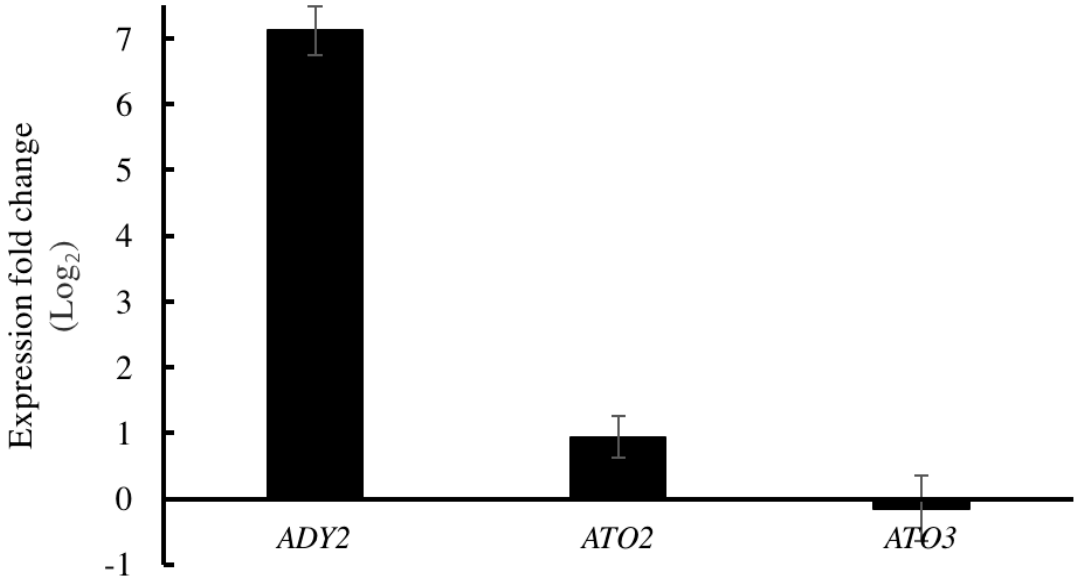

Figure 2-5. *ADY2* is induced during growth on acetate relative to glucose. a) Expression fold change of *ADY2*, *ATO2* and *ATO3* during growth on 60 mM acetate for 20 hours: After 20 hours of culture, expression of *ADY2* and *ATO2* in 100 mM glucose-grown *C. neoformans* cells was compared against that of 60 mM acetate-grown cells. Fold changes were represented as Log_2 values such that on average *ADY2* expression increased 137-fold ($2^{7.17}$) while *ATO2* increased 1.91-fold ($2^{0.94}$). Error bars indicate standard deviation from the mean of triplicate expression fold change values.

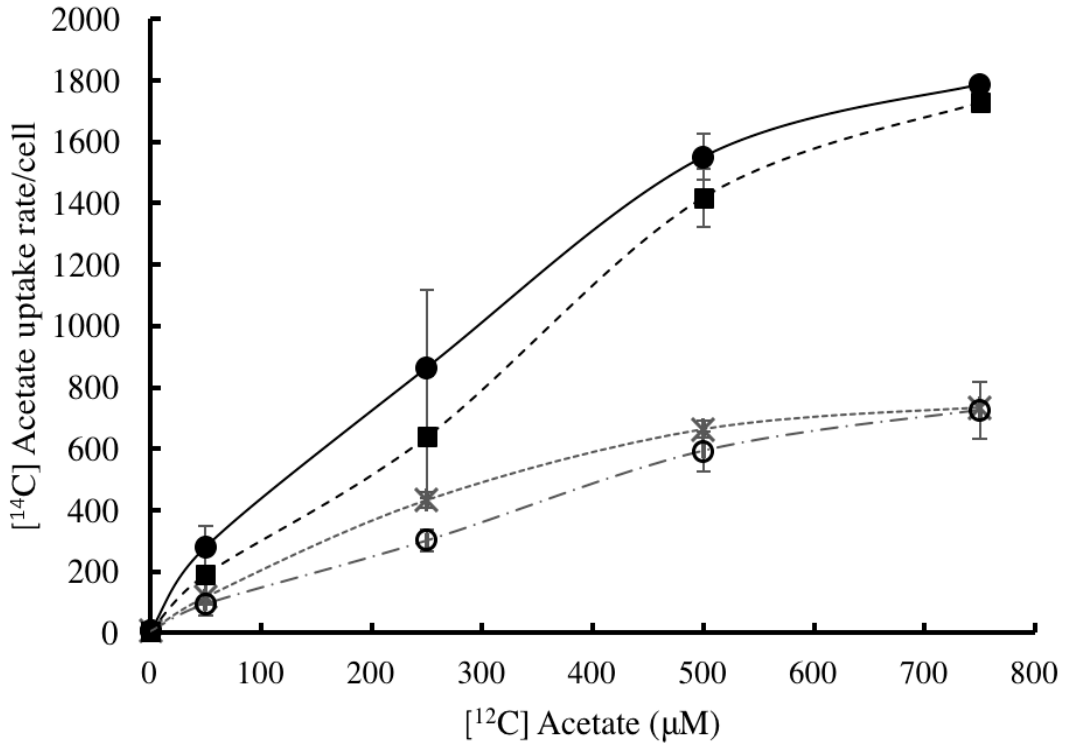

Figure 2-6. Ady2 is essential for facilitated acetate uptake after growing cells in glucose. *C. neoformans* cell suspensions of H99 —●—, *ady2* ···■···, *ato2* - ■ -, and *ady2ato2*—○ - were grown in YPD to an OD 600 of 1.0 (~100,000 cells/μL) then washed and incubated for 5 minutes in a 40:1 mixture of unlabeled acetate to labeled acetate and intracellular [^{14}C] acetate was measured by a scintillation spectrophotometer. The rate of uptake per cell was plotted against μM acetate. Error bars indicate standard deviation from the mean of triplicate values.

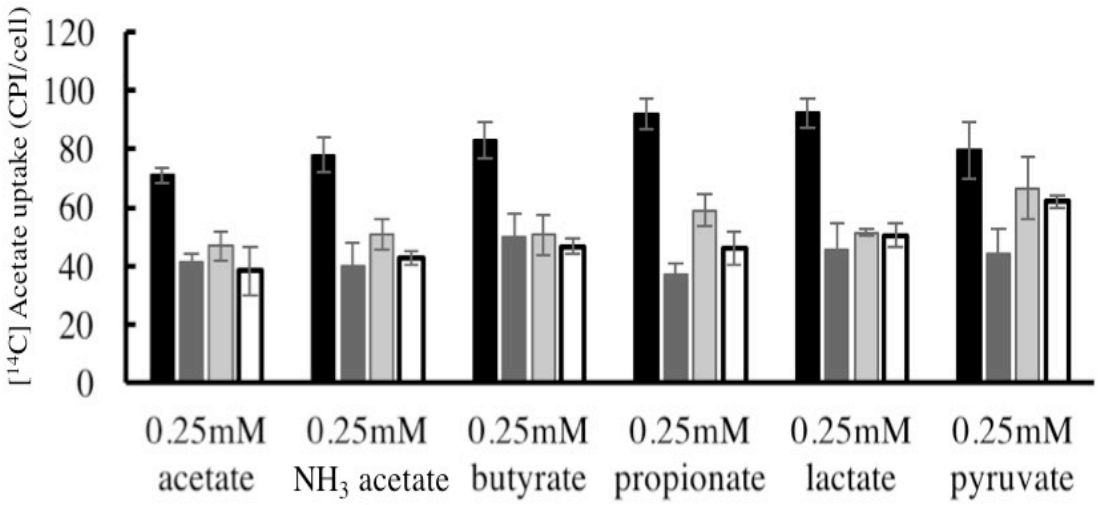

Figure 2-7. After prolonged starvation Ato2, like Ady2 is required for acetate uptake and they are specific for acetate in the presence of other carbon sources. Glucose grown *C. neoformans* were washed and transferred into 0.5 % acetate for 20 hours then incubated with a 40:1 ratio of unlabeled acetate, equimolar NH_3 and acetate mixture, butyrate, propionate, lactate and pyruvate (250 μM) to [^{14}C] acetate (6 nM). Error bars indicate standard deviation from the mean of triplicate values.

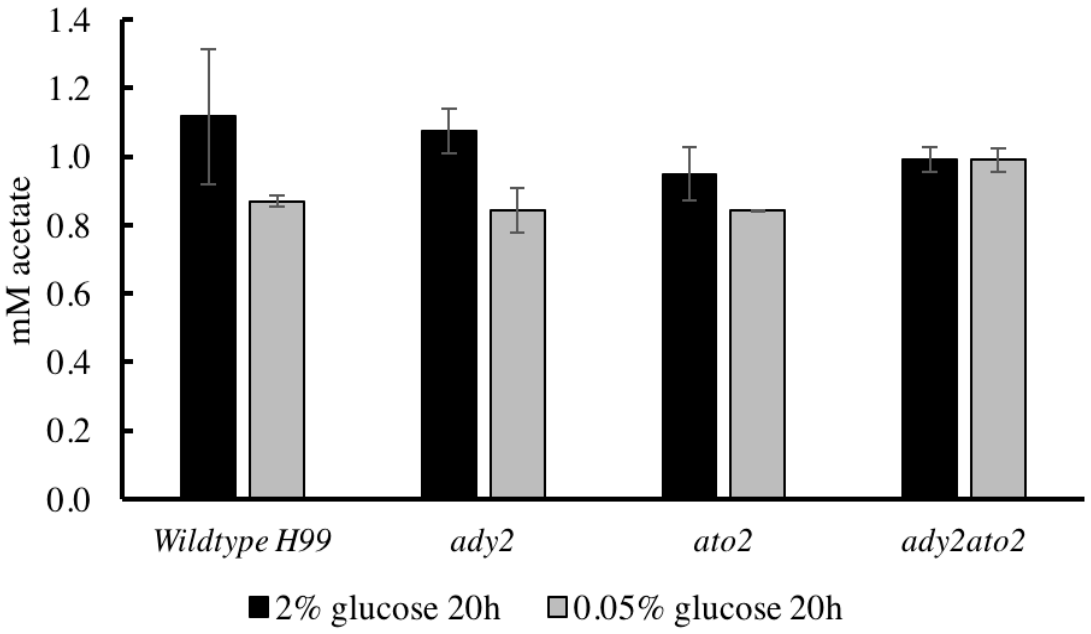

Figure 2-8. Loss of Ady2 and Ato2 does not affect acetate export. Levels of extracellular acetate in the culture supernatant were measured by hydroxamate assay. 75 µL of hydroxamate reaction mixture (0.4 M Tris at pH 7.5, 80 mM $MgCl_2$, 2.4 M hydroxylamine, and 90 µM ATP disodum salt hydrate) was mixed with 225 µL of the culture supernatant. The mixture was agitated thoroughly then incubated for 5 minutes at 37ºC. *Methanosarcina thermophila* acetate kinase (Ack) was added to the reaction to a concentration of 0.023 ng/µL, homogenously mixed and incubated at 37ºC for 15 minutes. At the 15-minute time point, the reaction was stopped with a 20 % trichloroacetate and $FeCl_3$ in 10 N HCl in 1:1 ratio and OD 540 was measured. Error bars indicate standard deviation from the mean of triplicate mM acetate concentrations.

a)

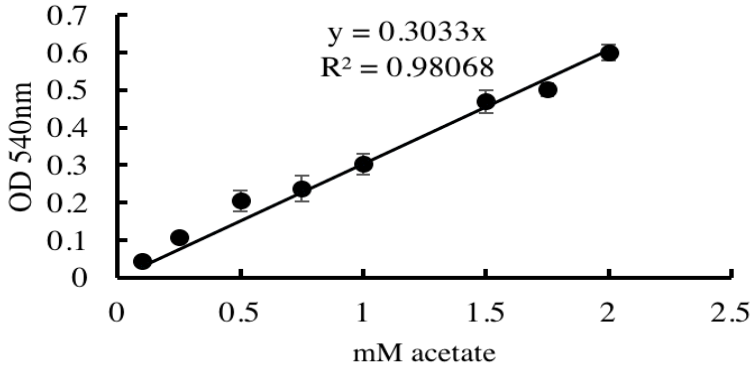

b)

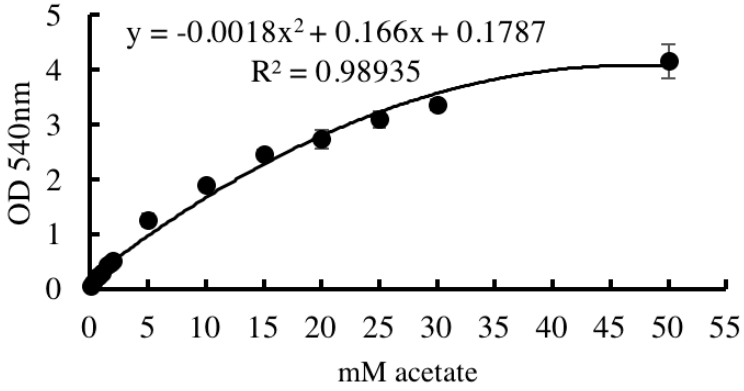

Figure 2-9. Hydroxamate assay signal has linear correlation to acetate concentration between 0.1 mM - 2 mM. To demonstrate sensitivity of the hydroxamate assay we used to detect levels of extracellular we generated a standard curve by performing the assay with known acetate concentrations. **a)** Linear relationship between acetate concentration ranging from 0.1 mM-2.0 mM and the hydroxamate assay signal **b)** Beyond 2 mM-50 mM acetate concentrations the linear relationship between acetate concentration and hydroxamate assay signal is lost. Error bars indicate standard deviation from the mean of triplicate values.

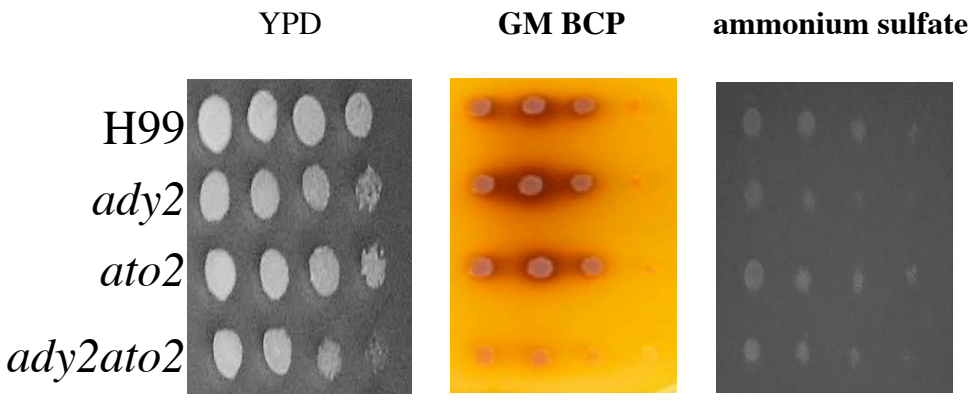

Figure 2-10. Ady2 and Ato2 additively contribute to extracellular environment alkalinization by NH_3 export. Glucose grown *C. neoformans* were washed and serial dilutions were spotted onto a standard YPD plate to provide optimum growth conditions. The medium GM-BCP containing glycerol, yeast extract, and the pH indicator bromocresol purple and adjusted to pH 3.3 was used to detect media alkalinization due to NH_3 export. YNB agar supplemented with 100 mM ammonium sulfate was used to investigate a role in Ady2 and Ato2 in ammonium uptake.

a)

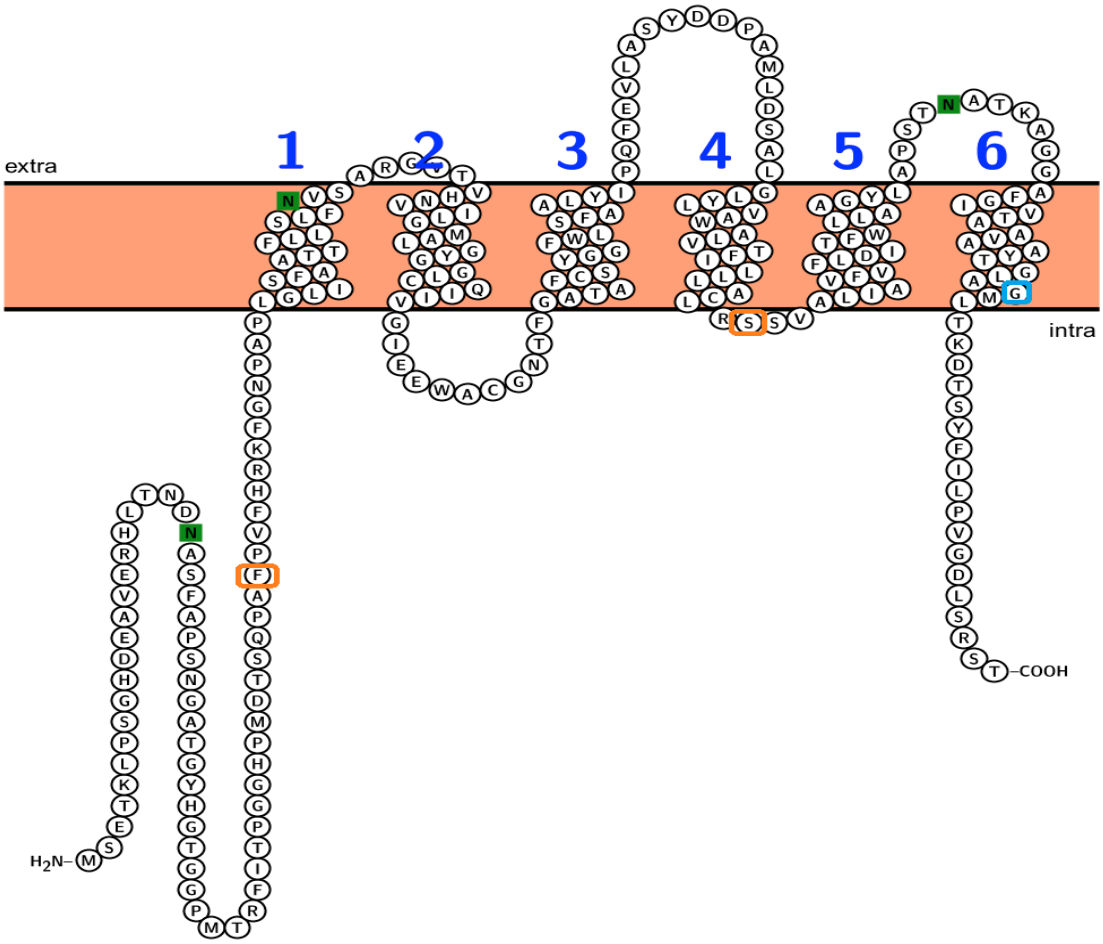

b)

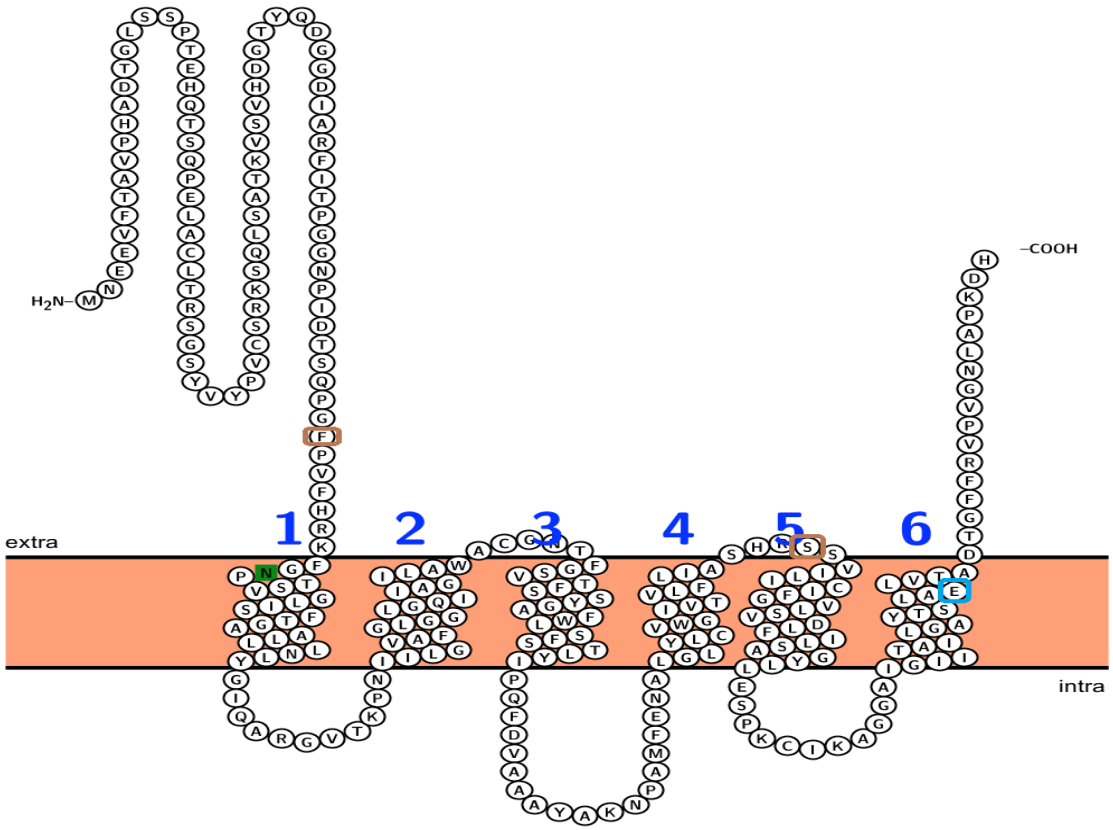

Figure 2-11. a) Predicted membrane topology of *Cryptococcus neoformans* Ady2. Using the program Protter, *Cryptococcus neoformans* Ady2 probable membrane topology was visualized. Ady2 N and C termini are speculated as being intracellularly localized. **b) Predicted membrane topology of *Cryptococcus neoformans* Ato2**. *Cryptococcus neoformans* Ato2 probable membrane topology was visualized using Protter. Ato2 N and C termini are speculated as being extracellularly localized. Residues that are circled align to *Y. lipolytica* Gpr1p that when mutated result in sensitivity to acetate (Gentsch et al., 2007)-blue indicates predicted intra-membrane location of the residues while orange indicates extracellular residue location.

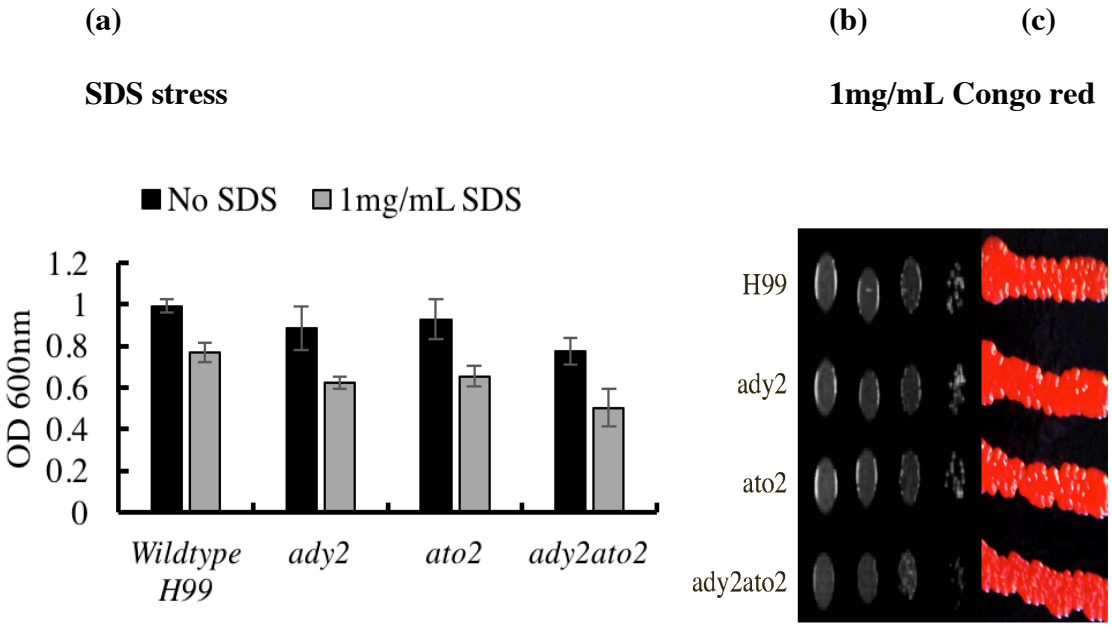

Figure 2-12: Loss of Ady2 and Ato2 does not compromise cell wall integrity during 20 hours of 1 mg/mL SDS stress (P>0.05 unpaired t test, GraphPad 7, Inc.) or Congo red stress. a) H99, *ady2*, *ato2* and *ady2ato2* were grown in YNB containing 10 mM glucose and 1 mg/mL SDS and 1 mg/mL Congo red. As a control, the same experiment was replicated without SDS. While growth was inhibited by SDS, the trend was consistent with growth rate during growth on 10 mM glucose lacking SDS, thus uncoupling the effect of SDS from the growth phenotype due to carbon source requirement of the mutant strains. Error bars were created from standard deviation from the mean of triplicate values. **b)** There was no growth defect during Congo red stress and **c)** Cells growing on Congo red took up the stain and appeared as pink colonies.

a)

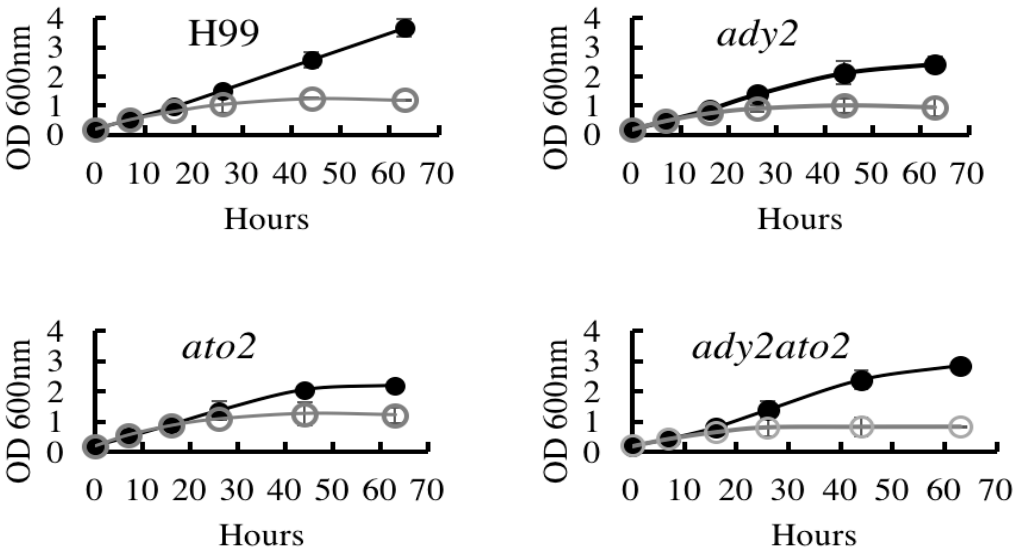

b)

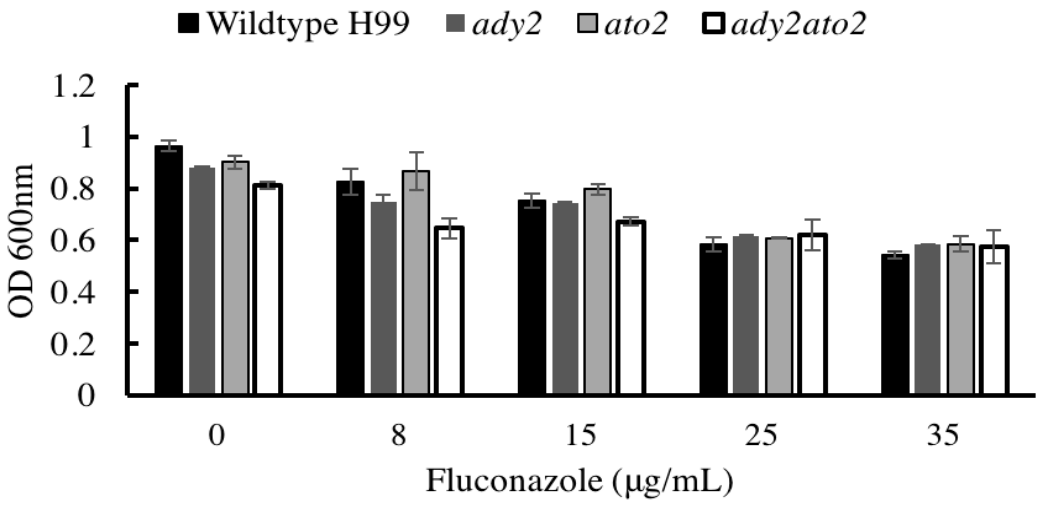

Figure 2-13: Loss of Ady2 and Ato2 does not impact fluconazole susceptibility (P>0.05, unpaired t test, GraphPad 7, Inc.). a) Growth curves of H99, *ady2*, *ato2* and

ady2ato2 were grown in YNB containing 0.2 % glucose and 8 μg/mL fluconazole (⊖) and compared to corresponding growth rate in the absence of fluconazole (●). **b)** H99, *ady2*, *ato2* and *ady2ato2* were grown in YNB containing 0.2 % glucose and 8 μg/mL, 15 μg/mL and 35 μg/ml fluconazole at 30ºC for 16 hours. As a control, the same experiment was replicated without fluconazole. Error bars indicate standard deviations from the mean of absorbance at OD 600nm values.

The role of Ady2 and Ato2 in virulence of *Cryptococcus neoformans*

[1]Grace N. Kisirkoi, [2]Stuart Levitz, [2]Charlie S. Specht, [2]Chrono Lee, [1]Yijian Qiu,

[1]Bridget Luckie, [1]James Morris, and [1]Kerry S. Smith

[1]Department of Genetics and Biochemistry

Eukaryotic Pathogens Innovation Center (EPIC)

Clemson University

Clemson, SC 29634

[2]Infectious Diseases and Immunology

Department of Medicine

University of Massachusetts Medical School

Worcester, MA 01605

To whom correspondence should be addressed:

[1]Kerry S. Smith

Office 864-656-6935

Email kssmith@clemson.edu

CHAPTER THREE

Abstract

Cryptococcus neoformans, the leading cause of fungal meningitis resulting in over 600,000 annual deaths, has adapted to survive in its mammalian host environment. Carbon metabolism is critical for virulence in *C. neoformans* and nonpreferred carbon sources such as acetate are likely essential energy sources during initial pulmonary colonization. We investigated the roles of two acetate transporters, Ady2 and Ato2, in the virulence of *C. neoformans*. Deletion of Ady2 and Ato2 led to a defect in growth at 37ºC, impaired capsule formation, led to higher susceptibility to phagocyte-mediated clearance, and instigated cell-cell aggregation phenotype resulting in flocculation during starvation conditions, and a diminished ability to modulate environmental pH while facilitating acetate uptake under starvation conditions. Moreover, high inducement of *ADY2* and *ATO2* during growth on glucose rich media versus nutrient limiting media suggested an involvement of Ady2 not only in acetate import but in overall adaptation to nutrient poor conditions at high pH. Loss of Ady2 and Ato2 caused diverse metabolic and cellular defects that together led to high attenuation of virulence, a complex phenotype governed by various adaptive properties of *C. neoformans*. These diverse phenotypes from loss of Ady2 and Ato2 suggest that acetate transport may be linked to homeostasis of intracellular acetyl-CoA pool, a central carbon metabolite essential for biosynthetic and cellular processes. Thus, the loss of Ady2 and Ato2 has far reaching effects: affecting crosstalk between effectors of the master-regulation of metabolism such as the cAMP-PKA signaling cascade, inhibiting alternative catabolic pathways during energy

limitation, and inhibiting protein, carbohydrate, lipid biosynthesis, cell growth and proliferation.

Introduction

From the approximately 1,000,000 annual incidences of the basidiomycetous *Cryptococcus neoformans* infections globally, over 600,000 yearly deaths result, the bulk of which are in Sub-Saharan Africa (Sloan and Parris, 2014). Following an initial pulmonary infection, cryptococcal cells encounter a nutrient deprived environment within the lungs as the invading cells are taken up by resident alveolar macrophages which are the first immune cells to interact with invading *C. neoformans* (Diamond et al., 1974). During murine pulmonary infection, the glyoxylate pathway, fatty acid beta-oxidation, gluconeogenesis, and amino acid synthesis are induced in *C. neoformans* suggesting metabolic adaptation to a nutrient limited environment (Hu et al., 2008). Moreover, acetate was the most abundant metabolite recovered from the lungs of infected Female Fisher rats (Himmelreich et al., 2003) consistent with the elevated transcript levels of proteins involved in acetate transport and metabolism. Specifically, acetyl-CoA synthetase (Acs) which catalyzes acetate activation to acetyl-CoA, and pyruvate decarboxylase, aldehyde dehydrogenase, xylulose 5-phosphate/fructose 6-phosphate phosphoketolase which catalyze acetate production, as well as two putative acetate transporters were induced during murine pulmonary infection (Hu et al., 2008; Kronstad et al., 2012). Furthermore, an *acs* mutant was attenuated in virulence and could not utilize acetate as the sole carbon source (Hu et al., 2008).

An immunocompetent host can effectively combat an initial *C. neoformans* pulmonary infection thus clearing it through Th1-like responses induced by classically activated macrophages rather than the ineffective alternatively activated Th2 responses

(Rohatgi and Pirofski et al., 2015). Neutrophils contain *C. neoformans* in the lungs within a granuloma then kill them oxidatively, non-oxidatively or with the aid of antimicrobial peptides (Rohatgi and Pirofski et al., 2015). In blood circulation, neutrophils have effective non-specific anticryptococcal response. However, in an immunocompromised host, the internalization of *C. neoformans* by activated macrophages can be counterproductive because the cryptococcal cells adapt to this environment and proliferate within macrophages. Phagocytosed cells can then non-lytically exit macrophages into the bloodstream or remain inside parasitized macrophages that traverse into blood circulation. While the intracellular environment within tissue resident phagocytes and in the lung mimics culture conditions in minimal media lacking preferred carbon sources, blood has elevated glucose which is maintained at an average of ~7.5 mM according to a rat model (Dunn-Meynell et al., 2009).

C. neoformans is uniquely adapted to its *in vitro* and *in vivo* environment, as it tightly regulates environmental pH, senses nutrients, adjusts metabolism, and actively evades the host's antifungal immune attempts. We have previously identified two transporters, designated as *ADY2* (CNAG_05678) and *ATO2* (CNAG_05266), from the Gpr1/Fun34/YaaH family of acetate transporters as being essential for modulating extracellular and intracellular environments thus heavily impacting pathogen survival in the environment and the host. During starvation in minimal media supplemented with acetate, *ADY2* is dramatically upregulated and both *ADY2* and *ATO2* are required for acetate uptake as a carbon source (Dissertation Chapter 2). Acetate taken up can be subsequently activated by Acs to acetyl-CoA to enter the central carbon metabolism after

depletion of preferred carbon sources such as glucose, whose metabolism results in carboxylic acid intermediates.

During infection, *C. neoformans* encounters a variety of host environmental niches that drastically vary pH and whose accumulation could be toxic to cells. Consistent with *C. neoformans*' metabolic versatility that makes it saprophytic, ammonia extrusion following gluconeogenic catabolism of NH_3 compounds could alkalinize environments to selectively high pH levels. This phenomenon is demonstrated during necrotropic colonization of dead plant tissue by fungi *Colletotrichum acutatum* and during invasion by commensal pathogen *Candida albicans*. This ability to raise environmental pH autoinduces hyphal morphogenesis, one of *C. albicans*' virulence factors (Vylkova et al., 2011) that leads to invasive host colonization. Pathogens' ability to sense and actively modulate their environments enhance their remarkable ability to prevail despite host attempts to expel them by creating harsh microenvironments. Media alkalinization by *C. albicans* was limited by presence of glucose, hence hypothesized to be glucose repressible (Vylkova et al., 2011). This observation suggests that pH is modulated in a carbon source dependent manner.

This study seeks to evaluate the roles played by Ady2 and Ato2 in *C. neoformans* virulence given their drastic contributions to the pathogen's propensity to adapt to unfavourable environments. Cells lacking Ady2 and Ato2 are unable to grow at human body temperature of 37°C, are diminished in capsule formation, and are generally impaired in their ability to cause mortality in mice. These diverse effects in addition to our previous studies on roles of Ady2 and Ato2 in metabolic adaptation (Dissertation

Chapter 2) suggest crosstalk between acetate transport, the resulting impact on intracellular acetyl-CoA pool and master-regulator of metabolism, stress responses and epigenetic regulation of cellular processes (possibly through the SNF/PKA signaling cascade).

Materials and methods

Strains and morphological characterization

The *C. neoformans ady2*, *ato2,* and *ady2ato2* knockout strains were kindly provided by Dr. James Kronstad (Michael Smith Laboratories, University of British Columbia, Vancouver, Canada). Independently created mutants of Ady2 and Ato2 from the Madhani collection (Jung et al., 2015) were checked as having similar phenotypes as mutants obtained from the Kronstad Lab. Strains were grown in the minimal medium, YNB (Difco™) supplemented with 0.2 % glucose at 30ºC with moderate aeration.

Flocculation was observed by cell-cell aggregation as *C. neoformans* cultures were grown to mid-log phase then resuspending them by vortexing and allowing them to settle such that the most flocculent strains would settle to the bottom of the culture tube faster. Fluorescent and light microscopy using an Axiovert® inverted microscope was then performed to examine *C. neoformans* cell-cell aggregation in relation to flocculation. To do this, a drop of Calcofluor White Stain (Sigma-Aldrich) was mixed with the *C. neoformans* strains and one drop of 10 % KOH on a slide after which a coverslip was placed over the sample and the set-up was incubated for 1 minute at ambient temperature followed by observing under the DAPI filter of the Axiovert® inverted microscope x40 magnification in comparison to the visible light filter.

To regenerate the single mutants for replication of phenotypes of individual null mutants, the Ady2 and Ato2 single mutants were crossed with KN99a and allowed to sporulate on Murashige and Skoog media (4.3 g/L Murashige and Skoog basal salt mixture from Sigma-Aldrich, 1mL/L of 1000x Murashige and Skoog vitamin solution

from Sigma-Aldrich, filter sterilized, mixed with 4 % sterile agar and adjusted to pH 5) at ambient temperature in the dark. Individual spores were obtained and allowed to germinate on YPD (Difco™) containing the respective selection antibiotics after which the strains were genotyped by PCR to confirm presence of the intended single gene and absence of its counterpart.

Examining virulence factors in *C. neoformans*

Capsule formation was induced by first washing overnight YPD cultures of H99, *ady2, ato2* and *ady2ato2* strains with sterile nanopure water then introducing 10,000 of these cells into a 2 mL culture of CO_2-independent media (Gibco™). This culture was then left to grow with aeration by shaking at 37ºC. A dense cell suspension was stained in India ink (VWR®) at a 1:1 ratio and the capsule formation discerned from the resistance of the capsule to India ink staining such that a halo occurred around encapsulated cells when observed by light microscopy. Colony morphology of encapsulated versus the unencapsulated cells was observed during growth of *C. neoformans* in capsule inducing plate media (CO_2-independent media for mammalian cell culture containing 2 % agar).

The ability to produce melanin and to grow at mammalian body temperature of 37ºC was investigated by first growing overnight cultures of individual and double mutants lacking *ADY2* and *ATO2* along with their wild type background (H99). These *C. neoformans* strains were then washed twice by pelleting 1 mL of culture in the same volume of sterile nanopure water, centrifuging at 3000 x g then resuspended in sterile nanopure water at an optical density (OD) 600 of 0.2. Their cell densities were confirmed to be equal by hemocytometer counting. For the melanin production analyses, four 10-

fold serial dilutions of these strains were spotted onto minimal media, YNB 2 % agar supplemented with 1 g/L glucose, 1 g/L L-asparagine, 3g/L KH2PO4, 250 mg/L MgSO4, 100 mg/L L-DOPA, 1 mg/L Thiamine HCl, adjusted to pH 5.6 and left to grow in the dark at 30ºC. Melanin production was also investigated with a higher *C. neoformans* cell density starting serial dilutions with 2 x 10^6 cells and subsequent 100-fold dilutions to investigate the roles of cell density and growth rate on melanin production.

For the experiments to investigate H99, *ady2, ato2* and *ady2ato2* mutants' thermotolerance at mammalian body temperature, overnight *C. neoformans* cultures were washed twice by pelleting 1 mL of culture in the same volume of sterile nanopure water, centrifuging at 3000 x g then resuspended in sterile nanopure water at an OD 600 of 0.2. After confirming equal cell density between the strains by checking their absorbance at 600 nm and counting them using a hemocytometer, four 10-fold serial dilutions of were spotted onto minimal media, YNB 2 % agar supplemented with 0.2 % glucose and on YPD plates containing 2 % agar then incubated at 37ºC.

Fungal killing by human neutrophils

C. neoformans cultures were first grown overnight in YPD cultures then washed thrice by pelleting at 300 x g for 5 minutes then resuspending in 1 mL PBS buffered at pH 7.4 (Gibco™) and diluting to 1,000 cells/uL. Venipuncture was performed on healthy blood donors to obtain peripheral blood of which 10 mL was coagulated to yield serum while another 10 mL was anticoagulated using 10 U of pyrogen-free heparin (Elkins-Sinn, Inc., Cherry Hill, N.J.) per mL. Holding the Falcon tube (Becton Dickinson) containing uncoagulated blood tipped at a slight angle, 5 mL of Mono Poly resolving

medium was dispensed in a slow steady stream over the medium's interface to avoid mixing. The Vacutainer™ (Becton Dickinson) containing coagulated blood and the falcon tube containing uncoagulated blood were centrifuged at 300 x g for 15 minutes at ambient temperature without breaks.

Serum was obtained from the Vacutainer™ while neutrophils were obtained from the second-densest fraction of the density-separated blood. The obtained neutrophils were resuspended in RPMI 1640 medium (Gibco™) which had been prewarmed at 37ºC. The neutrophil suspension was then pelleted by centrifuging at 300 x g at ambient temperature. Contaminating red blood cells were lysed using 500 µL of 1x Red Blood Cell Lysis Buffer (Roche). The resulting neutrophils were resuspended to a density of 1000 neutrophils/µL in RPMI 1640 medium prewarmed at 37ºC. A coculture of 80,000 neutrophils and 10,000 *C. neoformans* cells was rotated for 2 hours at 37ºC and then pelleted by centrifugation at 300 x g for 5 minutes. Neutrophils were lysed osmotically by incubating them in 1mL of sterile nanopure water for 10 minutes followed by vortexing. Triplicates of 100x dilutions were done to determine % surviving *C. neoformans* = (untreated CFU/treated CFU) x 100.

Fungal killing by mouse derived J774.16 cell line

Overnight *C. neoformans* cultures were grown in YPD cultures then washed thrice by pelleting at 300 x g for 5 minutes then resuspended in 1 mL PBS buffered at pH 7.4 (Gibco™) and diluting it to 1,000 cells/µL. The J774.16 mouse macrophage cell line was passaged weekly in 10 mL Dulbecco's Modified Eagle Medium (DMEM; Gibco™ Life Technologies) supplemented with 10 % heat-inactivated fetal calf serum, 1 % non-

essential amino acids, 100 µg/mL penicillin-streptomycin, and 10 % NCTC-109 medium (all from Gibco™ Life Technologies). A coculture of 80,000 macrophages activated with 10 nM phorbol myristate acetate (PMA) and 10,000 *C. neoformans* cells opsonized with 1 µg/mL mAB18B7 (kindly provided by Dr. Arturo Casadevall, Johns Hopkins Bloomberg School of Public Health) was rotated for 2 hours at 37°C then was pelleted by centrifuging at 300 x g for 5 minutes. For the 24-hour phagocytosis assay, un-engulfed *C. neoformans* were gently aspirated from the coculture after 1 hour of co-incubation. Macrophages were lysed osmotically by incubating them in 1 mL of sterile nanopure water for 10 minutes followed by vortexing. Triplicates of 100x dilutions were spotted onto YPD plates for quantification and survival was determined by the equation: % surviving *C. neoformans* = (untreated CFU/treated CFU) x 100.

Investigating virulence of *C. neoformans* in the C57BL/6 mouse model

To investigate the roles of Ady2 and Ato2 in virulence during infection of the vertebrate mouse model, *Cryptococcus neoformans* strains H99, *ady2*, *ato2* and *ady2ato2* were cultured overnight in 3 mL of YPD then diluted to $2x10^5$ cells/mL in PBS buffered at pH 7.4 (Gibco™). C57BL/6 mice 6-7 weeks old received an oral tracheal infection of 10,000 *C. neoformans* strains in two biological replicates with five mice per strain. The oral tracheal infection was delivered using a finely tipped pipette inserted into the mouth of temporarily anaesthetized mice such that 50 uL of *C. neoformans* cell suspension was aspirated down the trachea.

Biological replicates were started on separate days and used two independent C57BL/6 mouse batches (Jackson Laboratories, Bar Harbor ME and Charles River

Laboratories, Wilmington, MA). Mortality was determined by observing mice every 24 hours and sacrificing moribund ones. To determine fungal load in the surviving mice the murine lungs were harvested, weighed and suspended in 4 mL of PBS buffered at pH 7.4 (Gibco™) containing 200 U/mL of Penicillin-Streptomycin solution supplied in 100x formulation (Gibco™). The lung tissue in PBS buffered at pH 7.4 was then mechanically ground using a tissue homogenizer (Miltenyi Biotec). Colony forming units (CFU) were determined by spotting homogenate suspension on Saboraud Dextrose Agar at pH 5.6 (Thermo Scientific™) and counting the resulting colonies. Kaplan Meier survival analysis graphs were generated using GraphPad Prism 5.

Examining the roles of Ady2 and Ato2 in pH modulation of media

C. neoformans strains were grown overnight in YPD at 30°C then pelleted by centrifugation and washed 3x using sterile nanopure water. The cells were resuspended to an OD 600 of 0.05 in YPD, YNB supplemented with 0.5 % acetate, and GM-BCP media containing glycerol, yeast extract, and the pH indicator bromocresol purple adjusted to acidic or alkaline pH using HCl or NaOH and grown at 30°C with aeration. pH indicator colour changes in cultures were monitored every 24 hours. A pH sensitive stain, pHrodo® (ThermoFisher, Inc.) was used to stain and image cells. To do this, dense cell suspensions were washed by centrifuging at 300 x g in PBS buffered at pH 7.4 then incubated with 5 μM pHrodo™ Red AM Intracellular pH Indicators in PowerLoad™ (ThermoFisher, Inc.) for 30 minutes at ambient temperature, then 30 minutes at 37°C to provide an indication of intracellular pH in live cells during culture. This preparation was then visualized under the rhodamine filter of the Axiovert® inverted microscope.

After twenty hours, total RNA was isolated as previously described (Dissertation Chapter 2) and according to the specifications of Aurum™ Total RNA Mini Kit (Bio-Rad™). Quantitative RT-PCR was performed using the Verso 1-step RT- qPCR SYBR Green ROX kit (ThermoFisher Inc.). Data was normalized to *UBC6* because of its highly stable expression (Llanos et al., 2015). Using the double delta Ct (cycle threshold) method ($2^{\Delta\Delta Ct}$) method described by Schmittgen TD and Livak KJ., (2008), the expression fold change of *ADY2*, *ATO2* and *ATO3* relative to the reference gene was determined. This double delta Ct method used comparative Ct (Cycle threshold) values, which indicated the number of RT-qPCR cycles completed before a fluorescent signal crossed the background noise's threshold. Hence the less the Ct value, the higher the abundance of the target nucleic acid.

Our comparative delta Ct method contrasted the target genes under experimental manipulations, *ADY2*, *ATO2* and *ATO3* relative to *UBC6* (CNAG_05765) the reference control gene whose expression must not change regardless of experimental manipulations (Llanos et al., 2015). Target gene Ct values were compared relative to the internal control *UBC6* such that values of target genes below those of *UBC6* indicated relatively reduced transcript levels while values of target genes above this defined threshold indicated that transcript levels were elevated. We also used an internal control encoded by the *ACT1*, which was compared against *UBC6* as a quality check as it is typically constitutively expressed despite experimental manipulations. To obtain fold change of gene expression in nutrient limited YNB relative to the nutrient rich YPD, which contains 2 % glucose, the Ct values of *ADY2, ATO2,* and *ATO3* against *UBC6* were compared within the growth

conditions and values presented in the form of fold change of gene expression in YNB supplemented with 0.5 % acetate, relative to fold change of gene expression in YPD.

The ability to modulate pH and survive at physiologically relevant pH of 4.5 and 7 was investigated by first growing overnight cultures of individual and double mutants lacking *ADY2* and *ATO2* along with the wild type H99. These *C. neoformans* strains were then washed twice by pelleting 1 mL of culture in the same volume of sterile nanopure water, centrifuging at 3000 x g then resuspended in sterile nanopure water at an OD 600 of 0.2. Their cell densities were confirmed to be equal by hemocytometer counting after which 2 µL of four 10-fold serial dilutions of H99, *ady2, ato2* and *ady2ato2* were spotted onto minimal media, YNB agar supplemented with 0.5 % acetate and adjusted to pH 4.5 and 7.0 then incubated at 30ºC.

Results

To assess the roles played by Ady2 and Ato2 in maintaining intact *C. neoformans* cell morphology, we evaluated the cells and culture suspensions of wild type H99 versus the mutant strains *ady2, ato2* and *ady2ato2* and found that *ady2ato2* was impacted by the loss of Ady2 and Ato2 at 30ºC in YNB supplemented with 0.2 % glucose. Unlike the wild type *C. neoformans* and the *ady2* and *ato2* strains which were in a dispersed single-celled monolayer, the *ady2ato2* strain clumped to develop strings of unseparated cells (**Figure 3-1a**). In addition to clumping at the microscopic level, the double mutant cells were flocculent as they clumped macroscopically such that their liquid cultures settled faster than their single mutant or wild type strains (**Figure 3-1b**).

We next investigated the contributions of Ady2 and Ato2 towards ability to remain viable and grow at mammalian body temperature, polysaccharide capsule as well as synthesis of melanin, the three major virulence determinants of *C. neoformans*. While *ady2* and *ato2* retained wild type levels of thermotolerance, the *ady2ato2* strain had a heightened thermosensitivity such that its growth was impaired at 37ºC (**Figure 3-2**). Moreover, loss of both Ady2 and Ato2 impacted capsule production. While the wild type and single mutant strains formed a capsule and hence were resistant to negative staining by India ink, leaving a halo around their encapsulated cells, the double mutant was impaired in capsule formation (**Figure 3-3a**). During these capsule-inducing conditions on agar, the unencapsulated strains formed textured colonies devoid of the glossy sheen morphology observed on the strains that still had capsule (**Figure 3-3b**). While melanization occurred in the single *ady2* and *ato2* mutants, the loss of both Ady2 and

Ato2 caused a defect in melanin production when a cell density starting from 10^4 cells was spotted on media containing dopamine (**Figure 3-4a**). However, increased cell density to start at $2x10^6$ resulted in melanization of all four strains (**Figure 3-4b**).

We investigated whether the presence of acetate transporters (which enable adaptation to the low pH that is characteristic of acetate) would also confer a survival advantage to *C. neoformans* killing by phagocytes, whose predominant environment is slightly acidic. Macrophages are the first resident immune effectors to contact and phagocytose invading cells then link host innate oxidative mediated killing, and adaptive antifungal mechanisms (Rohatgi and Pirofski et al., 2015). However, macrophages can be parasitized and support cryptococcal proliferation (Diamond and Bennet, 1973). We observed that neither individual nor double mutants of Ady2 and Ato2 were differentially killed by mouse macrophage-like cell lines during a 2 hour coculture (**Figure 3-5**). However, after the 24-hour phagocytosis assay, *ato2* and *ady2ato2* but not *ady2* were susceptible to macrophage antifungal activity (**Figure 3-5**).

We also looked into the roles played by Ady2 and Ato2 during *C. neoformans* killing by neutrophils, which contain *C. neoformans* infection within a granuloma in the lungs. Neutrophils in blood also phagocytose *C. neoformans*. They execute anticryptococcal action oxidatively, non-oxidatively or with the aid of antimicrobial peptides (Rohatgi and Pirofski et al., 2015). Neutrophils are effective in cryptococcal clearance even in the absence of *C. neoformans* opsonization (Miller and Mitchell, 1999). Unlike macrophages, human neutrophils were able to kill the double *ady2ato2* mutant

significantly more efficiently than the wild type (P=0.0045, GraphPad Prism 7, Inc. unpaired t-test) or the single mutants (P>0.5) after a 2 hour coculture (**Figure 3-5)**.

Our cumulative virulence-associated observations of mutants lacking Ady2 and Ato2 being defective in major virulence determinants of *C. neoformans* in addition to preferential killing of *ady2ato2* by neutrophils led us to investigate the virulence roles of Ady2 and Ato2 in a mouse (C57BL/6) model. Not surprisingly, the double *ady2ato2* mutant was highly attenuated in virulence such that the mouse group infected with this strain continued to survive and did not succumb to infection despite the groups infected with H99, *ady2* and *ato2* having died from infection approximately 15 days earlier (**Figure 3-6**). However, upon sacrificing the surviving mice after 50 days of the experiment, the fungal load was maintained at an average of the original inoculum of 10,000 *C. neoformans* (**Figure 3-6**).

We investigated the possibility that Ady2 and Ato2 have a role in environmental adaptation to physiologically relevant environment that *C. neoformans* encounters and must adapt to during infection. To do this we observed relative growth rates of H99, *ady2, ato2* and *ady2ato2* as well as gene expression of acetate transporters during nutrient deprived environments at slightly acidic (macrophage-like) and slightly alkaline conditions (similar to human blood and brain environments) against the basis of nutrient rich YPD**.** We uncovered a role of Ady2 and Ato2 in modulating *C. neoformans* environmental pH such that the cells actively acidified the extracellular environment in a nutrient-dependent manner as seen by 20 hour and 72 hour *C. neoformans* cultures maintaining a yellow colouration characteristic of acidic pH as illustrated on the cell free

panel (**Figure 3-7**). Moreover, we observed yellowing of the area surrounding the colonies growing on nutrient rich YPD agar (**Figure 3-7**). **Figure 3-8a** shows H99, *ady2, ato2,* and *ady2ato2* after 20 hours and 72 hours of growth as they alkalinize acidic GM-BCP. The cell free panel indicates the colour calibration of media at varying pH. This progression of media alkalninization is also shown on plate cultures as the colonies turn colour between day 2-6 before alkalinizing the media. The *ady2ato2* strain alkalinized the media relariveley slower than other strains.

When stained with the cytosolic pH stain, pHRodo, cells from the 5-day spot fluoresced (**Figure 3-8b**). After 48 hours of growing in test tube cultures, *ady2* and *ady2ato2* strains were slower than H99 and *ato2* strains in media alkalinization (**Figure 3-8c**) while by 60 hours, H99, *ady2*, *ato2* but not *ady2ato2* had alkalinized GM-BCP (**Figure 3-8d**). Hence all the strains- H99, *ady2*, *ato2* and *ady2ato2* grow in GM-BCP but *ady2ato2* is slow to alkalinize it. Alkaline pH altered nutrient acquisition needs of *C. neoformans* growing in YNB supplemented with 0.5% acetate such *ady2* and *ady2ato2* but not *ato2* were growth-impaired (**Figure 3-9**). However, growth to wild type levels was observed in YNB supplemented with 0.5% acetate at pH 4.5 even though there was a general growth decline in acidic compared to neutral pH (**Figure 3-9**). During growth in nutrient rich YPD at varying pH of 4.5, 7 and 8, *ADY2* expression was consistently uninduced (**Figure 3-10**). However, its transcript levels were elevated at pH 7 and 8 during growth in YNB supplemented with 0.5% acetate, but not at the acidic pH 4.5 which is below Pka of acetate (**Figure 3-10**). *ATO2* remained uninduced during growth in nutrient rich YPD at pH 7. However, at pH 4.5 and 8 it is slightly downregulated.

Throughout growth in YNB supplemented with acetate at pH 4.5, 7 and 8, *ATO2* was not induced. (**Figure 3-10**).

Overall, *C. neoformans* growing in nutrient limiting conditions instigate pH modulation towards alkaline conditions during which Ady2 was highly upregulated relative to glucose rich YPD.

Discussion and conclusions

In a previous study, we identified Ady2 as being the acetate transporter induced and required for uptake of deprotonated acetate during nutrient limitation. Moreover, Ato2 was required after prolonged exposure of *C. neoformans* to starvation (Dissertation Chapter 2). The requirement of acetate transporters during *in vivo* conditions that mimic the physiological environment encountered by *C. neoformans* during establishment of an initial lung infection led us to predict that acetate transport would play a significant role in *C. neoformans* pathogenicity by mediating metabolic adaptation to the different environmental niches afforded by the host.

In this study we sought to investigate the impact of loss of *ADY2* and *ATO2* on *C. neoformans* virulence. We expected that this diminished ability to execute metabolic adaptation to harsh physiologically-relevant conditions would impact *C. neoformans* capacity to persist in the host, thus resulting in diminished virulence. Therefore, we first explored the general morphology of H99, *ady2, ato2,* and *ady2ato2* followed by characterization of these strains during conditions that resulted in induction of virulence factors and survival in physiological niches both *in vitro* and *in vivo*. We found that loss of Ady2 and Ato2 led to cell-cell aggregation (**Figure 3-1a**) resulting in flocculation characterized by cell-cell aggregation forming clumps that settle in a pellet in liquid culture (**Figure 3-1b**). This phenotype is typically seen in the yeast *S. cerevisiae* after stopping cell division due to nutrient limitation (Smit et al., 1992).

A comprehensive look into genes that affect colony morphology implicated the *SNF1/PKA* pathway, a master programmer of metabolic and transcriptional activities of

cells in response to nutrient availability (Voordeckers, et al., 2012). Therefore, the impairment of *ady2ato2* strain in utilizing acetate as a sole carbon source to generate acetyl-CoA, a key central metabolic energy source, is in line with this flocculation phenotype. This clumping morphology is also typically seen in bacteria and yeast cells with increased expression of adhesins or adhesion proteins (Bumgarner et al., 2009; Schembri et al., 2004). Evidence of involvement of the *SNF1/PKA* signaling cascade in adaptation of the yeast *S. cerevisiae* to nutrient limitation (Voordeckers, et al., 2012) and in *C. neoformans* virulence factors (Hu et al., 2008) led us to hypothesize that disrupting Ady2 and Ato2 would perturb metabolism adaptation and the interconnections between virulence factor expression and pathogenesis. Consistent with this hypothesis, we found that loss of Ady2 and Ato2 led to impairment in major *C. neoformans* virulence determinants, specifically, defect in thermotolerance of mammalian body temperature (**Figure 3-2**), and impaired capsule formation (**Figure 3-3a**) also characterized by wrinkled, non-glossy colony morphology (**Figure 3-3b**).

C. neoformans Snf1 was found to be essential for virulence, melanin production, and growth on acetate at 37°C (Hu et al., 2008), which is similar to our observations of the thermosensitivity of *ady2ato2* and requirement of Ady2 during growth on acetate. We therefore infer that the effect of loss of Ady2 and Ato2 in regulating activity of acetate uptake may have impacted the intracellular acetyl-CoA pool such that loss of acetate transporters led to dysregulation of acetate flux. We hypothesize that this caused undesirable fluctuation in the pool of cellular acetyl-CoA, thus impacting cellular metabolic expenditures and the virulence-associated capsule acetylation hence deficient

attachment in the *ady2ato2* strain. We recommend performing an assay to determine intracellular levels of acetyl-CoA using commercially available kits. The PicoProbe Acetyl CoA Assay kit (Abcam) provides excellent sensitivity at pmol concentrations with the advantage of distinguishing and quenching CoA that are not complexed to acetate (Zhang et al., 2016).

Like *C. neoformans*, the bacterium *Escherichia coli* has a capsule whose polysaccharides provide immune and environmental protection hence classified as a virulence determinant. Schembri et al (2004) demonstrated that *E. coli* capsule shields the function of antigen 43 (Ag43), a self-recognizing adhesin that confers flocculation and cell-cell aggregation. Therefore, the observed cell-cell aggregation, wrinkled colony morphology and flocculation of the *ady2ato2* double mutant *C. neoformans* could be a result of impaired capsule attachment that leaves cell surface adhesins exposed. Western blots with specific antibodies to detect differentially shed capsule in supernatants of H99, *ady2, ato2* and *ady2ato2* strains during capsule inducing conditions could reveal a role of acetate transporters in capsule attachment.

Additionally, flocculation of *ady2ato2* may be attributable to this strain's disrupted homeostasis of intracellular acetyl-CoA reserves as a result of acetate uptake defect. This may in turn interfere with acetylation-mediated interconversion of chitin into chitosan, a fungal cell wall component that is required for bud separation resulting in flocculation and is quantifiable (Baker et al., 2007). In the event of failure in cell separation, flocculent cells would not be readily dispersed by mechanical agitation techniques such as sonication (Baker et al., 2007). Should such cells be mechanically

dispersed, it would be irreversible. Flocculent *Cryptococcus* strains are typically virulence-attenuated (Zaragoza et al., 2006; Wormley et al., 2005; Wang et al., 2012), which could partly be due to efficient clearance as a result of their diminished ability to evade immune recognition. These results from exposed cell surface antigens that become easily discernable by the host innate and humoral immune components upon loss of the capsule envelope.

Similar to observations of the flocculent clump+ strains reported by Zaragoza et al., (2006), we observed that unlike the wild type H99 and single mutant strains, *ady2* and *ato2*, the flocculent *ady2ato2* strain was relatively more susceptible to clearance by PMA-activated J774 macrophage-like cell line and human neutrophils. Zaragoza et al., (2006) observed that clump+ *C. neoformans* exhibited higher adherence to macrophage-like cell lines and were therefore more efficiently phagocytosed. Ady2 and Ato2 contributed to clearance by these phagocytes. Moreover, *ady2ato2* mutant's susceptibility to phagocytes anticryptococcal activity (**Figure 3-5**) was consistent with its capsule deficiency because the capsule has been reported to play a significant antiphagocytic role of *C. neoformans* by macrophages (Harrison and Levitz, 2002; Mukherjee and Casadevall, 1995), dendritic cells (Vecchiarelli et al., 2003) and neutrophils (Dong and Murphy, 1997). Mukherjee and Casadevall (1995) observed that complement-mediated phagocytosis of *C. neoformans* was dependent on the subcellular location of the major opsonin, complement component 3 (C3) in the polysaccharide capsule. They reported that an increase in capsule size diminished complement-mediated phagocytosis and pathogen clearance. These findings suggested a capsule-aided immune evasion

mechanism involving disruption of the location of C3 deposition hence inability to opsonize *C. neoformans* for host immune recognition (Zaragoza et al., 2003).

Impairment of the *ady2ato2* strain in melanin formation (**Figure 3-4a**) is likely linked to a relatively slower growth rate of this strain as it starts to melanize when a higher cell density is used (**Figure 3-4b**). Melanin formation results from phenoloxidase-mediated polymerization of such diphenolic compounds as dopamine (Rhodes et al., 1982). In the mammalian host, *C. neoformans* are hypothesized to utilize the diphenolic catecholamines in the brain to synthesize melanin hence protecting themselves against free radicals and successfully disseminating in the host (Jacobsen and Tinnel, 1993). Melanization was found to be protective against reactive oxygen and nitrogen species, and therefore conferred resistance to *C. neoformans* killing by macrophages' oxidative compounds (Wang and Casadevall, 1994).

The *ady2ato2* growth defect in the mammalian temperature, 37ºC was consistent with our hypothesis that disrupting acetate transport could upset crosstalk between effectors of the *SNF1/PKA* signaling cascade between metabolism adaptation and virulence factor elaboration. This hypothesis was also supported by Alspaugh et al., (2002) who observed that *C. neoformans SNF1* (the yeast ortholog of mammalian PKA) and its second messenger, cAMP are integral to the virulence factors; capsule and melanin formation and in virulence in a mouse model. Moreover, the fungal plant pathogen *Neurospora crassa* deficient in *PKA* are temperature sensitive and have an abnormal morphology (Bruno et al., 1996). Our findings suggest that Ady2 and Ato2 could be involved in this signaling pathway through nutrient sensing to relay survival

mechanisms that confer persistence in the host, thus enhancing the virulence of *C. neoformans*.

This temperature sensitivity to mammalian body temperature and capsule defect led us to hypothesize that this strain would be have virulence attenuation in the vertebrate (mouse) model (**Figure 3-6**). We hypothesized that the metabolic adaptation role of acetate transport could be induced by the dynamic mammalian environmental niches which provide a multiplicity of challenges that *C. neoformans* must either adapt to or modulate in order to facilitate persistence in the host. This neutral-alkaline pH is initially encountered as *C. neoformans* cells gain access to the lung tissue followed by a slightly acidic pH and nutrient limitation inside activated phagocytes that ingest them. Once in blood circulation, fungemia exposes *C. neoformans* to 5-7.5 mM glucose and a slightly alkaline pH of 7.4. Increase in pH compromises membrane proton gradient and diminishes uptake of nutrients as observed during growth of *C. neoformans*.

We also observed that Ato2 had a role in acetate uptake during prolonged starvation. Moreover, this study demonstrated that nutrient rich conditions in YPD caused media acidification (**Figure 3-7**) while nutrient limiting conditions under study led to media alkalinisation (**Figure 3-8, Figure 3-9**). This suggested that nutritional status affected pH dependent metabolic signaling. A connection between the pH responsive transcription factor, Rim 101 and the cAMP/PKA master regulator of nutritional-mediated control of cellular and biosynthetic cascades was observed in *C. neoformans* such that Rim101 mutants were defective in growth during alkaline conditions (Kronstad et al., 2011). Consistent with our observation that during growth in the glucose-rich YPD,

C. neoformans actively acidifies the media, Vylkova et al., (2011) observed that *C. albicans* media alkalinization was glucose repressible.

The ability to modulate pH is essential for optimal function of proteins during relevant conditions. Hence this study's observation of conditional pH adjustment by *C. neoformans* wild type, *ady2* and *ato2* single mutants but not the *ady2ato2* double mutant in response to preferred carbon source availability, suggests an involvement of Ady2 and Ato2 in active adaptation to dynamic niches of physiological relevance. A deletion of *C. albicans ATO5*, a *C. neoformans ADY2* and *ATO2* homolog, led to a defect in media alkalinization (Vylkova et al., 2011). A high pH generally affects nutrient bioavailability to *C. neoformans* especially during starvation. Changes in pH beyond ideal pKa of alternative carbon source affects overall charge, thus diminishing passive diffusion of alternative carbon sources across membranes and necessitating energy dependent nutrient uptake of charged carbon sources. This is substantiated by our observation that *ADY2* was both transcriptionally elevated (**Figure 3-10**) and required for acetate uptake during nutrient limitation at high pH but not during growth in nutrient rich YPD.

Our observation of induction of *ADY2* in nutrient limited YNB supplemented with 0.5 % acetate suggests a role of Ady2 in adaptation to nutrient limiting conditions in a pH dependent manner. Overall, *ATO2* was uninduced relative to *ADY2* (**Figure 3-10**) suggesting it is not involved in transcriptional pH regulation under the conditions tested. A slight fold change (2 and below) down-regulation of *ATO2* was observed in YPD at pH 4.5 and pH 8. As two-fold transcript variation is the cutoff below which gene expression changes are considered valid based on correlation of RT-qPCR and microarray analyses

(Rajeevan et al., 2001a; Rajeevan et al., 2001b), we interpreted this as *ATO2* being uninduced in both nutrient rich YPD and nutrient limited YNB supplemented with acetate. This observation of *ATO2* not being induced in neither YPD nor nutrient limited YNB supplemented with acetate (**Figure 3-10**) was expected as Ato2 was consistently not required for *C. neoformans* growth or acetate uptake until cells were subjected to prolonged starvation **(Dissertation Chapter 2).**

Generally, loss of Ady2 and Ato2 converged phenotypes, which together led to high attenuation of virulence, a complex phenotype governed by various adaptive properties of *C. neoformans*. From our observations of the role of acetate transport in metabolic adaptation that influences *C. neoformans* virulence, we hypothesize that regulation of acetate metabolism plays a central role in the cAMP/PKA signaling cascade, which master-regulates metabolism, facilitates catabolic pathways during energy limitation, and inhibits protein, carbohydrate, lipid biosynthesis, cell growth and proliferation. Pathogenic fungi characteristically induce this complex signaling cascade resulting in virulence-associated phenotypes during growth in physiological pH. Similarly, these adaptive features enable *C. neoformans* to colonize and persist in the host. The key players in these signaling cascades have not been characterized, we therefore recommend a comparative genome-scale characterization of the wild type H99 against the highly virulence attenuated *ady2ato2* strain to elucidate the coexpression networks and identify candidate genes that may be key players in this complex virulence phenotype.

References

Alspaugh JA, Pukkila-Worley R, Harashima T, Cavallo LM, Funnell D, Cox GM, Perfect JR, Kronstad JW and Heitman J, 2002. Adenylyl cyclase functions downstream of the Gα protein Gpa1 and controls mating and pathogenicity of *Cryptococcus neoformans*. *Eukaryotic Cell*, **1:**75-84.

Baker LG, Specht CA, Donlin MJ, Lodge JK, 2007. Chitosan, the deacetylated form of chitin, is necessary for cell wall integrity in *Cryptococcus neoformans*. *Eukaryotic Cell*. **6:**855-867.

Bruno KS, Aramayo R, Minke PF, Metzenberg RL and Plamann M, 1996. Loss of growth polarity and mislocalization of septa in a *Neurospora* mutant altered in the regulatory subunit of cAMP-dependent protein kinase. *The EMBO Journal*, **15:**5772.

Bubb WA, Wright LC, Cagney M, Santangelo RT, Sorrell TC and Kuchel PW, 1999. Heteronuclear NMR studies of metabolites produced by *Cryptococcus neoformans* in culture media: identification of possible virulence factors. *Magnetic Resonance in Medicine*, **42:**442-453.

Bumgarner SL, Dowell RD, Grisafi P, Gifford DK, Fink GR, 2009. Toggle involving cis-interfering noncoding RNAs controls variegated gene expression in yeast. *Proceedings of the National Academy of Sciences*, **106:**18321–18326.

Diamond RD, Bennett JE, 1973. Growth of *Cryptococcus neoformans* within human macrophages *in vitro*. *Infection and Immunity* **2:**231-236.

Diamond RD, May JE, Kane MA, Frank MM, Bennett JE, 1974. The role of the classical and alternate complement pathways in host defenses against *Cryptococcus neoformans* infection. *Journal of Immunology,* **112:**2260–2270

Dong ZM, and JW Murphy, 1997. Cryptococcal polysaccharides bind to CD18 on human neutrophils. *Infection and Immunity*, **65:**557-563.

Dunn-Meynell AA, Sanders NM, Compton D, Becker TC, Eiki JI, Zhang BB and Levin BE, 2009. Relationship among brain and blood glucose levels and spontaneous and glucoprivic feeding. *The Journal of Neuroscience*, **29:**7015-7022.

Harrison TS, and SM Levitz, 2002. *Cryptococcus neoformans* and macrophages. *Mycology Series*, **14:**539-558.

Himmelreich U, Allen C, Dowd S, Malik R, Shehan BP, Mountford C and Sorrell TC, 2003. Identification of metabolites of importance in the pathogenesis of pulmonary cryptococcoma using nuclear magnetic resonance spectroscopy. *Microbes and Infection*, **5:**285-290.

Hu G, Cheng PY, Sham A, Perfect JR and Kronstad JW, 2008. Metabolic adaptation in *Cryptococcus neoformans* during early murine pulmonary infection. *Molecular Microbiology*, **69:**1456-1475.

Jacobson ES, Tinnell SB, 1993. Antioxidant function of fungal melanin. *Journal of Bacteriology,* **175:**7102–7104.

Kronstad JW, Hu G and Choi J, 2011. The cAMP/protein kinase. A pathway and virulence in *Cryptococcus neoformans*. *Mycobiology*, **39:**143-150.

Kronstad J, Saikia S, Nielson ED, Kretschmer M, Jung W, Hu G, Geddes JM, Griffiths EJ, Choi J, Cadieux B and Caza M, 2012. Adaptation of *Cryptococcus neoformans* to mammalian hosts: integrated regulation of metabolism and virulence. *Eukaryotic Cell*, **11:**109-118.

Levitz SM, Harrison TS, Tabuni A and Liu X, 1997. Chloroquine induces human mononuclear phagocytes to inhibit and kill *Cryptococcus neoformans* by a mechanism independent of iron deprivation. *Journal of Clinical Investigation*, **100:**1640.

Llanos A, François JM and Parrou JL, 2015. Tracking the best reference genes for RT-qPCR data normalization in filamentous fungi. *BMC Genomics*, **16:**1.

Miller MF, Mitchell TG, 1991. Killing of *Cryptococcus neoformans* strains by human neutrophils and monocytes. *Infection and Immunity* **59:**24-28.

Mukherjee S, Lee SC and Casadevall A, 1995. Antibodies to *Cryptococcus neoformans* glucuronoxylomannan enhance antifungal activity of murine macrophages. *Infection and Immunity*, **63:**573-579.

Rajeevan MS, Ranamukhaarachchi DG, Vernon SD, Unger ER, 2001a. Use of real-time quantitative PCR to validate the results of cDNA array and differential display PCR technologies. *Methods*. **4:**443-51.

Rajeevan MS, Vernon SD, Taysavang N, Unger ER, 2001b. Validation of array-based gene expression profiles by real-time (kinetic) RT-PCR. *The Journal of Molecular Diagnostics*. **1:**26-31.

Rhodes JC, Wicker LS, Urba WJ, 1980. Genetic control of susceptibility to *Cryptococcus neoformans* in mice. *Infection and Immunity*. **29:**494-499.

Rohatgi S and Pirofski LA, 2015. Host immunity to *Cryptococcus neoformans*. *Future Microbiology*, **10:**565-581.

Schembri MA, Dalsgaard D, Klemm P, 2004. Capsule shields the function of short bacterial adhesins. *Journal of Bacteriology*, **186:**1249–1257.

Schmittgen TD and Livak KJ, 2008. Analyzing real-time PCR data by the comparative CT method. *Nature Protocols*, **3:**1101-1108.

Sloan DJ and Parris V, 2014. *Cryptococcal meningitis*: epidemiology and therapeutic options. *Clinical Epidemiology*, **6:**169-182.

Smit G, Straver MH, Lugtenberg BJ and Kijne JW, 1992. Flocculence of *Saccharomyces cerevisiae* cells is induced by nutrient limitation, with cell surface hydrophobicity as a major determinant. *Applied and Environmental Microbiology*, **58:**3709-3714.

Vecchiarelli A, Pietrella D, Lupo P, Bistoni F, McFadden DC and Casadevall A, 2003. The polysaccharide capsule of *Cryptococcus neoformans* interferes with human dendritic cell maturation and activation. *Journal of Leukocyte Biology*, **74:**370-378.

Voordeckers K, De Maeyer D, Zande E, Vinces MD, Meert W, Cloots L, Ryan O, Marchal K and Verstrepen KJ, 2012. Identification of a complex genetic network underlying *Saccharomyces cerevisiae* colony morphology. *Molecular Microbiology*, **86:**225-239.

Vylkova S, Carman AJ, Danhof HA, Collette JR, Zhou H and Lorenz MC, 2011. The fungal pathogen *Candida albicans* autoinduces hyphal morphogenesis by raising extracellular pH. *MBio*, **2:**e00055-11.

Wang Y, Casadevall A, 1994. Susceptibility of melanized and nonmelanized *Cryptococcus neoformans* to nitrogen- and oxygen-derived oxidants. *Infection and Immunity*, **62:**3004-3007.

Wang L, Zhai B and Lin X, 2012. The link between morphotype transition and virulence in *Cryptococcus neoformans*. *PLoS Pathogens*, **8:**e1002765.

Wormley FL, Jr, Heinrich G, Miller JL, Perfect JR, Cox GM, 2005. Identification and characterization of an *SKN7* homologue in *Cryptococcus neoformans*. *Infection and Immunity*, **73:**5022–5030

Zaragoza O, Taborda CP and Casadevall A, 2003. The efficacy of complement-mediated phagocytosis of *Cryptococcus neoformans* is dependent on the location of C3 in the polysaccharide capsule and involves both direct and indirect C3-mediated interactions. *European Journal of Immunology*, **33:**1957-1967.

Zaragoza O, Casadevall A, Fries BC, 2006. Characterization of a flocculation-like phenotype in *Cryptococcus neoformans* and its effects on pathogenesis. *Cellular Microbiology*, **8:**1730–1739.

Zhang Y, Zhao Z, Ke B, Wan L, Wang H, Ye J, 2016. Induction of posttranslational modifications of mitochondrial proteins by ATP contributes to negative regulation of mitochondrial function. *PloS One*. **3:**e0150454.

a)

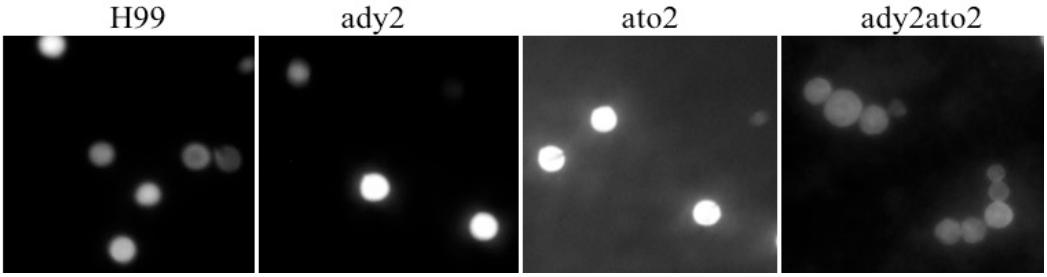

b)

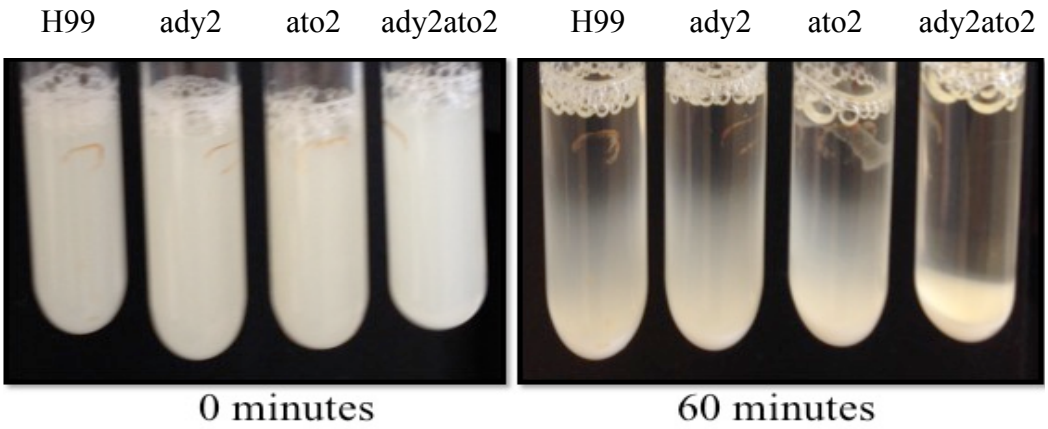

Figure 3-1. Loss of Ady2 and Ato2 causes flocculation and cell-cell aggregation: **A. Strains and morphological characterization. a)** Cell-cell aggregation was observed by fluorescent microscopy of Calcofluor White-stained *C. neoformans* under x40 magnification. **b)** *C. neoformans* wildtype, *ady2*, *ato2,* and *ady2ato2* were grown in the minimal medium, YNB supplemented with 0.2 % glucose. Flocculation from cell-cell aggregation of *C. neoformans* cultures grown to mid-log phase was observed by simultaneously resuspending the liquid cultures, then allowing them to settle such that the most flocculent strain was the first to settle at the bottom of the culture suspension.

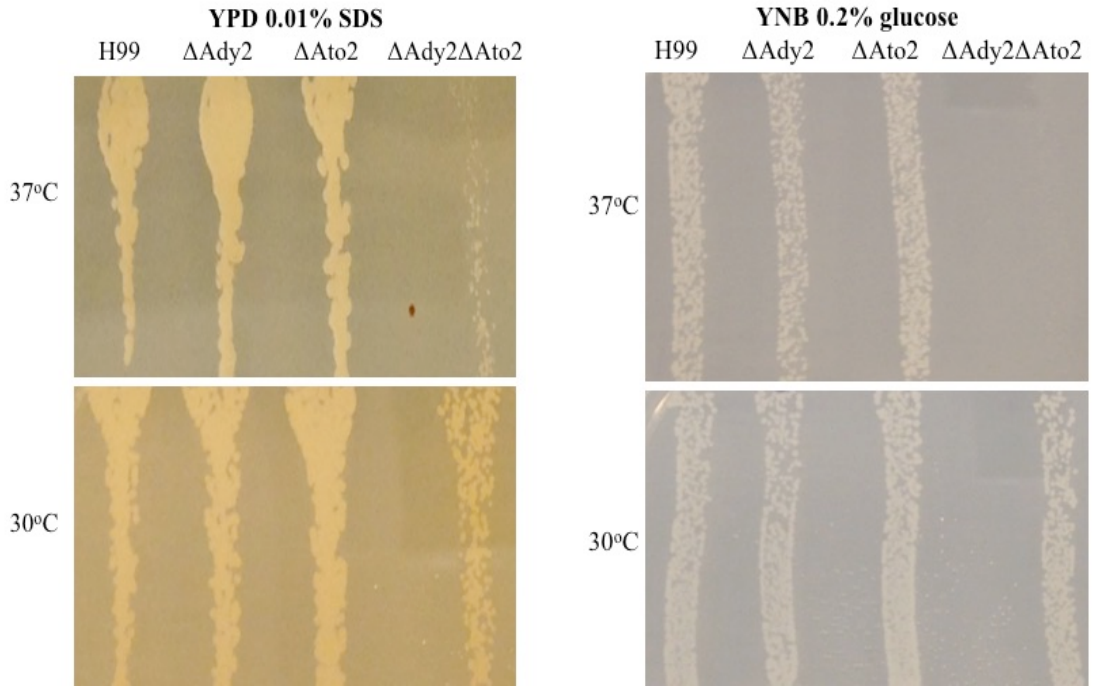

Figure 3-2. Loss of Ady2 and Ato2 impairs ability of *C. neoformans* to thrive at human body temperature. H99 and mutants lacking *ADY2* and *ATO2* were grown in overnight YPD starter cultures at 30°C to log phase then washed and 10,000 cells were spotted onto plates and allowed to roll in columns on YPD plates containing a membrane stressor and YNB plate supplemented with 0.2 % glucose. They were incubated at 37°C and contrasted to 30°C-grown cells.

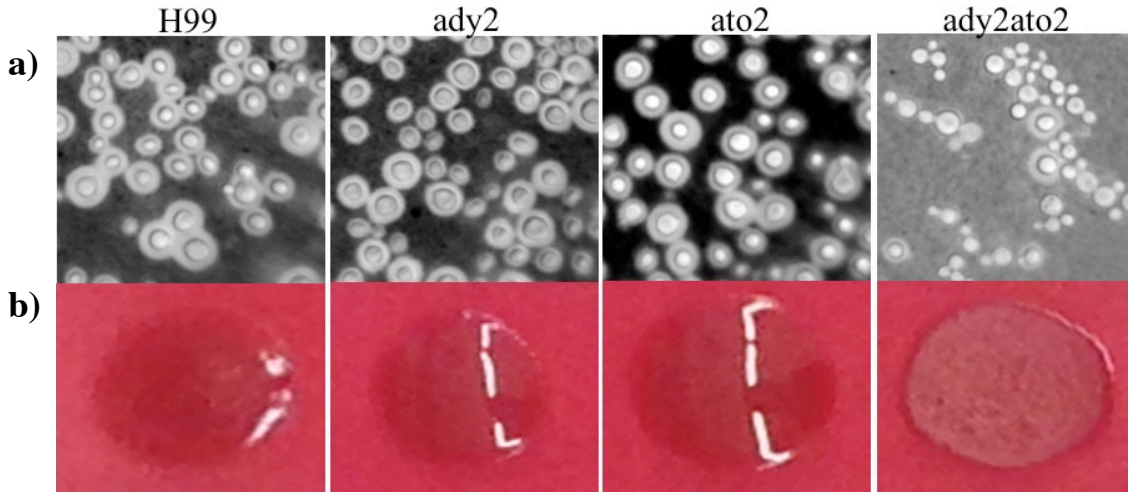

Figure 3-3. Loss of Ady2 and Ato2 impairs ability of *C. neoformans* to secrete capsule. **a)** Overnight YPD cultures of H99, *ady2*, *ato2* and *ady2ato2* were grown in CO_2-independent media at 37ºC. A dense cell suspension of the strains was stained in India ink at a 1:1 ratio and the capsule was visualized as a halo around encapsulated cells when observed by light microscopy. **b)** Colony morphology of encapsulated H99, *ady2*, and *ato2* versus the unencapsulated *ady2ato2* was observed on capsule inducing agar (CO_2-independent media for mammalian cell culture containing 2 % agar).

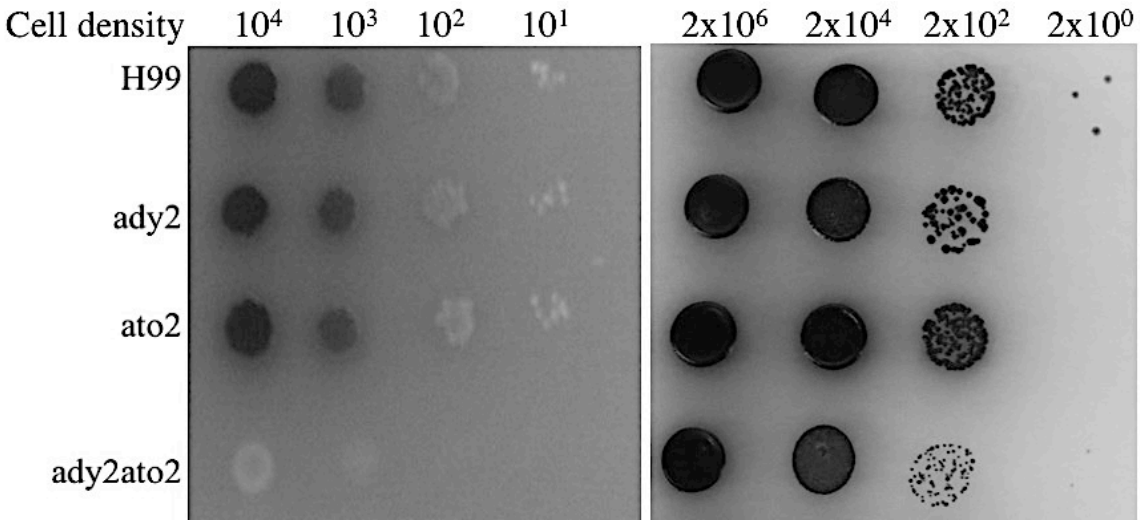

Figure 3-4. Loss of Ady2 and Ato2 slows melanization of *C. neoformans* in a cell density and growth rate dependent manner. H99, *ady2, ato2*, and *ady2ato2* strains were grown in overnight YPD starter cultures at 30ºC to log phase, washed in sterile nanopure water and 10,000 cells were spotted onto synthetic media plates supplemented with 1 mM dopamine at 4 serial dilutions. The cells were then left to grow in the dark at 30ºC and melanin production was observed by dark pigmentation of the colonies.

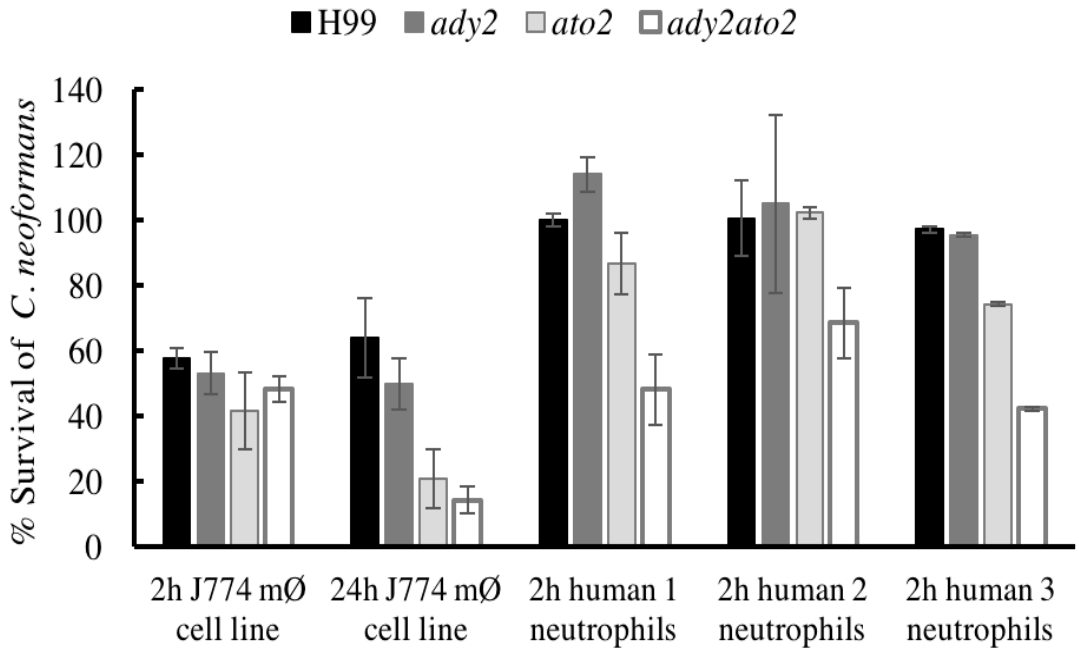

Figure 3-5. Ady2 and Ato2 contribute to *C. neoformans* survival during coculture with phagocytes. Overnight H99, *ady2, ato2* and *ady2ato2* cells were grown in YPD and resuspended to 1,000 cells/μL in PBS. 80,000 activated J774.16 macrophages (mØ) and 10,000 opsonized *C. neoformans* were cocultured at 37ºC with gentle shaking for 2 hours or 24 hours. Macrophages were lysed and percent surviving CFUs was determined. For neutrophils coculture with *C. neoformans*, blood and serum were obtained from three healthy human blood donors (human 1, human 2 and human 3). Human neutrophils were concentrated. 80,000 neutrophils and 10,000 *C. neoformans* cells were cocultured for 2 hours at 37ºC. Percent surviving CFU of *C. neoformans* were determined. Error bars indicate standard deviation from the mean CFU.

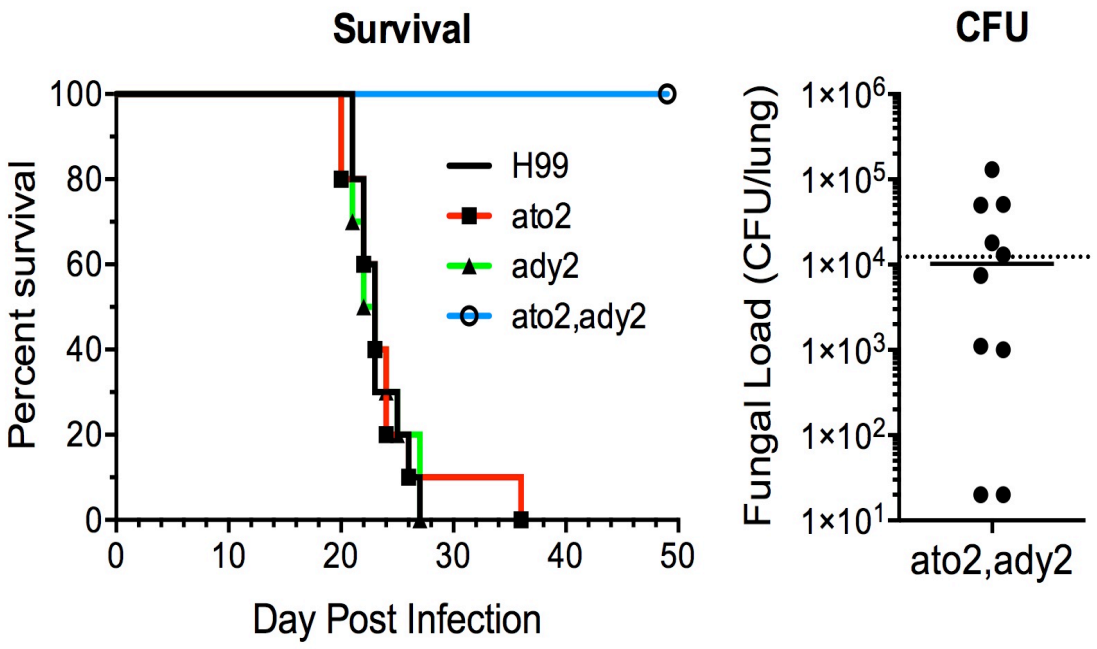

Figure 3-6. Ady2 and Ato2 are collectively essential for virulence of *C. neoformans*. Using a finely tipped pipette inserted into the mouth, 10,000 *C. neoformans* were inoculated into temporarily anaesthetized C57BL/6 mice (6-7 weeks old) in two biological replicates with five mice per H99, *ady2*, *ato2*, and *ady2ato2* strain. Mortality was determined every 24 hours. To determine fungal load in the mice infected with *ady2ato2* strain murine lungs were harvested, weighed and homogenized. Colony forming units (CFU) from lung were determined. This experiment was performed in the Levitz lab, Infectious Disease and Immunology, Department of Medicine, University of Massachusetts Medical School, Worcester, MA.

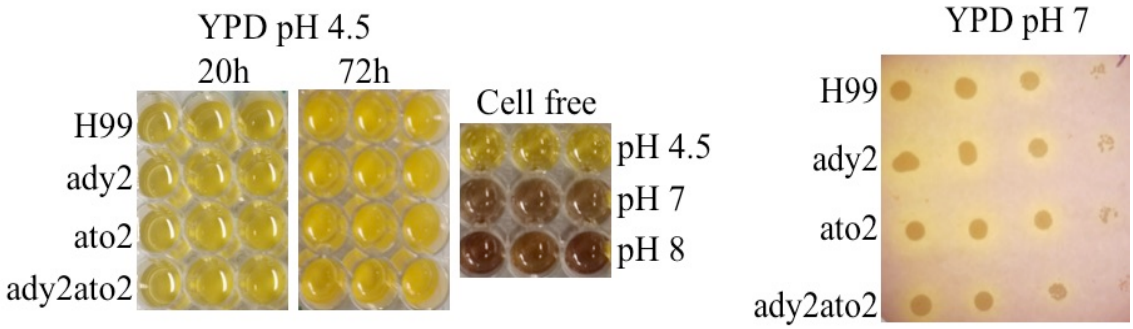

Figure 3-7. Ady2 and Ato2 are not essential for acidifying YPD. The ability to modulate pH in nutrient rich YPD containing the pH indicator, bromocresol purple was investigated by inoculating YPD liquid media with H99, *ady2*, *ato2* and *ady2ato2* strains then incubated at 30ºC Colour changes were observed after 20 hours and 72 hours. Colour changes relative to pH were calibrated by cell free media adjusted to pH 4.5, pH 7 and pH 8. Four 10-fold serial dilutions of H99, *ady2*, *ato2* and *ady2ato2* started at OD 600 of 0.2 were spotted onto YPD agar containing the pH indicator, bromocresol purple adjusted to pH 4.5 and 7.0 then incubated at 30ºC.

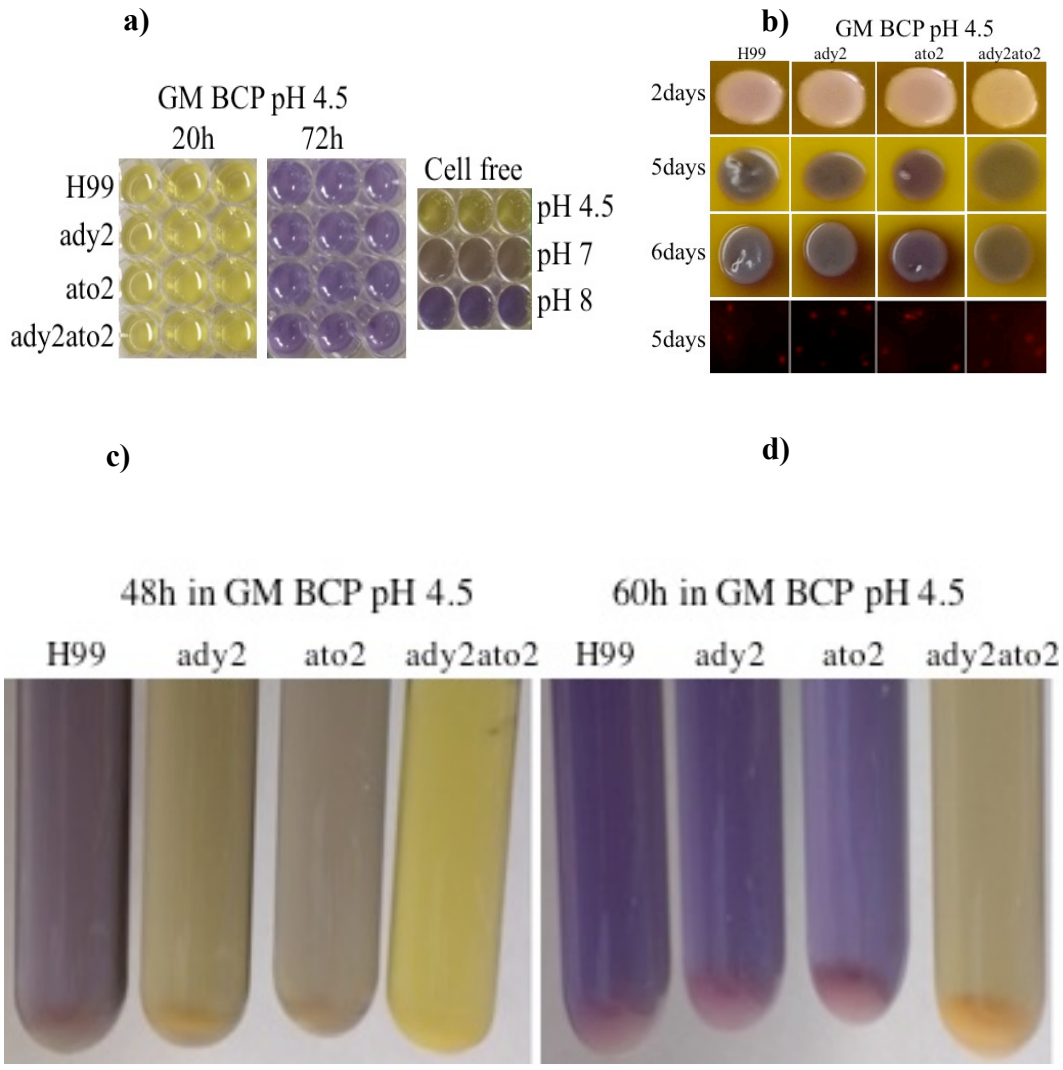

Figure 3-8. Ady2 and Ato2 are required to raise pH of nutrient poor media.

Four 10-fold serial dilutions of H99, *ady2, ato2* and *ady2ato2* started at OD 600 of 0.2 were spotted onto GM-BCP agar and liquid cultures supplemented with 0.5 % acetate and adjusted to pH 4.5. The set up was incubated at 30ºC. **a)** Cells growing at pH 4.5 alkalinize GM-BCP after 72 hours as indicated by the colour calibration of the cell-free GM-BCP **b)** *C. neoformans* growing for 48 hours in GM-BCP media initially adjusted to pH4.5. The lowest panel shows a cytosolic pH sensitive stain, pHRodo® which was used

to stain cells as their pH adjusted and colony colour changed. **c)** H99, and *ato2* are the first to start alkalinizing GM-BCP while **d)** *ady2* and especially *ady2ato2* are slow in GM-BCP alkalinization.

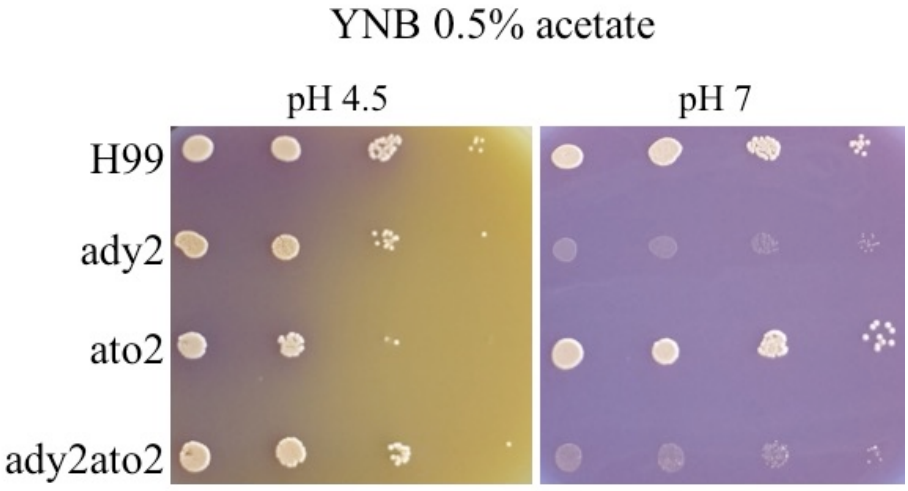

Figure 3-9. Ady2 is essential during growth on acetate at high pH. Four 10-fold serial dilutions of H99, *ady2, ato2* and *ady2ato2* were spotted onto minimal media, YNB agar supplemented with 0.5 % acetate and adjusted to pH 4.5 and 7.0 then incubated at 30ºC.

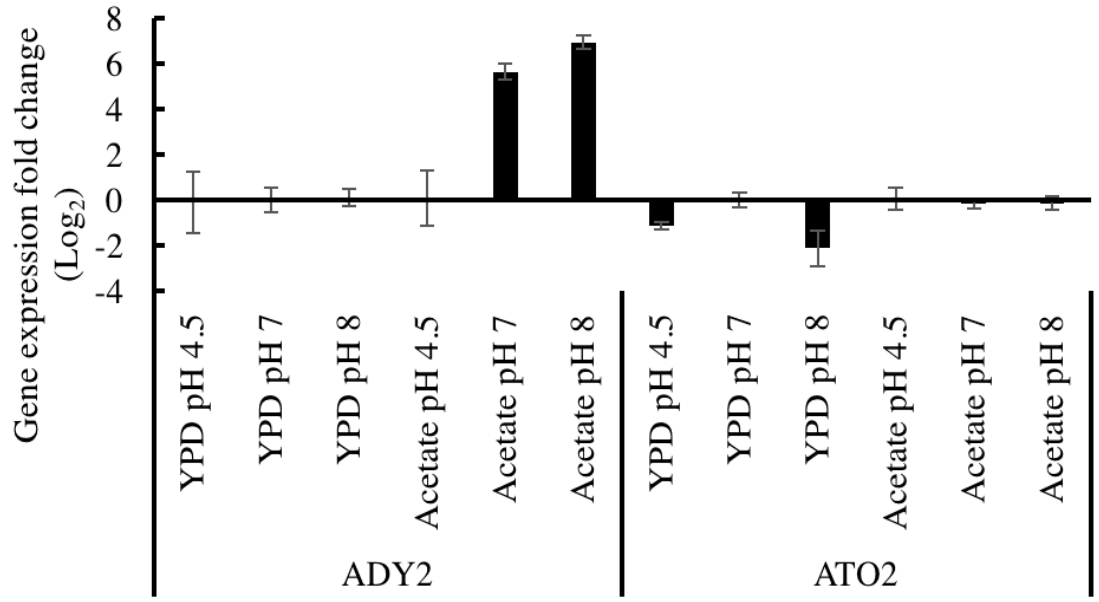

Figure 3-10. *ADY2* is upregulated in acetate at high pH while *ADY2* and *ATO2* are not induced in YPD at varying pH. After 20 hours of *C. neoformans* growth in YPD and YNB supplemented with 0.5 % acetate (acetate) at their respective pH at 30ºC, total RNA was isolated and quantitative RT-PCR (RT-qPCR) was performed. Resulting data on expression of *ADY2* (CNAG_05678) and *ATO2* (CNAG_05266) were analyzed relative to the reference (*UBC6*) and control genes (*ACT1*) as described by Schmittgen TD and Livak KJ., (2008). Error bars indicate standard deviation from mean Log_2 of gene expression fold change values.

Investigating the roles of *Cryptococcus neoformans* Ady2 and Ato2 in virulence during infection of the invertebrate model, *Galleria mellonella*

Grace N. Kisirkoi, Bridget Luckie, Lauren Tracy, and Kerry S. Smith

Department of Genetics and Biochemistry

Eukaryotic Pathogens Innovation Center (EPIC)

Clemson University

Clemson, SC 29634

To whom correspondence should be addressed:

Kerry S. Smith

Office 864-656-6935

Email kssmith@clemson.edu

CHAPTER FOUR

Abstract

Our observations of a defect of the *ady2ato2* double mutant strain during growth at 37ºC and capsule formation conditions, led us to speculate that *ady2ato2* would not be as virulent as H99 because of a possible interactive role of Ady2 and Ato2 that contribute to virulence of *Cryptococcus neoformans*. This is because ability to grow at mammalian body temperature of 37ºC and secrete a characteristic polysaccharide capsule are known virulence determinants of *C. neoformans* (Kronstad et al., 2011). The transcript levels of genes encoding acetate transporters and acetyl-CoA synthetase (Acs) were elevated during mouse lung infection (Hu et al., 2008). Furthermore, expression studies of *C. neoformans* phagocytosed by lung alveolar macrophages, which combat an initial infection, reveal a glucose- and amino acid-poor environment (Feldmesser et al., 2000; Feldmesser et al., 2001). Therefore, this likely necessitates utilization of such nonpreferred carbon sources as lactate and acetate early in establishment of a pulmonary infection (Barelle et al., 2006; Lorenz et al., 2004). Facilitated uptake of acetate could be an important survival strategy when carbon-sources are limiting. We postulated that acetate transporters shuttled acetate for subsequent activation by Acs to acetyl-CoA thus feeding into central carbon metabolism and adaptation to mammalian niches, hence facilitating virulence. The wax worm larvae *Galleria mellonella* has been demonstrated to be an invertebrate model for a number of bacterial and fungal pathogens (Mylonakis, et al., 2005; Garcia-Solache, et al., 2013; Sabiiti, et al., 2011). We demonstrated that both the *ady2ato2* double mutant was avirulent to this model at 37ºC while the single

ady2 and *ato2* mutants had attenuated virulence. As an *acs* null mutant was attenuated in virulence in the mouse model, we included it in our *G. mellonella* experimental groups to provide a mouse model parallel. Here, we further highlight a role in virulence of *ady2* and *ato2* as observed in the *G. mellonella* larvae.

Introduction

The wax moth larva, *G. mellonella* is an inexpensive model used to evaluate the virulence of numerous pathogenic fungi and bacteria (Mylonakis, et al., 2005; Garcia-Solache, et al., 2013; Sabiiti, et al., 2011). It is a good model because its size and morphology allows systemic introduction of known concentrations of inoculum as its proleg if slightly depressed opens up an aperture where a needle containing inocula or drug is inserted and reseals without significant trauma. This helps immune responses to capitalize on the invading infection rather than tissue repair. The ability to live at human body temperature, yield results similar to mouse trials, low-maintenance requirements, and capacity to respond to known antimicrobial agents that typically clear or ease infections in humans all make *G. mellonella* desirable as a virulence model especially for organisms whose pathogeneses involve systemic circulation (Mylonakis, et al., 2005; Garcia-Solache, et al., 2013; Sabiiti, et al., 2011).

As a cryptococcal model, *G. mellonella* mimics the mammalian system's immune reactions consisting of structural, passive, cellular, and humoral responses to infection including phagocytosis, melanization, and encapsulation of large invading pathogens by hemocyte layers (London, 2006). Like the mammalian system, *G. mellonella* survival is improved by anticryptococcal treatment using amphotericin B, flucytosine or fluconazole given to a larva post infection with *C. neoformans* (Mylonakis et al., 2005). The cost effectiveness, ease of experimental manipulations, similarity to mouse trials, and relevance to mammalian immune reactions made *G. mellonella* an exceptionally desirable model organism for our purposes before embarking on the costlier mouse trials

graciously performed by the Levitz lab as described in **Chapter 3**. Necessity of mouse trials was highlighted by a few concerns about *G. mellonella*. Its genome is yet to be sequenced, limiting its genetic tractability. Moreover, lack of such visceral organs as lungs and brain limits the scope of virulence studies that could be used to decipher disseminated *C. neoformans* at the point of pulmonary colonization and cryptococcal meningoencephalitis (Garcia-Solache, et al., 2013).

Materials and methods

In order to determine relative virulence of H99, *ady2, ato2* and *ady2ato2 C. neoformans* strains, *G. mellonella* were infected and handled through a technique adapted from Kozubowski and Heitman (2010) and London (2006). The strains were cultured in yeast extract peptone dextrose (YPD-Difco™) medium at 30ºC to mid-log phase. Residual cells were collected by centrifugation, then washed thrice in phosphate buffered saline (PBS) buffered at pH 7.4 (Difco™). The washed cells were then resuspended to a concentration of 1 X 10^5 cells/μL. Prior to injection, the area of inoculation was swabbed with 70 % ethanol to prevent interfering systemic cross-infection with surface bacterial normal flora of *G. mellonella*. 10 μL of the cell suspension was injected using a 10 μL Hamilton syringe into the left terminal pseudopod region of the larvae. A control group received 10 μL of sterile, cell-free PBS.

Larvae were incubated at 37ºC. Determining CFU counts was performed 48 hours post infection by first immobilizing and anaesthetizing the larvae at -20ºC for 15 minutes. Immobilized larvae were then suspended in 1 mL of sterile PBS buffered at pH 7.4 (containing 1 % of PenStrep stock containing 10,000 μg/mL of Penicillin and Streptomycin, ThermoFisher™). Larvae were then ground using a 607 Mini-BeadBeater 16 (MIDSCI™) for 30 seconds to obtain a homogenate of full larval contents. 5 x 10^3 dilutions of these homogenates were spread onto YPD plates such that should the inoculum size have stayed constant in the infected larvae 200 colonies would be obtained. Plates were incubated at 30ºC and colonies were counted 48 hours later. Melanization and mortality resulting from infection was checked by counting dead *G. mellonella* every

24 hours and was plotted on a Kaplan-Meier plot generated by Kaleidagraph version 3.51 (Synergy Software, Reading, PA). The survival studies were performed in biological duplicates with each experimental treatment having ten individuals while the treatments used to determine melanization had five individuals per group.

Results and discussion

We investigated the relative virulence of *C. neoformans* H99, *ady2, ato2* and *ady2ato2* strains in the *G. mellonella* invertebrate model and observed a requirement of Ady2 for virulence in this model. Loss of Ady2 led to highly attenuated virulence of *ady2* and *ady2ato2* while null mutation of Ato2 and Acs had reduced virulence (**Figure 4-1**). The *G. mellonella* infected with wild type H99 strain all died by the fourth day that this experiment was carried out followed by the *ato2*-infected group, which died by day seven. When the experiment was terminated on day nine, 10 % of the *acs*-infected, 90 % of the *ady2*-infected, and 90 % of the *ady2ato2*-infected were still alive. This suggested that *ady2* and *ady2ato2* strains are avirulent while *ato2* and *acs* srains are virulence-attenuated in the *G. mellonella* invertebrate model under the conditions tested (**Figure 4-1**). This suggests that Ady2 is essential for virulence under the conditions tested while Ato2 and Acs contributes to full virulence of *C. neoformans*. The Acs observation was similar to results from mice experiments by Hu et al., (2008).

After 48 hours of infection, the highest CFU count obtained was 250,000 in an *ato2*-infected larva, which is 4-fold lower than the original inoculum (**Figure 4-2**). Approximately 80 % of the larvae had CFUs below our detectable threshold, suggesting that they were still successfully combating *C. neoformans* infection after 48 hours. We recommend a similar study to check CFU after prolonged infection as opposed to 48 hours and determine the relative roles of Ady2 and Ato2 in proliferation and persistence of *C. neoformans* in the host. The infected *G. mellonella* also mounted an active immune response to the infection as demonstrated by their melanization (Browne and Kavanagh.,

2013) (**Figure 4-3a**). Between 20-25 % of the H99, *ady2,* and *ato2*-infected larvae had melanized while the avirulent *ady2ato2* had not (**Figure 4-3b**).

The virulence associations of *ADY2* and *ATO2* to the *C. neoformans* major virulence determinants of capsule formation, and ability to grow at 37ºC as described in **Chapter 3** also complement our observations of a virulence phenotype in *G. mellonella*. Despite the desirable traits of *G. mellonella* of being inexpensive, experimentally manipulable at various temperatures, and significant similarities with mammalian cell mediated immune reaction to infection, lack of such visceral organs as lungs and brain limits the mouse-*Galleria* parallels at the point of pulmonary colonization and cryptococcal meningoencephalitis (Garcia-Solache, et al., 2013). The mouse infection route described in **Chapter 3** mimics the natural infection of humans. Similar to our mouse model results described in **Chapter 3**, we saw consistency in the *G. mellonella* as the *ady2ato2* was just avirulent. Although a recent study did not find a consistent correlation between *Galleria* and murine virulence in clinical strains, a correlation did exist between *Galleria* and murine virulence in highly passaged laboratory strains, such as the H99 strain used in our studies (Bouklas et al., 2015).

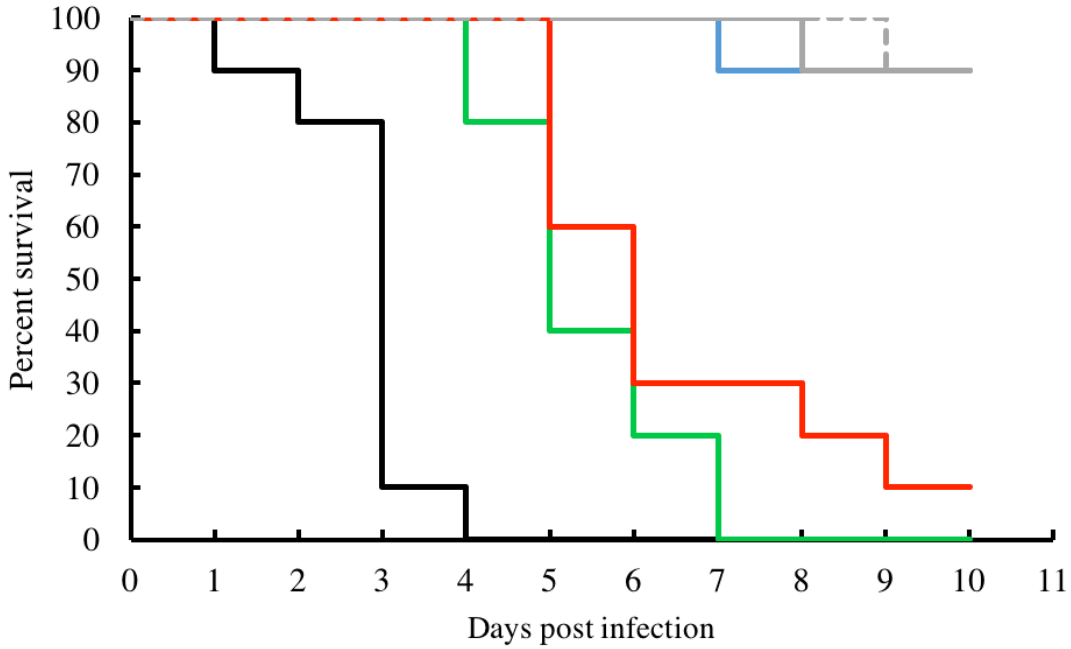

Figure 4-1. Ady2 is essential for virulence in *G. mellonella*: *Cryptococcus neoformans* strains H99 (—), *ady2* (—), *ato2* (—), *ady2ato2*, (—), *acs* (—) were cultured overnight in 2 mL of YPD, then diluted to 1 x 10^5 cells/mL in PBS buffered at pH 7.4. 10 µL of the cell suspension and *Cryptococcus* - free PBS (- - -) was injected into the last left proleg of 0.27 g-0.33 g white, non-melanized *G. mellonella* in two biological replicates with ten larvae per strain. Mortality was determined by observing larvae every 24 hours and removing dead or moribund ones.

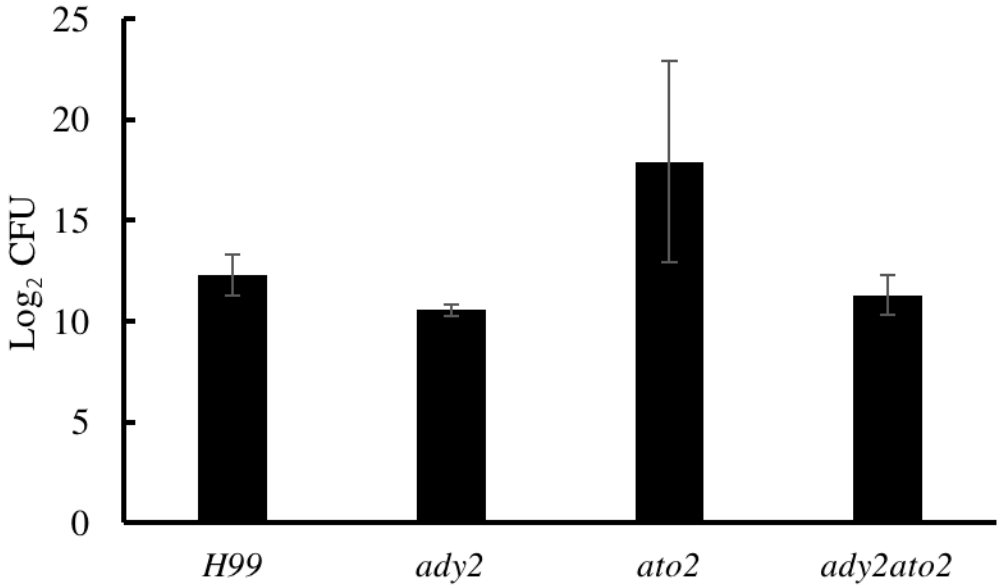

Figure 4-2. After 48 hours of infection, CFU counts of *C. neoformans* H99, *ady2, ato2* and *ady2ato2* in *G. mellonella* are below the original infection load of Log_2=20 ($1x10^6$). *G. mellonella* were infected with H99, *ady2, ato2* and *ady2ato2* and incubated at 37°C. After 48 hours, their lysates were obtained and spotted onto YPD plates to determine CFU counts. Error bars indicate the standard deviation from the mean CFU.

a)

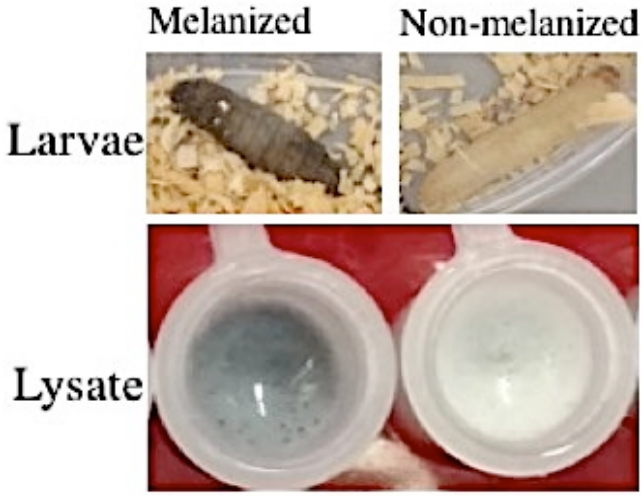

b)

Strain in *G. mellonella*	H99	*ady2*	*ato2*	*ady2ato2*
Percent melanized *G. mellonella*	20	20	25	0

Figure 4-3. After 48 hours of infection, Ady2 and Ato2 contributed to larva melanization. a) The melanized larvae and lysates of *G. mellonella* infected with H99, *ady2*, and *ato2* but not *ady2ato2* were observed to have darkened. **b)** Percent melanization of *G. mellonella* infected with H99, *ady2*, *ato2* and *ady2ato2* and incubated for 48 hours at 37°C was determined.

References

Barelle CJ, Priest CL, MacCallum DM, Gow NA, Odds FC and Brown AJ, 2006. Niche-specific regulation of central metabolic pathways in a fungal pathogen. *Cellular Microbiology*, **8:**961-971.

Bouklas T, Diago-Navarro E, Wang X, Fenster M, Fries BC, 2015. Characterization of the virulence of *Cryptococcus neoformans* strains in an insect model. *Virulence*, **6**:809-813.

Browne N, Kavanagh K, 2013. Developing the potential of using *Galleria mellonella* larvae as models for studying brain infection by *Listeria monocytogenes*. *Virulence*, **4:**271-272.

Feldmesser M, Kress Y, Novikoff P and Casadevall A, 2000. *Cryptococcus neoformans* is a facultative intracellular pathogen in murine pulmonary infection. *Infection and Immunity*, **68:**4225-4237.

Feldmesser M, Tucker S and Casadevall A, 2001. Intracellular parasitism of macrophages by *Cryptococcus neoformans*. *Trends in Microbiology*, **9:**273-278.

Garcia-Solache MA, Izquierdo-Garcia D, Smith C, Bergman A, Casadevall A, 2013. Fungal virulence in a Lepidopteran model is an emergent property with deterministic features. *mBio*, **4:**1-9.

Hu G, Cheng PY, Sham A, Perfect JR, Kronstad JW. 2008. Metabolic adaptation in *Cryptococcus neoformans* during early murine pulmonary infection. *Molecular Microbiology*, **69:**1456-1475.

Kozubowski L and J Heitman, 2010. Septins enforce morphogenetic events during sexual reproduction and contribute to virulence of *Cryptococcus neoformans*. *Molecular Microbiology,* **75:**658-675.

Kronstad JW, Attarian R, Cadieux B, Choi J, D'souza CA, Griffiths EJ, Geddes JM, Hu G, Jung WH, Kretschmer M. and Saikia S, 2011. Expanding fungal pathogenesis: *Cryptococcus* breaks out of the opportunistic box. *Nature Reviews Microbiology*, **9:**193-203.

London R, Orozco BS, Mylonakis E. 2006. The pursuit of cryptococcal pathogenesis: heterologous hosts and the study of cryptococcal host–pathogen interactions. FEMS *Yeast Research*, **6:**567-573.

Lorenz MC, Bender JA and Fink GR, 2004. Transcriptional response of *Candida albicans* upon internalization by macrophages. *Eukaryotic Cell*, **3:**1076-1087.

Mylonakis E, Moreno R, El Khoury JB, Idnurm A, Heitman J, Calderwood SB, Ausubel FM, Diener A, 2005. *Galleria mellonella* as a model system to study *Cryptococcus neoformans* pathogenesis. *Infection and Immunity*, **73:**3842-3850.

Sabiiti W, May RC, Pursall ER, 2011. Experimental models of cryptococcosis. *International Journal of Microbiology*, **2012:**1-10

Western blot analysis to confirm full length mCherry::Ady2 following fluorescent microscopy

Grace N. Kisirkoi and Kerry S. Smith

Department of Genetics and Biochemistry

Eukaryotic Pathogens Innovation Center (EPIC)

Clemson University

Clemson, SC 29634

To whom correspondence should be addressed:

Kerry S. Smith

Office 864-656-6935

Email kssmith@clemson.edu

CHAPTER FIVE

Abstract

The *Cryptococcus neoformans* acetate transporter Ady2 is required and induced by acetate during growth in minimal media supplemented with low acetate (≤ 0.5 %) (**Chapter 2**). In order to determine the subcellular localization of Ady2 particularly during conditions when Ady2 is required we tagged the N terminal region of Ady2 using mCherry under constitutive expression, transformed the construct into *ady2* strains lacking *ADY2* with the dual goal of complementing this strain as well as subcellular localization by fluorescent microscopy. We determined stable construct integration and protein translation using Western blot and found that *mCHERRY* had been cleaved in subsequent generations, and eventually not present when genomic DNA was analyzed. Consistent with this observation, the subsequent generations of this fluorescent *ady2ADY2* strain gradually lost ability to grow in minimal acetate as sole carbon source, a trait characteristic of strains stably expressing wild type *ADY2*. This suggested that the N-terminally tagged *mCHERRY::ADY2* strain had not been stably integrated or an ectopic construct was not heritable in subsequent passaged generations.

Introduction

In a bid to determine the subcellular localization of Ady2 during varied conditions, we tagged *ADY2* at its N terminal with *mCHERRY* using the plasmid pLKB55, graciously provided by Dr. Lukasz Kozubowski (Clemson University). To do this, we created a construct that fused *mCHERRY* upstream of *ADY2* under the constitutive expression of *GPD1* (glycerol-3-phosphate dehydrogenase) promoter as published (Kozubowski et al., 2011). We identified the pLKB55 vector with the *mCHERRY::ADY2* by PCR, Using PDS-1000/He™ biolistic particle delivery system (Bio-Rad™), we transformed the construct into mutant strain intending for the dual purpose of complementing this *ady2* strain and characterizing nutrient-mediated localization of Ady2. We then determined stable integration and translation of mCherry::Ady2 using Western blot analysis.

Materials and methods

Construction of *mCHERRY::ADY2*

Plasmid DNA was isolated from an overnight pLKB55 cultures grown at 37ºC in LB (ThermoFisher™) containing 100 µg/mL Ampicillin (ThermoFisher™). This plasmid also contained the gene that confers Hygromycin resistance (*HYG*). Genomic DNA was also isolated from an overnight wild type, H99 culture grown at 30ºC in YPD (Dicfo™). The open reading frame (ORF) of *ADY2* in addition to 0.3 kb upstream was amplified using forward primers that introduced the NheI restriction endonuclease recognition site ($^{5'}$GCTAGC$^{3'}$) and reverse primer that introduced the Pac1 restriction endonuclease recognition site ($^{5'}$TTAATTAA$^{3'}$) and alleviated the *ADY2* ORF stop codon. These restriction endonuclease sites were also in the pLKB55 vector downstream of *mCHERRY* into which *ADY2* was cloned. The *mCHERRY::ADY2* construct was under the constitutive expression of the *GPD1* promoter.

Biolistic Transformation of *mCHERRY::ADY2* into *Cryptococcus neoformans*

Biolistic transformation was performed according to the methods described by Taylor et al., (2015) and the Molecular Mycology Course Handbook (2016).

Strain preparation: Using primers that anneal to the pLKB55 backbone, *ADY2* insertion downstream of *mCHERRY* was confirmed. The full length *mCHERRY::ADY2* would be 2.63kb while an empty vector would result in a 0.3kb amplicon. Confirmed transformant's plasmid DNA was isolated and 5 µg was introduced into *C. neoformans* strains lacking *ADY2* with the dual goal of complementing this strain and determine the subcellular localization of *ADY2*. To do this, the *ady2* strain was grown overnight in YPD

at 30ºC. An equivalent of OD 600 = 3.0 of cells were pelleted by centrifugation at 3,000 x g, resuspended in 5 mL of sterile nanopure water and 200 uL of this suspension was spread onto transformation plates (YPD supplemented with 1 M sorbitol). These plates were allowed to grow at 30ºC for 3 hours.

DNA preparation: DNA macrocarrier membranes (Bio-Rad™) were dipped into 100 % Ethanol (ThermoFisher) and set aside to dry in a petri-dish containing Drierite® (ThermoFisher). 10 uL of vigorously vortexed gold beads, 5 μg of plasmid DNA containing the *mCHERRY::ADY2* construct, 10 μL of 2.5 M $CaCl_2$, and 2 μL of 1 M spermidine-free base, were then added to microfuge tubes and incubated at ambient temperature for 10 minutes. 500 μL of 100 % Ethanol was then added, vortexed, and pelleted by vortexing at 300 x g for 1 minute. The supernatant was aspirated and discarded then this process was repeated once more. 12 μL of 100 % Ethanol were then added and the microfuge tube was vortexed for 30 seconds. This gold bead-DNA mixture was aspirated and dropped at the center of the dried macrocarrier membrane. The newly wet membrane was then placed back into the petri-dish containing Drierite® and allowed to dry completely for about 3 minutes.

Operating the PDS-1000/He™ biolistic particle delivery system: The vacuum pump was switched on then the pressure valve (a silver knob) on the helium tank was turned counterclockwise to attain a pressure of 2200 psi visible on the pressure gauge. The DNA-containing macrocarrier membrane was then placed in its silver holder, DNA-side up. A mesh screen (Bio-Rad™; replaced during each biolistic transformation) was dipped in 100 % isopropanol (ThermoFisher) and placed into the disc chamber of the

white plastic mounting plate. After this, the holder containing the DNA-containing macrocarrier membrane was mounted onto the mesh DNA-side down. The cap was screwed and this assembled set-up was placed in the highest slot. The biolistic machine was then turned on using the red button to the left and the rupture disc holder that hangs from the ceiling of the machine was taken out utilizing a torque wrench to first loosen it by twisting it to the left. Once completely removed, a 1550 psi rupture disc (Bio-Rad™) prewashed in 100 % isopropanol was placed in the holder. The holder was then screwed back and tightened using a torque wrench by twisting it to the right; the distance between the rupture disc and macrocarrier was about 0.375 inches. The disk chamber was thoroughly cleaned using a 70 % Ethanol swab and the petri-dish containing *ady2* cells (that had been incubated for 3 hours at 30°C) was placed on the petri-dish holder (lid off) in the third slot of the biolistic particle delivery system chamber. The chamber door was shut and secured then the "vacuum" button was pushed down once until the vacuum gauge reached about 29 Hg (within 15 seconds). Quickly, the vacuum button was released to resume the down position while switching to pressing the "hold" button. At this point, the "fire" button was held until a 'pop' sound was made indicating the ruptured disc then the "fire" button was immediately released. The "vent" button was pressed to vent the chamber to 0 psi. The YPD 1 M sorbitol plate was removed when the chamber attained atmospheric pressure and the biolistic machine was turned off and cleaned using a 70 % Ethanol swab. The helium gas was turned off by turning the knob clockwise; the vacuum pump was then turned off.

Selecting *mCHERRY::ADY2* transformants: To allow the cells to recover, the YPD 1 M sorbitol plates were incubated for 3 hours at 30°C after which all the cells were scraped and evenly spread onto a YPD plate containing 100 µg/mL of Hygromycin (ThermoFisher) for selection as the pLKB55 vector carrying the *mCHERRY::ADY2* construct contained *HYG*. These plates were then incubated at 30°C for up to 72 hours during which the plates were observed every 24 hours and individual colonies from these plates were patched onto fresh YPD plates containing 100 µg/mL of Hygromycin. Colony transformants seen to be able to grow in YNB (Difco™) agar supplemented with 0.2 % acetate (unlike the initial *ady2* strain before *mCHERRY::ADY2* had been introduced) were subcultured for protein isolation, western blotting and fluorescent microscopy. This construct remains episomal and does not get integrated into the *ADY2* locus.

Protein isolation

Six individual colonies of *Cryptococcus neoformans* transformed with an *mCHERRY::ADY2* construct, and the wild type H99 (serves as the negative control), cultures were subcultured to grow overnight in YPD. An equivalent of OD 600 = 3 or up to 5 x 10^7 cells were harvested and washed by centrifugation at 300 x g for 1 minute using 1 mL ice cold sterile nanopure water before resuspending in 100 uL of sterile nanopure water. From these cells total denatured proteins were isolated according to the protocol described by Kushnirov (2000). To do this, 100 uL of 0.2 M NaOH was added to the cell suspension and the setup was incubated for 10 minutes at ambient temperature before centrifuging at 3000 x g. The supernatant was then carefully discarded and the resulting pellet was resuspended in 50 µL sodium dodecyl sulfate (SDS) buffer (0.06 M Tris-HCl pH 6.8, 4 % ß-mercaptoethanol, 5 % glycerol, 2 % SDS and 0.0025 % bromophenol blue). At this stage, samples could either be stored at -20°C or further processed by heating immediately at 95ºC for 3 minutes followed by a 30-second centrifugation at 3000 x g before either storing the samples at -20°C or proceeding to a denaturing SDS-PAGE gel prior to performing a western blot. 20 µL of these samples were then separated on SDS-PAGE gels at a voltage of 150 for 45 minutes.

Western blotting

Denatured proteins in the gel were then transferred to a nitrocellulose membrane using a sandwich assembled as follows: first a thick filter paper prewetted in transfer buffer (5.8 g Tris base, 2.9 g glycine, 200 mL MeOH, 3.75 mL of 10 % SDS and 795 mL of sterile nanopure water), followed by a nitrocellulose membrane also prewetted in

transfer buffer, the SDS-PAGE gel containing denatured proteins, and finally another thick filter paper prewetted in transfer buffer. This sandwich was arranged on the bottom platinum anode of a Trans-Blot SD Semi-Dry Transfer Cell (Bio-Rad™) after which the top was secured and its semi-dry chamber layered with of transfer buffer (approximately 100mL), the blot was ran for 40 minutes at 16 volts. At the end of a successful transfer, the nitrocellulose membrane should have gained the proteins originally from the SDS-PAGE gel, which can be ascertained if a prestained ladder that was initially visible on the SDS-PAGE gel is now visible on the nitrocellulose membrane and has faded from the SDS-PAGE gel. The nitrocellulose membrane was then washed for 5 minutes in 20 mL of TNT (1% of Tris-Cl pH 8.0, 3% of 5 M NaCl, 0.05% of Tween 20 in 1 L of sterile nanopure water) wash buffer with gentle shaking.

To inhibit non-specific binding of antibodies, the nitrocellulose membrane was then blocked in TNT wash buffer containing 1 % of nonfat milk for one hour at ambient temperature with gentle shaking. After blocking, the nitrocellulose membrane was incubated for one hour at ambient temperature with gentle shaking in the mouse-derived primary Anti-mCherry antibody (1C51, Abcam) which was freshly diluted 2,000 fold (5 μL of antibody in 10mL of blocking solution). After one hour had elapsed, the nitrocellulose membrane was washed thrice in TNT for 5 minutes per wash with gentle shaking. The nitrocellulose membrane was then incubated for another one hour in the secondary antibody solution (a 10,000-fold dilution, that is 1uL of the goat anti-mouse IgG H&L HRP from Abcam, in 10 mL of the blocking solution). This was followed by three additional wash steps in TNT, each 5 minutes with gentle shaking. For visualization

of the target protein, we used the ECL western blotting substrate (Pierce™) mixed in equal volume, to incubate the nitrocellulose membrane for 5 minutes before drying the nitrocellulose membrane, sealing it in clear wrapping paper and blotting it on a film in a dark room then developing an X-Ray film (ThermoFisher™) using an AFP X-Ray Film Processor (AFP Manufacturing Co.).

Results and discussion

To determine stable *mCHERRY::ADY2* construct integration and subsequent protein translation, we used western blot to analyze proteins isolated from six colonies subcultured from a *C. neoformans ady2* strains that had been transformed (**Figure 5-1**). Despite antibody detection of expressed mCherry, this did not contain the full ~64kDa mCherry::Ady2 and was only 24kDa. This suggests that *mCHERRY::ADY2* is either not heritable, or it is simply not stably integrated but gets cleaved in subsequent generations as these six strains also lost ability to grow in minimal concentrations of acetate, implying a loss of functional Ady2. The stability of ectopically integrated constructs introduced by biolistic transformation varies from 17.5 % - 100 %, while frequency of homologous recombination is about 10 % (Lin et al., 2015). It is therefore likely that the ectopically integrated pLKB55 containing the *mCHERRY::ADY2* was not stable. Arras et al., (2015) have described a protocol for stable complementation of *C. neoformans* genes into a "safe haven" locus that stably integrates and is heritable. We are currently exploring this site to be used in expressing C-terminally tagged *ADY2* also with the dual purpose of complementing the *ady2* strain, or any other genes of interest driven by their endogenous promotors.

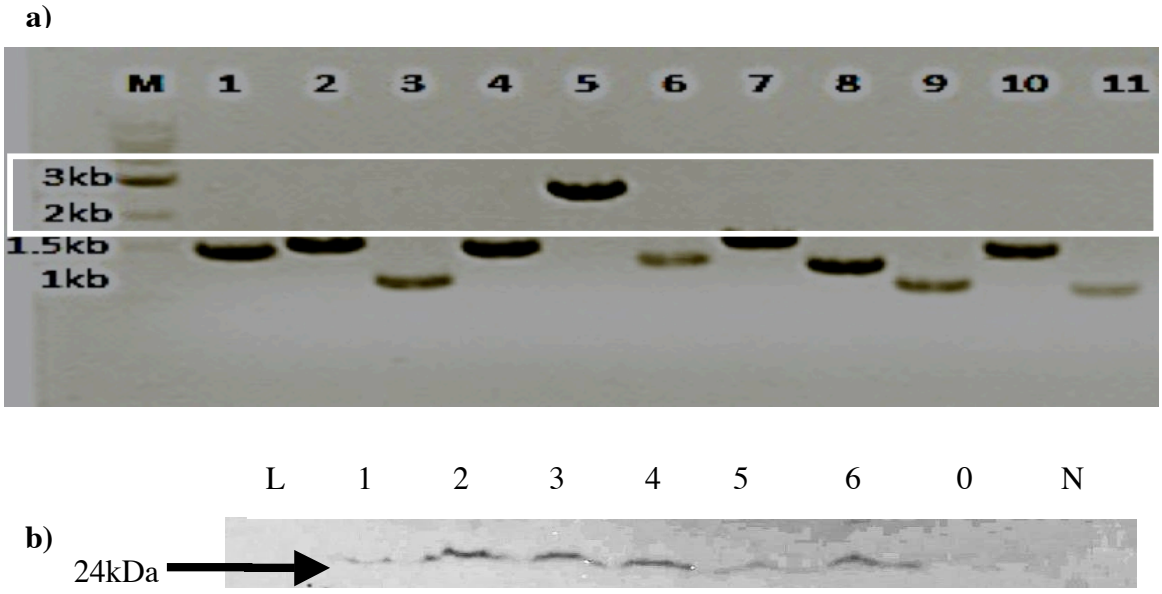

Figure 5-1: *mCHERRY::ADY2* construction. From wild type genomic H99, *ADY2* was amplified and cloned into pLKB55 and **a)** 11 transformants were checked by colony PCR for amplicon sizes (Lanes 1-11) corresponding to *mCHERRY::ADY2* (2.63kb) against a molecular ladder lane (M) followed by biolistic transformation of confirmed vectors into *C. neoformans*. The colony on lane 5 had the correct amplicon size. **b)** Fluorescent *C. neoformans* transformants were subcutured and heritability of full length mCherry::Ady2 confirmed western blot. The lanes as labeled contain: L=prestained Ladder (shows up on nitrocellulose membrane but not developed film as it is not recognized by antibodies). 1-6=individual colonies from transformations with mCherryAdy2 construct in pLKB55. 0=colony with same properties as 1-6 except that the cell numbers were low before protein isolation hence low yield. N=H99 (negative control).

a) Amplifying 1.6kb of 0.3kb 5' + *ADY2 ORF*
5’ Primer: GGAACGCTAGCTATGTCTGAAACGAAGCTCCC
3’ Primer: GGAACTTAATTAATACGATAGATGGGGGCAAGTCGGG
b) Confirming 2.63kb *ADY2::mCHERRY*
5’ primer: GGAACCTGTCGCTTGCGTCATCGTAGTA
3’ primer: GGAACGGGAGGGTGTACATCCTTTTCC

Table 5-1: Primers used to generate and confirm *mCHERRY::ADY2*: Primer set **a)** was used to amplify the ORF (open reading frame) of *ADY2* in addition to a preceeding 0.3kb 5’ region was amplified resulting in a 1.6kb fragment. This was then cloned into the Nhe1 and Pac1 restriction endonuclease sites of the pLKB55 vector. Using primer set **b)**, 11 transformants were checked by colony PCR for amplicon sizes (Lanes 1-11) corresponding to *mCHERRY::ADY2* (2.63kb) against a molecular ladder lane. This primer set anneals to the backbone of the pLKB55 such that without the *ADY2* insert, a 0.3kb amplicon would be obtained.

References

Kozubowski L, Aboobakar EF, Cardenas ME and Heitman J, 2011. Calcineurin colocalizes with P-bodies and stress granules during thermal stress in *Cryptococcus neoformans*. *Eukaryotic Cell*, **10:**1396-1402.

Kushnirov VV, 2000. Rapid and reliable protein extraction from yeast. *Yeast*, **16:**857-860.

Lin X, Chacko N, Wang L, Pavuluri Y, 2015. Generation of stable mutants and targeted gene deletion strains in *Cryptococcus neoformans* through electroporation. *Medical Mycology*. **53:**225-34.

Molecular Mycology Course Handbook, 2016. Current approaches to fungal pathogenesis, experiment 4: Transformation of *Cryptococcus neoformans*.

Taylor T, Bose I, Luckie T, Smith K, 2015. Biolistic Transformation of a Fluorescent Tagged Gene into the Opportunistic Fungal Pathogen *Cryptococcus neoformans*. JoVE (Journal of Visualized Experiments). **97:**e52666.

The role of acetate transport in environmental adaptation and pathogenicity of *Cryptococcus neoformans*

Grace N. Kisirkoi

Department of Genetics and Biochemistry

Eukaryotic Pathogens Innovation Center (EPIC)

Clemson University

Clemson, SC 29634

CHAPTER SIX

Conclusions and recommendations for further studies

This dissertation provides novel insight into the roles of acetate transporters in the environmental adaptation and pathogenicity of *Cryptococcus neoformans*, the most frequent cause of fungal meningitis. With this new insight, there ensued additional testable hypotheses, which provide opportunities for continued investigations. This chapter will cover the conclusions drawn from these two studies in relation to ongoing experimental manipulations. Based on these conclusions, I will make future recommendations for continued investigations.

The first of these studies demonstrated a complementary role of the acetate transporters, Ady2 and Ato2 in environmental adaptation. This is because their cumulative loss compromised the pathogen's ability to buffer surrounding pH to alkalinity, attributable to ammonia export. Moreover, plate growth assays identified Ady2 but not Ato2 as indispensable for *C. neoformans*' survival during physiologically relevant starvation conditions replicated in minimal media supplemented with low acetate concentration. A slight contribution of Ato2 to survival in minimal media supplemented with acetate, as well as a reiteration of the essentiality of Ady2 was seen during growth on liquid minimal media supplemented with low acetate. However, upon increased acetate concentration in the media, these transporters are not essential as is depicted by growth at wild type levels. Confirmation of the relative contribution of these acetate transporters to acetate transport was further highlighted by a dramatic upregulation of *ADY2* during growth on acetate, while the less effectual *ATO2* was only slightly

upregulated. These observations further suggest that acetate is a signal that induces expression of these genes, hence their expression allows for versatile adaptation to low nutrient environments and may crosstalk with the cAMP/PKA cascade.

As expected, initial uptake rates of radiolabeled acetate following overnight growth in nutrient rich YPD identified a requirement for Ady2 but not Ato2 in acetate uptake. However, upon an additional passage of cells into nutrient poor YNB supplemented with acetate for an additional twenty hours, Ato2 also became required for acetate uptake. This finding led to the conclusion that both Ady2 and Ato2 are involved in acetate uptake, however Ato2 plays a significant role following prolonged exposure to starvation conditions and it acts to supplement Ady2 function in meeting the cell's energy requirements. Ady2 and Ato2 were not essential for acetate export as delineated by wild type levels of acetate using the techniques used to measure extruded acetate.

Assuming that our technique of measuring acetate export had enough resolution to distinguish acetate export from any other analogous byproduct(s) that could react with assay reagents to give signal, I am led to hypothesize that yet another protein may be performing this task. This is highly likely because experimental evidence of *Saccharomyces cerevisiae* Fps1p suggests that this membrane aquaglyceroporin channel allows export of dissociated acetate across the membrane. Knockouts of Fps1p accumulate acetate slower than wild type cells and are more resistant to acetate toxicity (Mollapour et al., 2007). Using the amino acid sequence of *S. cerevisiae* Fps1p, a BLASTp search of *C. neoformans* failed to identify an ORF of significant sequence identity. Moreover, there is yet another uncharacterized member of the acetate transporter

Gpr1/Fun34/YaaH, Ato3, whose roles may entail acetate export. Therefore, I propose that acetate export efforts be undertaken to characterize Ato3 with reference to acetate export and carbon source requirements.

The colourimetric assay which we used to determine acetate export depended on conjugation of acetate assumed to be exported into the culture supernatant with hydroxamate and detecting its colourimetric intensity with the aid of spectrophotometry. However, I cannot completely rule out the possibility that the apparent lack of distinction between wild type and mutant cells' acetate export could be due to low resolution of the hydroxamate assay. In this case, acetate signal could be indistinguishable from such structural analogs as butyrate and propionate, which could react with hydroxamate assay reactants. This is especially because the target analyte is an enzymatic byproduct from a culture supernatant that could contain these analogs. Although published results of the hydroxamate assay are robust, alternative approaches could serve to confirm observations in this studies using analytical techniques that target acetate as the specific analyte, or a metabolomics approach that surveys patterns of excreted metabolites in the supernatant, among them acetate.

I was able to optimize a gas chromatography flame ionization detection (GC/FID) protocol (**Table 6-1**). Preliminary data obtained from this optimized protocol could be used to design experiments to detect a target analyte or plan an exploratory metabolomics analysis. The FID's detection strategy is mass-flow rate dependent thus allowing for direct detection of the analyte acetate. This avoids the uncertainties that could arise from contaminant-prone derivatization. The physical properties of acetate governed our

experimental design. Its volatility and thermostability met the criteria for ideal analytes to be used in GC analysis. Moreover, as acetate exists in a polar state, the ideal column was polar as well. This polar ZB-FFAP column held on to the polar acetate until its boiling point was reached at which acetate eluted off the column and proceeded to detection. The GC/FID yielded such robust reproducibility that the standard deviation of the mean elution time (3.73 minutes) of standard acetate concentrations was ± 0.03 minutes. This accuracy was maintained during sample analysis of the culture supernatant such that the acetate elution peak was at a mean of 3.77 ± the standard devioation of 0.002 minutes. However, as the free access to the MUAL equipment had a sample number cap, we could only run samples in N=1 per strain following 30 and 48 hour-long growth in the minimal media, YNB supplemented with 2 % glucose.

Overall, we observed that after 30 hours of culture, acetate recovered in the supernatant of wild type, the individual null mutants of *ADY2* and *ATO2* was statistically comparable. However, the acetate concentration of the double mutant dropped below the detection limit of the assay (**Table 6-2**). On the other hand, after 48 hours of culture, only the wild type strain had detectable acetate (**Table 6-3**). This could point to an involvement of Ady2 and Ato2 in acetate export. However, the low sample size limits statistical power and calls for replications of the experiments using statistical and biological replicates to ascertain the roles of *ADY2* and *ATO2* in acetate export.

I further propose a larger scale survey of metabolites in culture supernatant with the aim of unearthing the metabolic processes being undertaken by each of the strains based on loss of a specific transporter. In such a large-scale screen, it is not feasible to

fully anticipate possible analyte thermostability, polarity or volatility. Therefore, liquid chromatography/mass spectrometry (LC/MS) as opposed to either GC/FID or GC/MS may provide a wider range of differential analyte separation than GC-based methods. Several optimization aspects of the separation technicalities are anticipated. To start with, investigators could assume that analytes of interest will be more polar than non-polar. Therefore, this would call for a polar column and non-polar initial solvent conditions. With increasing polarity in the solvent, analytes of interest will be released from the column relative to their increasing polarity. The MS component would serve to ionize the separated analytes and use a mass/charge ratio to identify and quantify it. Alternatively, an MS/MS technique could be applied such that it bypasses the LC separation. In this case, the sample (culture supernatant) could directly be injected into an MS/MS analyzer, which allows for tandem mass spectrometry in several concurrent mass analyzers either in time or in space. Adjustments of ionization intensities could be made to fragment polymerized compounds and determine whether they are sugars, amino acids, or ammonium, or carboxylic acids. Their relative abundance in each *C. neoformans* acetate transporter mutant strains would give insight into the diverse roles being played by these proteins and further illuminate their functions and mechanisms of action.

Results detailed in this dissertation further led to the conclusion that Ady2 is required for cellular membrane uptake of deprotonated acetate when concentrations fall below a threshold that diffusion only would suffice to meet the cell's energy demands during starvation. Another conclusion that we arrived at is that the mutant phenotypes we observed are a direct consequence of loss of function of acetate transporters as opposed to

pleiotropic effects arising due to membrane disruption. This is because membrane transport employs membrane bound or membrane associated proteins, whose correct integration collectively contributes to intact membrane integrity. Additionally, under the conditions tested, Ady2 and Ato2 did not contribute to fluconazole resistance. However, because acetate is a precursor for ergosterol synthesis and ergosterol is the target for fluconazole, we propose a different approach than was used in this study to further investigate a possible relationship between acetate transport and fluconazole susceptibility. To do this, I suggest media constitution of acetate and fluconazole in the minimal YNB as opposed to adding fluconazole to a glucose-containing rich medium. This approach would limit the carbon source availability. Consequently, a reduced ability to take up acetate for ergosterol biosynthesis under these starvation conditions could result in the *ADY2* mutants having vulnerability to fluconazole. As Vanden Bossche et al., (1992) found that the fluconazole resistant *Candida glabrata* isolate (B57149) had a higher [^{14}C]-acetate uptake rate, we are currently characterizing the roles of Ady2 and Ato2 during conditions that necessitate acetate uptake.

Since my data supported a requirement for Ady2 and Ato2 in acetate transport and eliminated non-specific effects from compromised membrane integrity, I was led to initiate an ongoing inquiry into the subcellular localization of these genes during varied conditions by tagging *ADY*2 with mCHERRY. I utilized the plasmid- pLKB55 graciously provided by Dr. Lukasz Kozubowski (Kozubowski et al., 2011) to create a construct that fused mCHERRY upstream of *ADY2* under the constitutive expression of *GPD1* (glycerol-3-phosphate dehydrogenase) promoter. This construct could also be used to

complement the *ADY2* null mutant strain by restoring phenotypes observed during growth on low acetate from loss of *ADY2*. Fluorescence microscopy indicated an elevated signal during the conditions concurrent with *ADY2* overexpression. I found that when cells were grown for 48 hours in minimal solid media supplemented with low acetate (0.2 %) during which *ADY2* is essential, localization occurs in punctate structures. However, during growth in higher acetate (0.5 %), localization is more diffuse with varied concentration of signal around the cell's periphery and within the cytoplasm (**Figure 6-1a** and **Figure 6-1b**).

Efforts to determine stable construct integration and protein translation using Western blot (**Chapter 5**) have revealed that *mCHERRY* is cleaved in subsequent generations, and eventually not present when genomic DNA was analyzed. Consistent with this observation, the subsequent generations of this newly generated strain gradually lost ability to grow in minimal acetate as sole carbon source, a trait characteristic of strains stably expressing wild type *ADY2*. This suggested that the N-terminally tagged *mCHERRY::ADY2* strain was not stably integrated or was not heritable as constructed. In the light of these subcellular localization observations, I propose genome-editing techniques to confirm these data using a native promoter modified from the "safe haven" trans complementation strategy (Arras et al., 2015). Moreover, the regulation of *ADY2* expression under its native promotor could also be investigated with technique. This strategy was originally created to complement null mutant *C. neoformans* strains by reintroduction of the wild type allele into a small gene-free region which allows for stable integration into this targeted region without disrupting other genes, and distinction of the

new complement strain from wild type contaminants (Arras et al., 2015). However, I propose tagging the C-terminus of *ADY2* using a fluorescent reporter such as *mCHERRY* with the aid of overlap extension PCR then introducing this fusion construct into the safe haven vector with the dual intent of complementing the null mutant *ady2* strain as well as determining the localization of *ADY2* under different conditions.

Alternatively, the CRISPR/Cas9 machinery as recently optimized for *C. neoformans* (Arras et al., 2016; Wang et al., 2016) to reduce off target genoome editing and enhance stable integration of the cassete of interest can be used. To do this, a fluorescent reporter can be fused to a 'dead' Cas9 whose nuclease activity is deactivated by D10A and H840A mutations similar to Chen et al., (2013). The CRISPR/Cas9 eliminates dependency on antibiotic resistance markers thus allowing multiplexing techniques and eliminating constraints faced by traditional genome editing techniques that are limited by running out of usable antibiotic resistance markers. Simultaneous fluorescent tagging of *ADY2* and *ATO2* with varied fluorescent reporters may be possible by designing short guide (sg) RNA to target the mutant dCas9::fluorescent tag fusion to its respective gene similar to Lackner et al., (2015). This multiplexing could further be extended to investigate interactions between acetate transport and assimilation or dissimilation by simultaneously tagging both a transporter and an acetate producing (such as acetate kinase) or utilizing enzyme (such as acetyl-CoA synthetase). The same dCas9, if untagged to a reporter could bind to *ADY2* or *ATO2* promotors to effect gene knockdown and titrate effects of their reduced expression. Further insight into acetate transporter function could be gleaned through CRISPR/Cas mediated tagging.

We suggest that for biochemical characterization of acetate transporters, the catalytically inactive dCas9 could also be fused to an affinity purification tag and purified prior to catalytic analysis for substrate specificities and structural analyses. The same sgRNA used to guide the fluorescently tagged construct described above could be used. Originally, the type II CRISPR/Cas system native to *Streptococcus pyogenes* was optimized to induce sequence-specific double strand breaks (DSBs) to knockout target genes either mediated by homogous recombination, or to induce missense mutations through non-synonymous nucleotide substitution mediated by non-homologous end joining DNA repair. With the aid of a Cas9 protein, the CRISPR machinery recognizes specific target DNA sequences steered by a short guide (sg)RNA and a protospacer adjacent motif (PAM) typically 20 nucleotides long (Sander and Joung, 2014).

The second of these studies identified Ady2 and Ato2 as having synergistic roles in virulence of *C. neoformans*. This conclusion was arrived at because of the highly attenuated virulence observed in *ady2ato2* such that infected mice never became moribund nor died. This leads us to hypothesize that the *ady2ato2* strain may have a protective effect by activating the immunity to effectively control disease from causing fatality. To study this, we hypothesize an experimental design of three test groups of C57BL/6 mice in addition to a positive control infected with wild type and a negative control group that would remain uninfected. Of the three test groups, one would be infected with 10,000 heat-killed *ady2ato2* cells, another group would receive an equal inoculum of viable *ady2ato2* cells. Moreover, this strain was heavily impaired in the major virulence factors-ability to grow at human body temperature, ability to produce

melanin - protective against unfavourable environments, and ability to produce capsule - a major immune modulator. This requirement of Ady2 and Ato2 for capsule formation and a connection to efficient phagocytic anticryptococcal clearance was demonstrated in this study. Efficient clearing of the double mutant by human phagoctyes and macrophages converged with the acapsular quality of the strain.

I hypothesize that capsule defects caused the double mutant strain to be more recognizable by phagocytes, hence it was easier to clear them during a coculture. Studies are ongoing to further characterize the roles of these acetate transporters during osmotic stress, different cell wall stresses and titrations of temperature using starvation media formulations instead of glucose-containing media that do not elicit significant phenotypes. Of particular interest is a study into the possibility of sorbitol to alleviate temperature sensitivity (Garcia et al., 2015) of *ady2ato2*, which we found was not differentially susceptible to cell wall and membrane pertubing Congo red and SDS. As weakened cell wall could result in temperature sensitivity and reduced viability yet *ady2ato2* has no obvious membrane or cell wall defect, possible phenotypic remediation of its thermosensitivity by sorbitol would suggest membrane or cell wall damage at the ultrastructural level and necessitate electron microscopy.

My general conclusion given the data on acetate transporters and their impact on *C. neoformans* virulence is that acetate transport plays a significant role in its pathogenecity by allowing adaptation to the different environmental niches afforded by the host. To elucidate the mechanisms employed in virulence association to acetate transport, we recommend several follow-up experiments. First, I suggest a whole-genome

survey of wild type and the double mutant strains through RNA-Seq. Through multiplexed gene expression information gleaned from wild type versus double mutant strains during infection, phagocyte coculture, growth at 37ºC, and capsule inducing conditions, we can determine differential expression patterns and tie them to virulence-associated mechanisms. Expression information about immune activation of different pathways could be gleaned from RNA-Seq. This could provide important information regarding the efficiency of immune-mediated pathogen clearance.

Secondly, an alternative infection to the one used in this study route could be used to introduce *C. neoformans* to C57BL/6 mice. In this study, an inhalation route was used to model the natural infection route. With this, the pulmonary environemnt is the initial infection site, which poses a difficulty in determining the role of genes under study during disseminated cryptococcal meningitis. Alternatively, a tail vein injection would ensure fast delivery to the brain and provide further insight into the roles played by acetate transporters during neural involvement, the stage that proves fatal in most human cases. My third suggestion involves an immunological study using enzyme linked immunosorbent assay (ELISA) to study the cytokines elicited by immune cells following invasion. Comparative analysis of responses of the avirulent *ady2ato2* mutant versus the wild type strain could reveal mechanisms that make it easier to abolish virulence of the double mutant strain.

In order to support prolific research on protein families that show promise as drug targets, I recommend a forward genetic approach using random mutagenesis to create unidentified mutants followed by a screen of these resulting mutants to identify those that

are defective in acetate transport. This would help generate a library of candidate genes that can be characterized to fully elucidate underlying mechansims responsible for acetate metabolism and relevant virulence links. Furthermore, I recommend expression and purification of the wild-type Ady2 and Ato2 followed by screening of a panel of compounds to identify inhibitors which when bound to these acetate transporters would phenocopy deletion of the *ADY2* and *ATO2* open reading frames. Additionally, the development of a manually curated 'smart' library could act as a repository for both published and highly proofed unpublished data. To do this, we suggest a ranking system to weight data guided by a research group's collective domain-specific knowledge. The aim of this would be to structure available data on a protein family into a searchable novel database. The eventual goal for this database would be to foster collaborative curation of large amounts of published and well-founded but unpublished data being continually churned by research groups. Consequently, predictive algorithms could be used to 'mine' patterns from data on specific proteins to generate hypotheses from discovery of models gleaned through automatic knowledge discovery. Not only will this allow for confident and efficient hypothesis generation, but it will also provide a platform for learning from unpublished negative data, hence elminate redundant experimental approaches and guide researchers towards novel approaches. Interactions between protein families could also be unearthed from high throughput genomics, proteomics metabolomics and other omics data.

I am manually curating this database "Eukaryotic Pathogens Hypothesis INnovation (EPHIN)" (coded by Steven Cogill, Stanford University, Emergency

Medicine, Palo Alto, Ca.) as a web application with a very small foot print. We are currently running our system on a windows 2012 server and our application is written using the fuelphp framework for the latest version of xamp which includes compatibility with php 5.6 and php 7. As of now our mysql database is 35 KB and our application is 15.7 MB. It is growing larger as we add more data to our classification forms. These forms were generated using overarching topics from manuscripts that had characterized GPR1/FUN34/YaaH family of acetate transporters. The forms provide a general profile for a protein, indicating the organism under study, the gene name(s) and sequence, protein name(s) and sequence, its functional annotations according to NCBI and Uniprot before highlighting possible genome edits used to study it. Specifically, it lets the curator select from such genome edits as deletion of complete open reading frames, protein segment truncation, site directed mutagenesis of defined non-synonmous amino acid substitution, overexpression, random mutagenesis and RNAi mediated gene knockdown. This is followed by a ranking the effect that this genome edit had on the organism or protein during such experimental conditions as carbon source utilization/substrate specificity, drug and inhibitor susceptibility, virulence determinants and colony/cell morphology.

Expression of a wild type allele during this conditions is also documented if the data is available. If data is published, links and references of all the publications are uploaded into the database. Analyses and information used to generate this database so far is illustrated in **Figure 6-2**. Pulling from all these sources, a snapshot of the weighted significance of this dissertation's study of *C. neoformans* Ato2 was generated as

illustrated in **Figure 6-3**. Alongside each snapshot generated is information on the number of studies used to generate it. The direction that creation of this database is forging will facilitate an objective understanding of pathogenicity and promote efficient use of resources on highly proofed research hypotheses from mining of large data sets. It will be extensible such that different protein families classification schemes can be created according to its specific factors.

The studies detailed in this dissertation have served to fill vital knowledge gaps on previoulsy uncharacterized *C. neoformans* acetate transporters by establishing their roles in pathogenesis and metabolic adaptations. These new insights have created new study questions that present opportunities for continued study as explored in this chapter.

References

Arras SD, Chitty JL, Blake KL, Schulz BL and Fraser JA, 2015. A genomic safe haven for mutant complementation in *Cryptococcus neoformans*. *PloS One*, **10:**e0122916.

Arras SD, Chua SM, Wizrah MS, Faint JA, Yap AS and Fraser JA, 2016. Targeted Genome Editing via CRISPR in the pathogen *Cryptococcus neoformans*. *PloS One*, **11:**e0164322.

Chen B, Gilbert LA, Cimini BA, Schnitzbauer J, Zhang W, Li GW, Park J, Blackburn EH, Weissman JS, Qi LS and Huang B, 2013. Dynamic imaging of genomic loci in living human cells by an optimized CRISPR/Cas system. *Cell*, **155:**1479-1491.

García R, Botet J, Rodríguez-Peña JM, Bermejo C, Ribas JC, Revuelta JL, Nombela C, Arroyo J, 2015. Genomic profiling of fungal cell wall-interfering compounds: identification of a common gene signature. BMC genomics. **16:**683.

Kozubowski L, Aboobakar EF, Cardenas ME and Heitman J, 2011. Calcineurin colocalizes with P-bodies and stress granules during thermal stress in *Cryptococcus neoformans*. *Eukaryotic Cell*, **10:**1396-1402.

Lackner DH, Carré A, Guzzardo PM, Banning C, Mangena R, Henley T, Oberndorfer S, Gapp BV, Nijman SM, Brummelkamp TR and Bürckstümmer T, 2015. A generic strategy for CRISPR-Cas9-mediated gene tagging. *Nature Communications* **6:**10237.

Mollapour M and PW Piper, 2007. Hog1 mitogen-activated protein kinase phosphorylation targets the yeast Fps1 aquaglyceroporin for endocytosis, thereby rendering cells resistant to acetate. *Molecular and Cellular Biology*, **27:**6446-6456.

Sander JD and Joung JK, 2014. CRISPR-Cas systems for editing, regulating and targeting genomes. *Nature Biotechnology*, **32:**347-355.

Vanden Bossche H, Marichal PATRICK, Odds FC, Le Jeune L and Coene MC, 1992. Characterization of an azole-resistant *Candida glabrata* isolate. *Antimicrobial Agents and Chemotherapy*, **36:**2602-2610.

Wang Y, Wei D, Zhu X, Pan J, Zhang P, Huo L and Zhu X, 2016. A 'suicide'CRISPR-Cas9 system to promote gene deletion and restoration by electroporation in *Cryptococcus neoformans*. *Scientific Reports*, **6:**1-13.

Time (minutes)	Temperature ramp	Temperature (◦C)	Hold time
0	10 ◦C/minute	80	1 minute
10		170	1 minute
	Technical conditions		
	Splitless liner		
	Injection volume - 2.0 µL		
	Purge flow – 2 mL/minute		
	Carrier gas - H2 at linear velocity of 45cM/s		
	Detector - FID		
	Polar column (ZB - FFAP):30 m X 0.25 mM X 0.25 µM		

Table 6-1. Optimized conditions used to detect acetate in culture supernatant with the aid of gas chromatography/flame ionization detection (GC/FID).

	30 hours	
Strain	**mM [acetate]**	**Retention time (minutes)**
H99	1.029	3.771
ady2	1.175	3.767
ato2	0.972	3.775
ady2ato2	0	none

Table 6-2. Concentrations of GC/FID measurements of acetate recovered in the supernatant of H99, *ady2*, *ato2* and *ady2ato2* strains grown at 30ºC in YNB supplemented with 0.2 % glucose for 30 hours (N=1).

48 hours		
Strain	**mM [acetate]**	**Retention time (minutes)**
H99	2200	3.759
ady2	0	none
ato2	0	none
ady2ato2	0	none

Table 6-3. Concentrations of GC/FID measurements of acetate recovered in the supernatant of H99, *ady2*, *ato2* and *ady2ato2* strains grown at 30ºC in YNB supplemented with 0.2 % glucose for 48 hours (N=1).

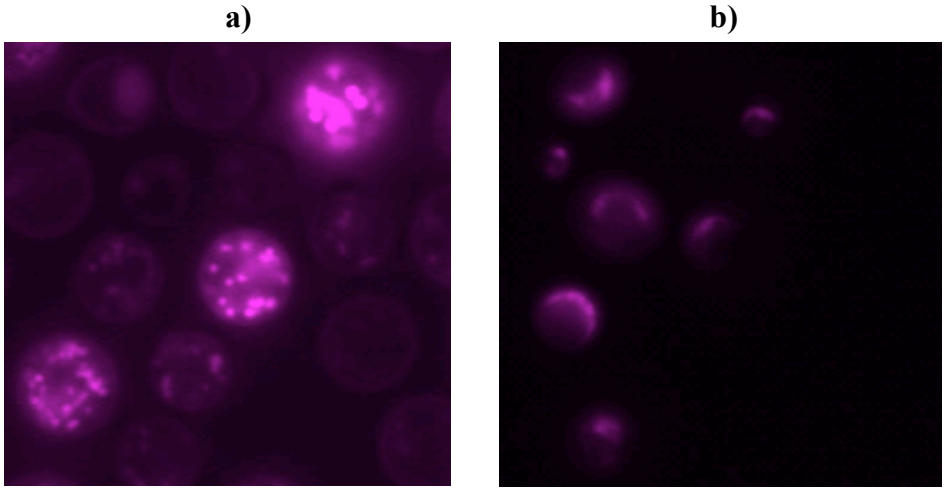

Figure 6-1. Localization of *mCHERRY::ADY2* during growth at 30ºC for 48 hours in YNB supplemented with **a)** 0.2 % acetate and **b)** 0.5 % acetate.

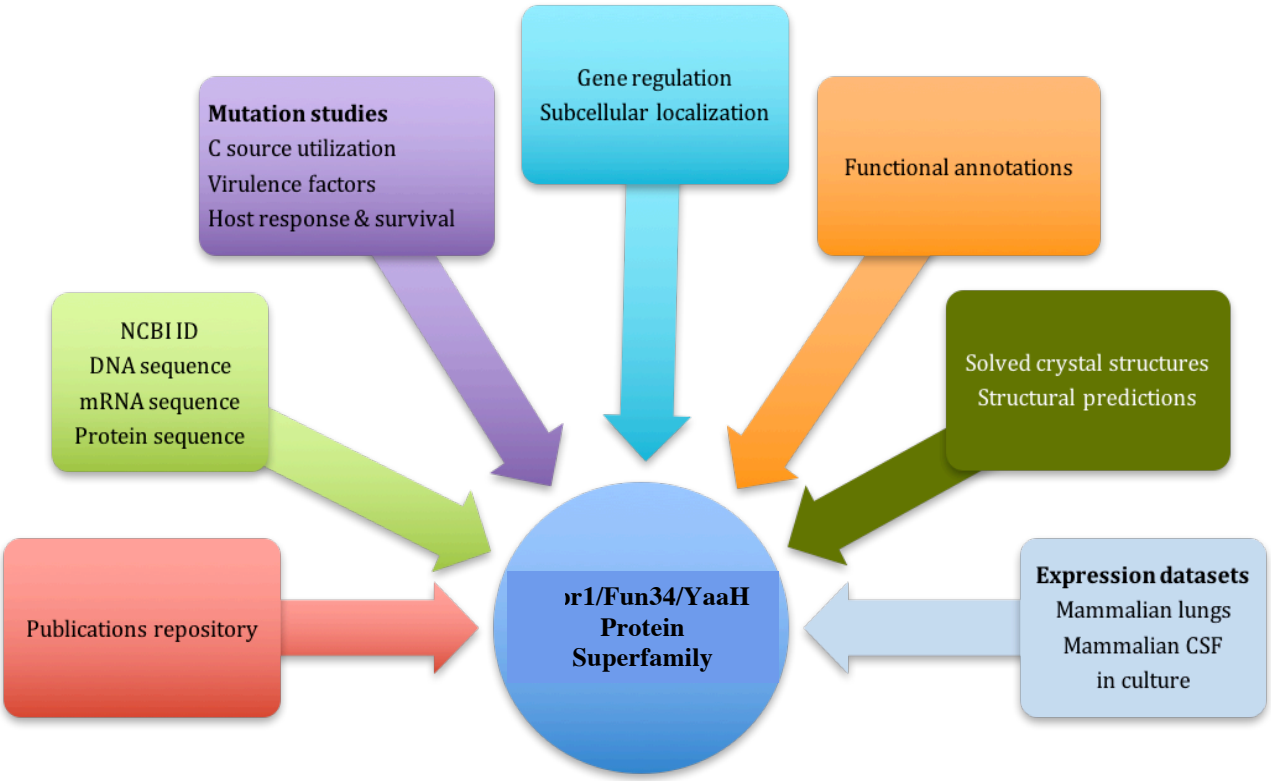

Figure 6-2. Eukaryotic Pathogens Hypothesis INnovation (EPHIN) database schematic. Analyses and information used to generate the extensible Eukaryotic Pathogens Hypothesis INnovation (EPHIN) database is presented on this schematic (Kisirkoi G. and Cogill S., unpublished). The system is running on a windows 2012 server and its application is written using the FuelPHP framework for the latest version of XAMPP and is compatible with PHP 5.6 and PHP 7.

***Cryptococcus neoformans* Ato2 snapshot**

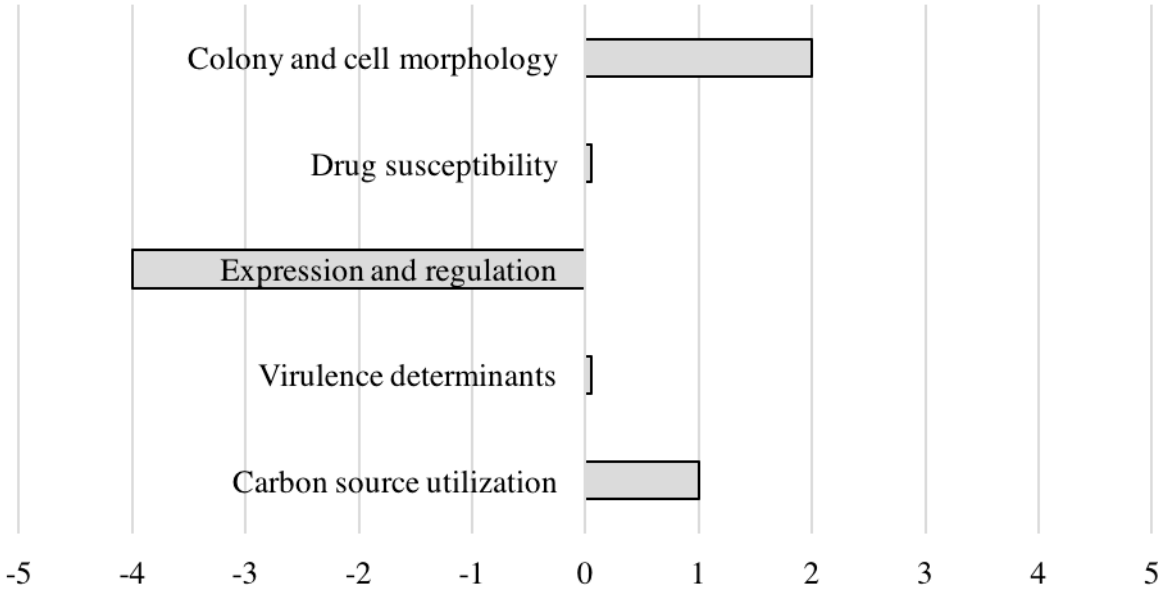

Figure 6-3. Data obtained from *Cryptococcus neoformans* experimental manipulations of Ato2 was uploaded onto EPHIN and used to create this snapshot (Kisirkoi G. and Cogill S., unpublished). The FuelPHP framework based on which EPHIN is created summarizes empirical data from published and unpublished sources into a snapshot.